METAL ION SPECIATION IN BLOOD PLASMA INCORPORATING 2-IMINO-4-THIOBIURET AS A POTENTIAL KIDNEY IMAGING AGENT IN NUCLEAR MEDICINE.

BY

KELEBILEONE MILDRED DITHEBE

A dissertation submitted in fulfillment of
the requirements for the degree of

Master of Science

University of the North West

2000

TABLE OF CONTENTS

ACKNOWLEDGEMENTS

I would like to give my sincere gratitude the following people:

1. NRF (National Research Foundation) and NECSA (Nuclear Energy Corporation of South Africa) for their financial support and again NECSA for allowing me to use their facilities for my research project.
2. University of the North West
3. Dr Neil Jarvis for his guidance and supervision throughout my work, Dr Werner Louw for helping me with the labelling and in general the Radiochemistry staff at NECSA for their support and guidance especially Mrs. Judith Wagener and Mr. Jan Rijn Zeevaart
4. My friends and family especially my parents who taught me to believe in God and to give my work unto Him and so my wishes will come true.
5. In brief, this "exercise" (research project) was more like a chemical reaction whereby reactants were (a). Hardworking
   (b). Determination
   (c). Perseverance
   (d). Endurance/ Tolerance

and the product being an MSc. Degree.

Hardworking + Determination + Perseverance + Endurance → MSc. Degree.

ABSTRACT

There is at present a need in several areas for a rational approach toward a ligand design, for selective complexation of metal ions in solution. Such areas would be, for example, design of complexes to act as imaging agents in the body.

Agents such as Dimercaptosuccinic acid (DMSA), Diethylenetriaminepentaacetic acid (DTPA), Mercaptoacetyltriglycine (MAG_3) and Glucoheptonate complexes to ^{99m}Tc have been used in the past for kidney imaging. However, investigational studies have shown that these agents, are taken up by the kidney, but imaging can only be done after a few hours. This long waiting period presents some hazards to the patients (high dose) during imaging. These observations have led to a need for new ligands that would easily be taken up by the kidneys (that is, imaging must be done immediately after injection).

In this study, a potentiometric technique will be used to investigate the behavior of 2-imino-4-thiobiouret (ITB) with some of the important blood plasma metal ions such as Ca(II), Mg(II), Ni(II), Cu(II) and Zn(II). Investigations were carried out, at 25°C and I= 0.15 mol dm^{-3} NaCl. A library of computer programs, ESTA was then used to calculate the formation constants from potentiometric data. The constants obtained were then introduced into a thermodynamic blood plasma model, ECCLES, to simulate processes in the body.

ITB was successfully labelled with ^{99m}Tc, the radionuclide of choice in imaging because of its availability, convenience, cost, excellent physical characteristics and low patient radiation dose.

General Abbreviations

ITB	2-Imino-4-thiobiouret
DTPA	Diethylenetriaminepentaacetic acid
DMSA	Dimercaptosuccinic acid
MAG_3	Mercaptoacetyltriglycine
HAG_3	2,3-Dihydroxysuccinic acid
ECMA	N,N' Ethylene (cysteine)(mercaptoacetamide)
DACH	1,2-Diaminocyclohexane
OIH	Orthoiodohippurate
p.i.	post injection
H^1 NMR	Proton Nuclear Magnetic Resonance
NQR	Nuclear Quadropole Resonance
GFR	Glomerular Filtration Rate
ERPF	Effective Renal Plasma Flow
EPO	Erythropoeitin
ECD	Ethylene cysteine dimer
N_2S_2	Diamine dithiolate
DNP	Renal tubular transport indicator
NECSA	Nuclear Energy Corporation of South Africa
ESTA	Equilibrium Simulation for Titration Analysis
ESTA2A	Optimisation module of ESTA
ESTA1	Simulation module of ESTA
Qbar / $\bar{Q}$	Deprotonation function, the average number of protons released per metal ion on complexation.
Zbar / $\bar{Z}$	Formation function, the average number of ligands bound per metal ion.
$\bar{Z}_H$	Protonation formation function, the average number of protons bound per ligand
$\bar{n}$	Average number of protons per ligand in the absence of metal ion
K_W	Water dissociation constant

β	Overall formation constant
pH	Negative logarithm of the free acid concentration
pA	Negative logarithm of the free ligand concentration
E_0	Electrode constant
L	Ligand
l.m.w	lower molecular weight
p.m.i	plasma mobilisation index
R	gas constant
T	absolute temperature
F	Faraday constant
I	Ionic strength

β	Overall formation constant
pH	Negative logarithm of the free acid concentration
pA	Negative logarithm of the free ligand concentration
E_0	Electrode constant
L	Ligand
l.m.w	lower molecular weight
p.m.i	plasma mobilisation index
R	gas constant
T	absolute temperature
F	Faraday constant
I	Ionic strength

CHAPTER 1 INTRODUCTION

1.1 Ligands Used As Potential Kidney Imaging Agents

Radionuclides of metals are most suitable for the production of radiopharmaceuticals as diagnostic and therapeutic tools. Radiopharmaceuticals are substance labeled with radionuclides that are routinely used in Nuclear Medicine Departments for the diagnosis and of diseases [1]. Radiopharmaceuticals are usually administered intravenously so that the tissue biodistribution will occur rapidly and the opportunity will be highest for radiopharmaceutical localization in the tissues of interest (eg. target organs) [2].

Nuclear Medicine is the field of medical practice that employs unsealed forms of radioactive materials for diagnosis and therapy. These clinical applications of radioactivity centre upon two different approaches, *in vivo* techniques being one approach [2].

In vivo techniques involve the administration of radioactivity to patients usually by oral or intravenous means. The majority of *in vivo* applications involve the determination of diagnostic information (such as organ function, shape or position) from a picture or image, of the radioactivity distribution within the organ or body part [2].

The diagnostic capability results from the gamma rays emitted by the agents employed in nuclear medicine, since these radiations become externally accessible for detection and imaging. Alternatively radionuclides that emit highly ionizing beta radiation that are absorbed locally are chosen for selective therapeutic irradiation of tissue malignancy [2].

Amidine ligands have recently been proposed as ligands for kidney imaging radiopharmaceuticals [3]. In this work, the ligand 2-imino-4-thiobiuret (ITB) will be studied. Ca^{2+}, Mg^{2+}, Zn^{2+}, $Ni^{2+}$and Cu^{2+} are some of the important

metal ions present in blood plasma. Investigational studies will be done to determine whether 2-Imino-4-thiobiouret (ITB) will be able to complex them at physiological pH.

Recent studies showed that more than 90% ITB could be labelled with ^{99m}Tc [4]. Formation constants for Tc cannot be measured potentiometrically because of its complex redox chemistry. Its oxidation states ranges from –1 to +7 state, the latter is the most stable [1]. This accounts for a rich range of complexes formed with technetium. TcO_4^-, has technetium in the +7 state, $[TcOCl_4]^-$, has technetium in +5, $[TcO(L4)_2]Cl$, has technetium in +1 state, where L4 is the deprotonated ITB. The latter is of importance to this work [3].

Blood plasma includes a range of different ligands (e.g amino acids, proteins), that could compete with ITB for metal ion complexation. Also, the metal ions present could compete with ^{99m}Tc for binding to ITB. This could interfere with the main purpose of using this ligand. This implies that, for a radiopharmaceutical to reach its organ of interest (the kidney), there must be minimal competition between ^{99m}Tc and the metal ions for ITB. If complexation between ITB and blood plasma metal ions occurs, it should not be at the physiological pH 7.4, because side effects resulting from mobilisation of metal ions from blood plasma may occur. Furthermore, interference with renal imaging may result.

Metal ions in biological systems are often in a state of equilibrium between two different oxidation states. The lower state can be stabilized symbiotically by adding soft ligands and the higher oxidation state by adding hard ligands. However, if we add very soft or very hard ligands, the metal ions will be completely anchored in one oxidation state and so the living process will be prevented. This is called poisoning. Well-known poisons are usually acids and bases which are strongly held, to the active sites of an enzyme, hence causing blockage.

Soft acid poisons bind strongly to sulfur groups and rob the organism of sulfur containing proteins such as those involving cysteine residues. On the other hand, soft base poisons, function by robbing the body of metal ions. At low

concentrations, these poisons act by blocking as they attach to the metals in metalloporphyrins and other metallo-enzymes. At high concentrations, they remove the metal ion entirely from the protein. This is when complexation results in precipitate formation [5].

By modifying the chelating ligand, the coordination sphere around the metal is charged and *in vivo* targeting can be adjusted in the complex. *In vivo* targeting can be achieved by manipulating the properties of a carrier molecule to determine biological distribution.

Several radiopharmaceuticals have been used to define renal anatomy and evaluate kidney function. The mercury compounds such as $^{197}HgCl_2$ and ^{203}Hg – chloromerodrin have not gained wide acceptance due to the low photon energy of ^{197}Hg (62-77 keV) and the comparatively high radiation dose to the kidney. The relative renal accumulation of the cortical imaging agent ^{99m}Tc- penicillamine (TPEN) has been shown to correlate with the relative creatinine clearance and effective renal plasma flow, but TPEN is not commercially available hence cannot be widely used.

^{99m}Tc-dimercaptosuccinnic acid (DMSA) is also an excellent cortical imaging agent, which permits accurate comparison of relative cortical accumulation without interference by pelvocalyceal activity. Animal studies *in vitro* have shown good correlation between the relative renal blood flow and subsequent reports have suggested that the relative renal uptake of DMSA *in vivo* correlates well with relative function [6]. However, some disadvantages are to be discussed below, regarding rate of uptake and radiation dose.

During recent years, ^{99m}Tc-MAG_3 (mercaptoacetyltriglycine) has gained wide acceptance because of its high extraction compared to any glomerular tracer. It has been proposed for overall clearance measurement. However, the purpose of clearance measurements is also to monitor renal function and to appreciate any change in function related to disease or treatment [7].

Investigational studies have also been done on certain ligands, in order to

establish their behavior when used as renal radiopharmaceutical agents. These include nitrogen bidentate donors such as biguanide and corresponding N1-substituted ligands [8]. These ligands have the ability to coordinate transition metals. The metallic ions are coordinated through the two imino groups.

Biguanides have gained attention for their hypoglycaemic activity and in particular metformin (1,1 dimethylbiguanide) is an antidiabetic medication, which has been used for more than 30 years. These classes of compounds have also been studied as antimalarial drugs and more recently for therapeutic treatment of pain, anxiety and memory disorders [9].

^{99m}Tc-biguanide (^{99m}Tc-Big) has shown the highest activity ratio for kidney or liver in mice due to its neutral oxo complex. Comparative studies were done with ^{99m}Tc-DMSA (Dimercaptosuccinic acid) to evaluate ^{99m}Tc-Big as a potential renal imaging agent. It was found out that, ^{99m}Tc-Big was cleared more quickly than ^{99m}Tc-DMSA and for the same acquisition times, the contrast in the whole body favoured ^{99m}Tc-Big.

It was also shown that, the estimated radiation dose absorbed by the kidneys and blood for ^{99m}Tc-DMSA, was significantly higher than for ^{99m}Tc-Big. These preliminary studies show that ^{99m}Tc-Big has favourable practical and dosimetric features for renal imaging as an alternative to ^{99m}Tc-DMSA. Although ^{99m}Tc-DMSA is the renal radiopharmaceutical currently used, it presents some disadvantages in terms of clinical applications. The best contrast imaging is achieved several hours after administration and the slow excretion leads to relatively high radiation dose.

Although a number of ^{99m}Tc complexes have been proposed as potential radiopharmaceuticals for morphological renal imaging, ^{99m}Tc-DMSA is widely recognised as the best radiopharmaceutical for kidney imaging, despite its limitations, such as long times to reach optimal renal uptake and the resulting radiation dose. Therefore, a new radiopharmaceutical that could reach a

peak uptake rapidly and clear quickly would represent a significant advantage for patients and for daily nuclear medicine practice [8], hence the purpose of this research. Here, a sulfur donor derivative of biguanide will be investigated.

Thiol groups have a well-known high affinity for binding to technetium. However, the high sensitivity of thiols for oxidation and problems during synthesis of thiol-containing ligands have encouraged the search for other technetium-binding functional groups as well [10].

1.2 Research Objective

The main idea of this research is to model the *in vivo,* blood plasma behavior of a ligand, 2-imino-4 thiobiuret (ITB), which can potentially be used for kidney imaging and renal function determination with the radiopharmaceutical agent, $^{99\,m}Tc$. It has been shown that ^{99m}Tc is well complexed by ITB at physiological pH 7.4 [4].

Blood plasma contains a host of ligands and metal ions, which can compete with ITB and ^{99m}Tc respectively in the radiopharmaceutical. Therefore, formation constants of important blood plasma metal ions such as Ca^{2+}, Mg^{2+}, Zn^{2+}, Cu^{2+} and Ni^{2+} will be measured potentiometrically. This enables prediction of side effects such as mobilisation of blood plasma metal ions by the ligand. Furthermore, selectivity of the ligand for ^{99m}Tc over blood plasma metal ions should become apparent.

The stability of the complexes *in vivo* and their biodistribution will be predicted by speciation modeling using the program ECCLES. Constants obtained will be introduced into a thermodynamic model of blood plasma, ECCLES, to calculate the speciation of metal ions of interest in the presence of the ligand. This information will be used in predicting the *in vivo* behaviour of the radiopharmaceutical agents.

1.3 Project Justification

Metal radionuclides are suitable in production of radiopharmaceuticals that can be used for diagnostic and therapeutic purposes. These have to be incorporated with ligands such as ITB and they must reach their target organ intact and remain stable for the residence time after administration [1].

Radionuclides such as ^{99m}Tc, ^{67}Ga, ^{123}I, ^{131}I and ^{186}Re when complexed with certain ligands, act as imaging agents. The most widely used agents for kidney imaging includes complexes with ligands such as DTPA, MAG_3, DMSA, Glucoheptonate, Dimethyl Ethyleneimine Phenol [DEn $(IP)_2$], Ethylene Dicysteine, ECMA, HAG_3, DACH. [1].

Several radiopharmaceuticals have been used to display renal anatomy and to estimate individual renal function. The search for a single agent that could perform both of these tasks has had a limited success. Mercury-labeled compounds were used in the past but even before introduction of ^{99m}Tc labeled pharmaceuticals, the mercury agents had not gained wide acceptance. This is because, the 6277 keV energy of ^{197}Hg is poorly suited to gamma cameras, ^{203}Hg has unfavourable dosimetry and both required 24-48 hours delay before scanning [11].

^{131}I Orthoidohippurrate (OIH), ^{99m}Tc-MAG_3 and ^{99m}Tc-N,N'-ethylene-di-L-cysteine (EC) are useful radiopharmaceuticals for evaluating renal function. The radiation characteristics of ^{99m}Tc are superior to those of ^{131}I, however the renal clearances of the ^{99m}Tc agents are less than that of OIH. Previous attempts to develop a ^{99m}Tc agent with a clearance that more closely approaches that of OIH have included variations of CO_2 groups of the EC ligand [12].

There are different radiotracers used under various conditions. These include the following;

Iodine-123 and Iodine-131 Hippuran (also called OIH [orthoiodohippurate]) are primarily renal function agent, useful in renal insufficiency for evaluation of function, visualization of the collecting system.

Technetium-99m glucoheptonate is most useful as a combination renal cortical imaging agent and renal function agent, used to evaluate overall function, but can be used for vascular flow and to visualize the renal parenchyma and collecting system.

Technetium-99m DMSA (Dimercaptosuccinnic acid) is used only as renal cortical imaging agent.

Technetium-99m DTPA (Diethylenetriaminepentaacetic acid) is used primarily as an imaging agent for renal blood flow studies and estimation of glomerular filtrate rate (GFR).

Technetium-99m MAG_3 is regarded primarily as a renal function agent with imaging capability. It is similar to hippuran but radiation dose is lower than that of hippuran. MAG_3 (Mercaptoacetyltriglycine) is reportedly more accurate with very poor renal function [13].

Technetium-99m EC (Ethylene dicysteine) suitable for clearance determinations, providing an index of tubular function. It is also ideal for measurement of ERPF [14].

Conflicting results have been expressed regarding reproducibility in ^{99m}Tc-DMSA planar renal image interpretation. An investigation to determine the level of interobserver variability among a large group of Belgian Nuclear Medicine physicians, who evaluated a randomly, selected samples of ^{99m}Tc-DMSA planar studies performed on children and adults has been carried out [15]. All patients were imaged on a digital γ camera computer system equipped with a low energy, high resolution, collimator (Elscint SP4 [Elschint, Haifa, Israel] or Sopha DSX Rectangular [Sopha Medical Vision, Buc,

France]). Scintigraphy was done 2-4 hours after injection of ^{99m}Tc-DMSA. The adult dose was 110 MBq (3mCi). The doses administered to the children were reduced according to guidelines of the European Pediatric Task Group. Examinations were done with patients in the supine position; collimator sides up, while the children were positioned directly on the collimator. The total acquisition time per image was variable. The age of the patient may play a role and reproducibility may be different in infants, older children and adults.

Some investigators have reported good interobserver reproducibility, whereas others considered that reproducibility was poor. These major divergencies are not surprising because of a large number of factors that may affect reproducibility [15].

^{99m}Tc has been the most widely used in imaging agents. The reason for this is that the behavior of ^{99m}Tc is known and it has shown some good results in the past [1]. ^{99m}Tc has been successfully used in radiopharmaceuticals as a non-invasive diagnostic agent. ^{99}Tc was first discovered in 1937 by Perrier and Segre. Two years later, ^{99m}Tc was discovered [16]. ^{99m}Tc is a labelling agent with low radiation dose and specially designed for the study of different specific parameters, such as renal parameters. The extensive search for a suitable renal radiopharmaceuticals can be understood from the view point that the kidney is vital organ responsible for the maintenance of composition of blood and extracellular fluid and thus deserves optimal diagnostic agents for its evaluation [17].

Because of the excellent imaging and low patient radiation dose of ^{99m}Tc, as well as its wide spread availability and low expense, it is the radionuclide of choice for procedures requiring short to medium time period [18].

The near ideal radionuclide characteristic of the ^{99m}Tc isotope makes it the isotope of choice for diagnostic nuclear medicine procedures. ^{99m}Tc has the advantage of a relative short half-life ($t_{1\backslash 2}$) of 6.02 hrs to permit the preparation of the radiopharmaceutical, the administration of it to the patient and to collect sufficient data to obtain meaningful images. ^{99m}Tc emits gamma radiation of

140 keV, which is sufficiently high to penetrate from deeply seated organs and is easily collimated and detected externally to the patient [1].

^{99m}Tc presents no contaminant beta – emission and it emits only low-energy auger electrons that minimize the absorbed radiation dose to the patient. The beta emissions resulting from the daughter isotope, ^{99}Tc, correspond to a negligible radiation dose to the patient while ^{99m}Tc is conveniently and effectively available on a daily basis from ^{99}Mo/ ^{99m}Tc generators [1].

The optimal imaging properties of ^{99m}Tc combined with the agent that has biological properties similar to PAH in animals can allow the clinician to study renal morphology, function and blood flow in a single non-invasive study. For instance, ^{99m}Tc-glucoheptonate and ^{99m}Tc-DMSA are adequate for morphologic evaluation. However, ^{99m}Tc-DMSA has a limitation of taking a long time to reach optimal renal uptake, which result in high radiation dose. Also, ^{99m}Tc-DTPA offers both functional and morphologic information and has been used in place of ^{131}I-OIH owing to its better radionuclide characteristics. However, owing to its rapid clearance, the morphological information remains inadequate. ^{99m}Tc-MAG_3, having similar properties to ^{131}I-OIH, has recently been introduced, and found to be more useful than DTPA or OIH. Unfortunately ^{99m}Tc-MAG_3 is quite expensive and is not readily available [19].

Therefore, much room is present for more improved kidney imaging agents. Consideration of ^{99m}Tc with a ligand giving rapid uptake and imaging followed by rapid clearance is highly desirable.

CHAPTER 2 LITERATURE REVIEW

2.1 The Kidney

2.1.1 Renal Physiology

The human body relies primarily on the kidney to maintain a constant osmolarity and concentrations of the predominate cations and anions. It also facilitates a constant pH, as well as excretes a number of metabolic products [19].

Kidneys are crucial for the body's urinary system. Their primary function is to detoxify the blood stream, filtering out impurities and waste products through tiny filters called nephrons. Each kidney contains about a million nephrons, within which tiny blood vessels called capillaries are intertwined with minute waste-carrying tubes called tubules. Wastes collected by these filters are passed on to the bladder through tubes called ureters, where they are excreted in the form of urine [20].

Kidneys have to eliminate end products of body metabolism. Furthermore, they have to maintain the balance of many constituents of the body fluids. In order for this purpose to be accomplished, three mechanisms must occur:

(i) glomerular filtration
(ii) tubular absorption
(iii) tubular secretion

For studying renal function, one can use radiopharmaceuticals that are eliminated by glomerular filtration, tubular secretion or by tubular fixation [21].

The most important concept in studying the kidney is recognition of the intimate relationship between structure and function. Among the clearance methods, the continuous infusion technique has been and continues to be a major method for investigational studies where accurate and precise

measurements of renal function are needed. The single injection clearance methods offer the great advantages of simplicity, ease of performance, low radiation dose and reasonable accuracy [22].

The kidneys through glomerular filtration (20%) and tubular secretion (80%) remove paraaminohippuric (PAH) acid. During a passage through a normal kidney, roughly 90% of the PAH is eliminated with the remaining amount returned to the circulation [19].

Kidneys also produce three important hormones, erythropoietin (EPO) which triggers the production of red blood cells in bones, renin, which regulates blood pressure, and vitamin D, which helps regulate the body's calcium balance necessary for healthy bones [20].

Life is greatly dependent on the equilibrium of the aqueous internal environment in which the cells of the body live and carry out their activities. This balance is achieved by the excretory and regulatory function of the kidneys as they regulate volume and composition of the extracellular fluid compartment. To perform this dual function the kidneys each contain approximately 1.3 millions structural and functional units termed nephrons.

The basic physiologic role of the nephron is to remove certain substances from blood plasma as it passes through the specialized vascular bed surrounding the nephron. In particular, excess water, metabolic end products (such as creatinine, urea, uric acid, sulfates, and phenols), as well as excess electrolytes (e.g. Na^+, K^+, and Cl^-) must be removed from the body.

The two basic mechanisms by which these processes are accomplished are:

(i) A large fraction of the total body fluid of the plasma passing through the glomerulus is filtered through the glomerular membrane and the visceral (inner) layer of the capsular epithelium into the capsular space (Bowman's space) of the nephron.

(ii) As this ultrafiltrate of plasma passes through the tubules, unnecessary materials are not reabsorbed. Substances required by the body, especially water, glucose and many electrolytes, are reabsorbed selectively into the plasma of the peritubular capillaries.

Thus, urine represents an aqueous solution of various materials rejected by the tubules of the nephron [23].

Evaluation of renal function requires the determination of the glomerular filtration rate (GFR) and in some cases of the effective renal plasma flow (ERFP) [24]. The standard techniques for determination of these parameters necessitates continuos intravenous administration of substances (Inulin and PAH), multiple urine collections, repetitive blood sampling and rather elaborate chemical analysis of plasma and urine specimens [25].

Creatinine clearance, very commonly employed as a measure of renal function, has significant limitations. It may often over or underestimate GFR, depending on the level of renal and tubular function. It is insensitive to early changes in the GFR and is subject to large errors due to the variability of tubular excretion of creatinine and to the difficulty in measuring the "true" level of endogenous creatinine free from non-creatinine chromogens as well as in obtaining complete urine collection. Furthermore, these techniques do not allow measurement of unilateral renal function without invasive ureteral catherization [25].

According to Woolfson et.al [26], a gradual increase in tubular secretion of creatinine, coupled with the difficulty in ensuring accurate 24 hour urine collections in patients with chronic renal failure means that, sequential creatinine clearance measurements can be misleading and emphasises the need for more definitive measurement. Although there is a close relationship between ERPF and glomerular filtration rate (GFR), it is easier to estimate the latter and inulin clearance is the most accurate.

Para-Aminohippurric acid is completely secreted by the kidney and allows for the most accurate estimation of renal plasma flow. However, the technique is laborious and ^{131}I-hippuran (^{131}I-HIP), which is almost exclusively secreted by the tubule with a clearance of 83% of that of para-aminohippuric acid, can be used in its place. Although handled like HIP, the clearance of ^{99m}Tc - mercaptoacetyltriglycine (^{99m}Tc-MAG_3) is 30% - 40% less due to increased protein binding, lower extraction and a smaller volume distribution. Effective renal plasma flow (ERPF) can be derived from MAG_3 clearance data but MAG_3 actually provides more important information about tubular function, which given the importance of tubulo-interstitial injury as a prognostic determinant, could be developed into a useful measurement [26].

The procedure for the determination of ERPF requires continuous intravenous injection of para-aminohippurate (PAH), complete urine collection and repetitive blood sampling. Measurement of kidney function with ^{131}I-orthoiodohippurate (^{131}I-OIH) has been investigated in the past by several authors including Schlegel and Hamway who proposed a camera-based technique to measure ERPF. ^{123}I-OIH has been introduced into nuclear medicine and possess several advantages over ^{131}I-OIH. This is because of the appropriate physical half-life, gamma ray energy and lack of beta emission, though ^{123}I-OIH is less practical due to its high cost and short shelf life [24].

^{131}I-OIH, although having similar biological properties as those of PAH, is suboptimal due to the use of the ^{131}I radiolabel. ^{131}I emits a 364 keV γ-photon, which results in poor spatial resolution and a β-particle, thereby increasing patient radiation dose to a significant extent. ^{123}I was introduced in place of ^{131}I to reduce these radionuclic problems. ^{123}I–OIH has better imaging properties due to its 159 keV γ-photon. Furthermore, the lack of beta emission reduces the radiation to the patient and allows the administration of higher doses, subsequently leading to a higher photon flux and enhanced spatial resolution. However, ^{123}I-OIH is not used in nuclear medicine due to

its 13 hours half-life and its relatively high cost [19]. Its half-life is longer than that of ^{99m}Tc whose labeling kits makes it (^{99m}Tc), to be a better agent.

The ability of molecules to be filtered depends on shape or charge with elongated, flexible molecules filtered more easily than spherical and neutral or positively charged molecules passing through more easily than anionic. Plasma proteins, such as albumin and transferrin and antibodies are too large to be filtered, and thus are retained in plasma. Many drugs and small molecules are bound to plasma proteins. The fraction in the plasma bound to these proteins effectively assumes the molecular weight of protein plus the small molecule. Thus, such small molecules are filtered at the glomerulus. An important criterion for potential radiopharmaceuticals for the measurement of glomerular filtration rates (GFR) is that they are bound to plasma proteins.

The principal segments of the nephron involved in the handling of renal radiopharmaceuticals are the glomerular capillaries and proximal tubular cells. The kidneys of a resting adult receive each minute approximately 1.25 litre of arterial blood, just under 25% of the cardiac output, via the afferent arterioles of the juxtamedullary and cortical nephrons. From this amount 16% to 20% is filtered by the glomeruli, a tuft of capillaries invaginated into the Bowman's capsule, the blind end of the nephron [17].

The permeability of these capillaries is 50 to 100 times that of the capillaries in the skeletal muscle. The resulting ultrafiltrate of blood has a similar composition to plasma except for the extremely low concentration of lipids and proteins with a molecular weight over 70,000 daltons for which glomerular filtration is minimal [17].

Cells lining the nephrons extract materials such as glucose, amino acids and water from the filtrate and return them to the blood in the reabsorption process. In addition, these cells extract materials from the blood and secrete them into urine. What begins as about 180 litres per day as filtrate ends up as 1 to 2 litres of urine [18].

2.1.2 Renal Anatomy

The renal arteries supplying blood to the kidneys, branch into arcuate and then interlobular arteries, and final branching results in afferent arterioles that supply blood to the glomeruli where plasma filtration takes place. After passing through the glomerular bed, the blood passes to a second peritubular capillary bed via the efferent arterioles.

Most of the efferent arterioles carry the blood supply to the cortex and proximal tubular cells. A small fraction goes to the medulla via bundles of efferent arterioles. This implies that, not all of the renal blood supply, is received by the proximal tubular cells, and compounds secreted in these cells may never be completely extracted in a passage through the renal circulation. This is important in understanding the concept of effective renal plasma flow (ERPR) measurement by secreted radiopharmaceuticals [18].

2.1.3 Renal Cancer

Renal cancer (renal adenocarcinoma or hypernephroma), can often be cured if it is diagnosed and treated when still localised in the kidney and to immediately surrounding tissue. The probability of cure is directly related to the stage or degree of tumour dissemination. Because a majority of patients are diagnosed when the tumour is still relatively localised and amenable to surgical removal, approximately 40% of all patients with renal cancer survive 5 years. Occasional patients with locally advanced or metastatic disease may exhibit indolent causes lasting several years. Late tumour recurrence many years after initial treatment occasionally occurs [27].

It is important to realise that while the kidney cancer is a serious illness, with timely diagnosis and treatment it can be cured. If found early enough, 5 years survival rate for patients with kidney cancer ranges from 79% to 100%, depending upon how early it is diagnosed [20].

2.2 Renal Radiopharmaceuticals

Renal excretion is a likely biodistribution property of molecules with a molecular weight less than 300 to 400. It is not surprising, therefore, that a large number of radiolabelled compounds have been proposed as renal radiopharmaceuticals. Most of them suffer from insufficient specificity and or lack of efficiency for renal excretion. Many are partially retained by the kidneys and thus exhibit multiple processes of renal excretion. In general, radiopharmaceuticals must have high specificity in both normal and diseased conditions. In addition, renal radiopharmaceuticals should reflect a single pathway so that quantitative measurements can be made in a simple manner [18]. Renal function studies with radionuclides are based on the physiological conditions of the renal excretion mechanisms and radiopharmacology [21].

Renal imaging agents are used to evaluate the anatomy and function of the kidneys. The performance of the kidney depends on its ability to carry out its three interrelated excretory, regulatory and endocrine functions. While the anatomy of the kidney can be determined with equal or greater resolution using X-rays, CAT scan, MRI or Ultrasound, its excretory function is most easily assessed by radio-scintigraphy. Small ionic scintigraphic agents are eliminated from the blood by the kidneys and are readily monitored by sequential camera images [18].

2.3 Technetium -99m (^{99m}Tc)

The most common type radioactive materials used in nuclear medicine are gamma ray emitters such as ^{99m}Tc, ^{67}Ga, ^{123}I, ^{201}Tl. These radionuclides can be quantified when localized within the body with modern instrumentation. Radiopharmaceuticals can be administered orally, intravenously or through intracavitary routes and they usually deliver lower doses of ionizing radiation than alternative radiographic technique [28].

The superior physical properties of ^{99m}Tc led to the evaluation of many chelating agents as potential radiopharmaceuticals. The kidneys

indiscriminately excrete low molecular weight polar compounds. Thus, many of the ^{99m}Tc chelates were excreted by the kidneys and were then proposed as ^{99m}Tc renal radiopharmaceuticals. Only a few have had extensive clinical use as ^{99m}Tc complexes that localize in the kidneys in sufficient amounts for static imaging.

^{99m}Tc is now the most widely used radionuclide in the practice of nuclear medicine. There are good reasons for this which include the following:

(i) Availability

The ^{99}Mo – ^{99m}Tc nuclide generator is an excellent source of ^{99m}Tc with half-life of 6.02hours. The half-life of ^{99}Mo is 67hours. The efficient column generator with alumina packing requires the use of irradiated enriched ^{98}Mo or "fission moly". However, the methylethyl ketone (MEK) liquid-liquid extraction system makes possible the use of natural molybdenum in the neutron activation process.

(ii) Physical characteristics

^{99m}Tc has excellent imaging characteristics for both gamma cameras and for rectilinear scanners. The radionuclide decays by internal transition.

(iii) Convenience

^{99m}Tc-pertechnetate is eluted in sterile, pyrogen-free saline; additional products are easily prepared because of simple chemistry and laboratory procedures. Commercially available synthetic kits add to the simplicity of preparing safe and effective labelled compounds.

(iv) Cost

^{99m}Tc-labelled compounds are now among the least expensive of radiopharmaceuticals and have a very high value-to-cost ratio.

(v) Radiation dose

The radiation dose to the patient from ^{99m}Tc-compounds is low despite the statistically significant large number of photons available [29].

Most of the ^{99m}Tc-complexes discussed above have been reported to show significant uptake and retention in the kidneys and were proposed as potential radiopharmaceuticals for morphological kidney imaging or determination of functional renal mass.

These agents include complexes of ^{99m}Tc with polyalcohols, hydroxyacids, mercapto acids, polypeptides, antibiotics and phosphonates. None of these is taken up in the kidneys entirely and considerable variation is noted in the rate and degree of uptake and duration of retention between various agents. Most of these complexes have been tested in humans and a limited numbers are now in clinical use [17,30].

Each ^{99m}Tc-complex has its own specific properties such as electron donor/acceptor, lipophilicity-hydrophilicity balance, redox potential, pK, chirality and isomerism. These specific properties are the key to molecular recognition by biological molecules. Simulation of molecular interactions between the predicted Tc-complexes and biological molecules is expected to give information at a molecular level, to the specific binding involving these species [31].

2.4 Kidney Imaging Agents

2.4.1 ^{99m}Tc- DTPA

^{99m}Tc-DTPA (Diethylenetriaminepentaacetic acid) (*fig. 2.1*) is taken up by the kidneys and is exclusively filtered by the glomerulus. It is also used to assess renal perfusion and to estimate the GFR. The serial dynamic images after intravenous injection of ^{99m}Tc- DTPA gives information about renal function [32].

^{99m}Tc- DTPA has been shown to behave as a glomerular filtrate agent. The biological properties as well as the physical characteristics of ^{99m}Tc make this a useful agent for diagnostic studies of the kidney. The possibility of using large administered doses while producing a low radiation dose to the patient results in being able to obtain information not possible with most other renal diagnostic agents [33]. ^{99m}Tc-DTPA was found very useful for evaluation of kidney and function with rectilineal scanners and gamma cameras [34].

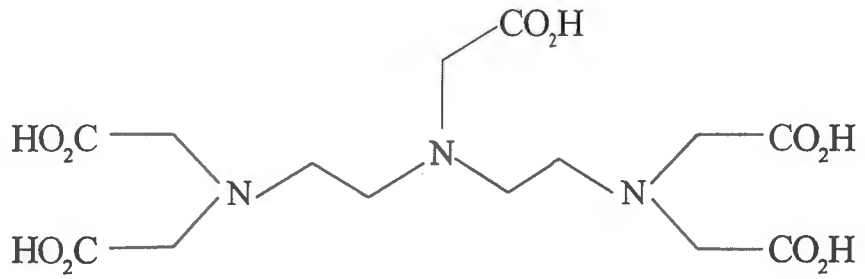

Figure 2.1: *Structure of DTPA.*

According to Taylor, *et.al* [35], ^{99m}Tc-DTPA is known to have excellent physical properties for imaging and gives a low radiation dose per imageable photon. While these characteristics permit rapid imaging during the first circulation to evaluate renal extraction efficiency of ^{99m}Tc-DTPA and other ^{99m}Tc renal agents may result in low target to background ratio and non-diagnostic images in patients with impared renal function [35].

When compared with ^{99m}Tc-EDTA, studies have shown ^{99m}Tc-DTPA to be more suitable for renal function due to its lower protein binding and high stability. However, studies showed that values reported for its stability constant range from 10^{17} to 10^{26}, which allow us to suppose that, complexes with different structures were involved in the respective determinations. Because of the far more favourable imaging and dosimetry characteristics of ^{99m}Tc, the continuous availability and the ease of preparation, ^{99m}Tc-DTPA is currently the agent of choice for radionuclide imaging clearance studies.

The rapid renal excretion of ^{99m}Tc-DTPA and its initial high renal uptake permit both static and dynamic imaging studies and a number of additional renal parameters can be assessed with this widely used renal radiopharmaceutical [36].

2.4.2 ^{99m}Tc- DMSA

^{99m}Tc-DMSA (Dimercaptosuccinic acid) (*fig. 2.2*) is used for imaging the morphology of the renal cortex.

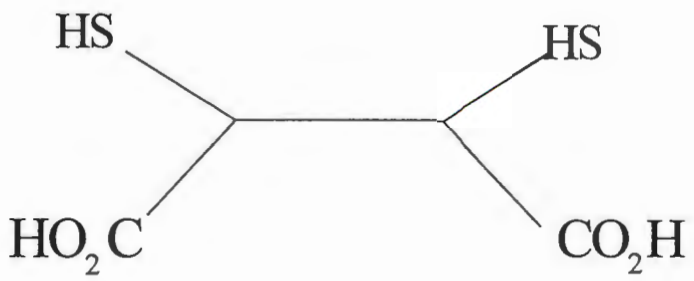

Figure 2.2: *Structure of DMSA.*

After intravenous injection, the agent is substantially bound to the protein and is thus not filtered by the glomerulus. After entering the kidney, it localizes in the cortex. It accumulates in the renal cortex and demonstrates functioning renal cortical mass [37].

2.4.3 ^{99m}Tc-MAG$_3$

^{99m}Tc-MAG$_3$ (Mercaptoacetyltriglycine) (*fig. 2.3*) is used as a renal imaging agent to assess renal function by monitoring agent passage into and through the kidney. The tracer is rapidly excreted by active tubular secretion [38].

Like ^{131}I – hippurate, MAG$_3$ is rapidly secreted by the renal tubules and a good correlation between hippurate and MAG$_3$ clearance has been found. Despite a lower extraction fraction of MAG$_3$, it seems possible to use it for determination of the effective renal plasma flow (ERPF) [39,40].

Because of the ^{99m}Tc label, MAG$_3$ provides superior image quality than ^{131}I–OIH and substantially less radiation to the patient in individuals with impaired renal function. The clearance of MAG$_3$ is proportional to the effective renal plasma flow (OIH clearance) and can be used as an index of renal function.

The favourable dosimetry and superior clinical applications of ^{99m}Tc-MAG$_3$ have resulted in an increased clinical use since its introduction in 1992 so that it now accounts for approximately 40% of the estimated 420,000 renal scans performed annually in the United States.

Although ^{99m}Tc-MAG$_3$ is regarded as the agent of choice for the renal imaging, there are significant differences between the biological behaviours of^{99m}Tc-MAG$_3$ and OIH. The plasma protein binding of Tc-99m-MAG$_3$ is relatively high and its plasma clearance in humans is about 65% of OIH. For this reason, the accurate renal plasma flow estimation with ^{99m}Tc-MAG$_3$ is relatively difficult. These problems have led to the search for other ^{99m}Tc labeled renal tubular function agents which would provide a direct measure of effective renal plasma flow (ERPF) [41].

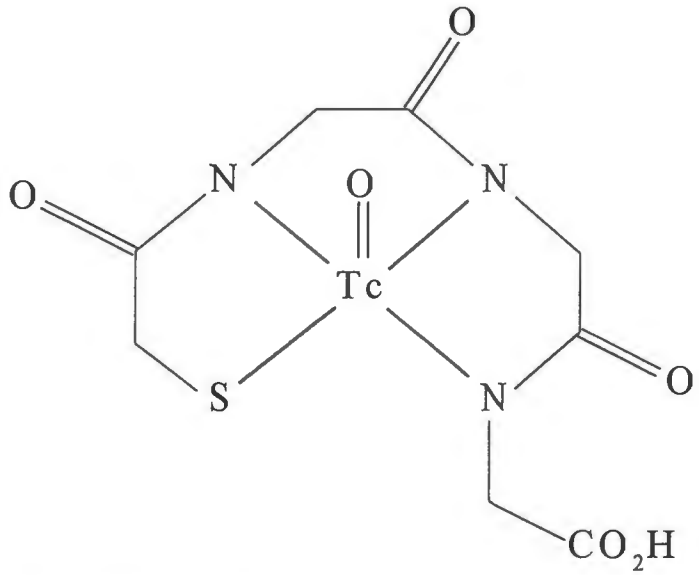

Figure 2.3: *Structure of Tc-MAG$_3$ complex.*

Camera-based clearance techniques are available commercially to measure the glomerular filtration rate (GFR) using ^{99m}Tc-DTPA and effective renal plasma flow (ERPF) using OIH. A preliminary camera-based technique to determine MAG_3 clearance has been introduced and appears to give good results. An accurate measurement of renal clearance requires a precise background correction. In this respect, MAG_3 has an inherent advantage over DTPA because the kidney extracts it much more efficiently. In normal volunteers, for example the 2 - 3 min renal uptake of MAG_3 was almost twice as great as the 2 – 3 renal uptake of DTPA [42].

All radiopharmaceuticals labeled with gamma emitting radionuclides of appropriate energy will provide imaging information. Agents that are primarily intended to produce anatomic rather than GFR or ERPF information are those that are retained by the kidney. Thus, the objectives for the development of this class are to produce an agent that results in a large fraction of the administered dose being retained with high specificity within a reasonable period.

Based on the observations of Paracelsus in the 16th century that the calomel (mercury chloride) caused diuresis, radiomercury compounds were

investigated as renal imaging agents by McAfee and Wagner in 1960. While up to 40% of administered radiomercuric chloride was retained by the kidneys both radiomercury alternatives. ^{197}Hg and ^{203}Hg have poor physical properties that limited their use [15].

Preparations which include ^{99m}Tc-Fe-ascorbate and ^{99m}Tc-Fe-ascorbate-diethylenetriamine penta-acetic acid (DTPA), known as Renotec behaved similarly with about 15% of the administered dose localizing in the kidneys. The use of sugar acids, gluconate in Australia and glucoheptonate (developed by New England Nuclear, North Billerica, MA) in the United States, formed more superior complexes with ^{99m}Tc and are still used.

2.4.4 ^{99m}Tc- Glucoheptonate

Various radiotracers such as ^{99m}Tc glucoheptonate (^{99m}Tc-GH) (*fig 2.4)* are known to concentrate in normal renal parenchyma. Both benign and malignant neoplasms are almost invariably shown to be non-functional in the delayed static scans using these renal radiotracers, while dynamic scintigrams (tracer angiograms) may demonstrate hypervascularity. A benign neoplasm such as oncocytoma could not be differentiated from malignant carcinoma by scintigraphy in the past. The only renal tumor that concentrates ^{99m}Tc-GH (glucoheptonate) consistently is neophroblastic nephromas in neonates [43].

^{99m}Tc-glucoheptonate is rapidly cleared from the blood with about 12% remaining after 1hour in humans. Early kidney values of over 15% at 15 minutes decrease to 10% by 1hour. Despite the relatively low fraction of the dose retained in the kidneys, the rapid blood disappearance and low levels found in other tissues allows ^{99m}Tc-glucoheptonate to provide useful image [15].

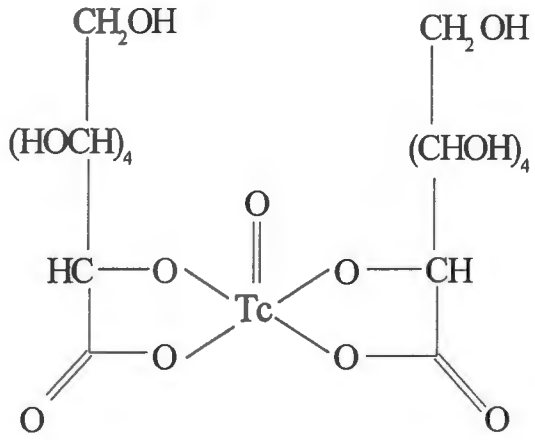

Figure 2.4: *Structure of Tc-Glucoheptonate complex.*

The ^{99m}Tc-DMSA complex, acts like the radiomercuric compounds. About 40-50% of it reaches its destination (kidneys) in 1hour after injection. Although the specificity of ^{99m}Tc DMSA is higher than that of glucoheptonate, the blood disappearance (30% remaining in the blood at 1hour) and the kidney uptake are slow processes. Thus, 3 hours post injection is the typical delay before imaging. A large fraction of ^{99m}Tc-DMSA binds to plasma proteins and thus is not available for filtration [15].

Early investigations on ^{99m}Tc-DMSA filtration were based on *in vitro* determination of ^{99m}Tc-DMSA protein - binding and the assumption that the nonprotein-bound portion of ^{99m}Tc-DMSA appears in the ultrafiltrate. Not only is this approach indirect, but the amount of bound protein varies considerably in different studies, as does the amount of estimated, nonprotein-bound, filtered ^{99m}Tc-DMSA. In order to determine how much ^{99m}Tc-DMSA is filtered and reabsorbed in the kidney, a direct approach of micropunture and microperfusion techniques were used. Control experiments were performed using ^{99m}Tc-DTPA, which is handled like Inulin *i.e.* without tubular transport or ^{99m}Tc pertechnetate, which serves as an indication of proximal tubular reabsorption.

According to Muller-Suur et.al [44], the results obtained showed that low fractions of ^{99m}Tc-DMSA entered the tubular lumen by glomerular filtration, and, ^{99m}Tc-DMSA in the tubular lumen is not actively or passively reabsorbed by the tubular epithelium. The following were also noted, ^{99m}Tc-DMSA is highly bound to plasma proteins in the circulating blood after injection and penetrates the glomerular filter at very low rates. The amount of ^{99m}Tc-DMSA present in the tubular system is completely excreted and not reabsorbed from the tubular fluid. Peritubular extraction must account for the uptake of ^{99m}Tc-DMSA in the proximal tubular cells of the renal cortex. ^{99m}Tc-DMSA is then bound to the plasma proteins, presumably with high binding constant and not further removed *i.e.* it accumulates with time in the kidney [44].

Despite the technical concerns, ^{99m}Tc- DMSA has proven to be clinically useful. High-resolution images, which facilitate quantifitation of renal mass, are obtained [15].

Radiopharmaceuticals such as ^{131}I-Orthoiodohippurate, is cleared from the plasma by glomerular filtration (~20%) and tubular secretion (~80%) with a total extraction efficiency by normal kidney of 70-90%. Unfortunately ^{131}I-OIH has poor imaging properties, a high radiation dose per imageable photon, and therefore it cannot be used to image renal perfusion [36].

2.4.5 ^{99m}Tc-EC

Verbruggen et.al pioneered the development of a new ^{99m}Tc labeled radiopharmaceutical, L, L ethylene-dicysteine (^{99m}Tc-EC). ^{99m}Tc- EC is a polar di-acid metabolite that is excreted from the kidney by active transport and easily labeled with ^{99m}Tc at room temperature [45].

^{99m}Tc-EC, a metabolite of ethylene cysteine dimer (ECD), is a new technetium labelled renal tubular function tracer which has been introduced as an alternative to ortho-iodohippurate (OIH) and with imaging qualities similar to ^{99m}Tc- MAG_3. There are several isomeric forms of ^{99m}Tc-EC, including the L, L isomer (*fig 2.5)*; the D, D isomer (*fig 2.6)*; and the D, L isomer (*fig 2.7)*.

Among them, the D, D form was found to have the highest extraction efficiency and clearance rate and thereby the greatest imaging potential. ^{99m}Tc-EC is a diamine dithiolate (N_2 S_2) complex and has similar molecular size to OIH. The carbonylglycine sequence of OIH is assumed to play a major role in its interaction with the transport proteins in the kidneys. It is therefore interesting that ^{99m}Tc-EC does not contain the carbonylglycine moiety which reconstitutes the side chain of OIH. Although the transport mechanism of ^{99m}Tc-EC remains to be determined, it is assumed that oxo technetium glycine structure of ^{99m}Tc-EC mimics the carbonylglycine moiety of hippuran and that the oxo technetium glycine structure fits with the tubular receptor proteins. Because of its low protein binding, ^{99m}Tc-EC is probably filtered by the glomeruli in substantial quantities.

The elimination of ^{99m}Tc-EC is principally via tubular transport. It is available in lyophilised kit form, which can be easily prepared at room temperature, but the compound remains stable for at least 8 hours. Both in normal individuals and patients, plasma clearance of ^{99m}Tc-EC has been reported to be around 0.75 of OIH clearance. The renal extraction ratio of ^{99m}Tc-EC is 0.70. The distribution volume of ^{99m}Tc-EC is twice that of ^{99m}Tc-MAG_3 (20% of the body weight) and slightly higher than that of OIH. The plasma protein bound fraction of the ^{99m}Tc-EC (30%) is significantly lower than that of ^{99m}Tc-MAG_3 and OIH.

There is a negligible uptake in liver and intestines. Within 1hour, 70% of ^{99m}Tc-EC is excreted in urine. ^{99m}Tc-EC provides the same scintigraphic information as ^{99m}Tc-MAG_3. The lower liver activity makes ^{99m}Tc-EC particularly attractive in patients with renal failure. The ^{99m}Tc-EC clearance can be accurately estimated from a single plasma sample obtained at 54 minutes after injection. From these observations, it can be deduced that ^{99m}Tc-EC is a suitable renal imaging agent and for some applications, it is even more attractive than OIH as, it provides an index of tubular function and yields high quality images. The extent to which ^{99m}Tc-EC is adopted for clinical use will depend upon its cost and availability [14].

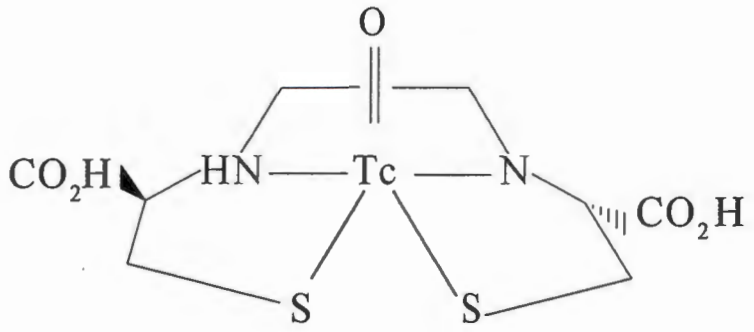

Figure 2.5: *L, L Cysteine isomer.*

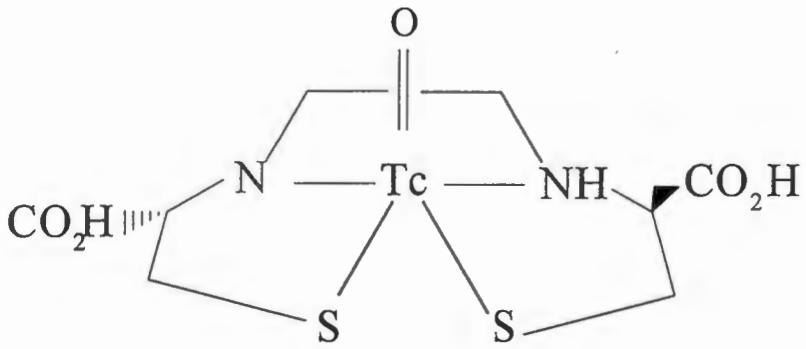

Figure 2.6: *DD-Cysteine isomer.*

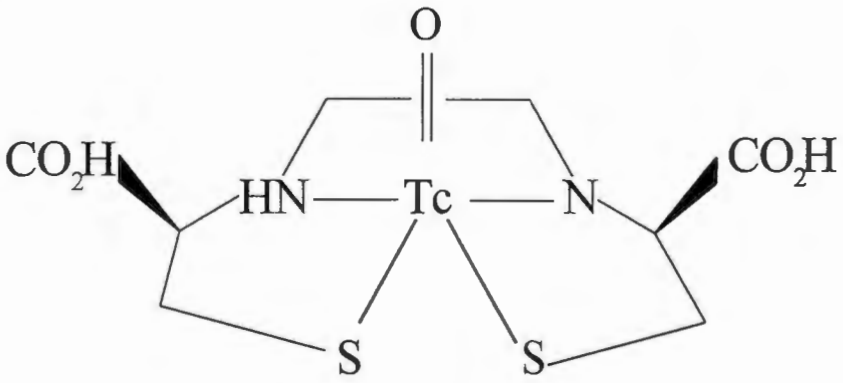

Figure 2.7: *D, L Cysteine isomer.*

Recent studies done by Ai-Yih-Wang [19], on the role of ^{99m}Tc-cysteine complex as a renal imaging agent, showed that renal excretion of ^{99m}Tc-cysteine was lower than ^{131}I-OIH. Approximately 91,8% of ^{131}I-OIH in the kidney is excreted within 60 minutes and only 75% of ^{99m}Tc-cysteine is

excreted within 60 minutes. The radioactivity that was transported to the kidney decreased to 0.35% at one-hour post – injection.

To determine the exact renal pathway of these radiopharmaceuticals, excretion was determined in rats under the influence of probenecid and 2,4 DNP (renal tubular transport indicators). Control results confirmed an obvious decline in renal excretion, the cumulative dose in urine of ^{99m}Tc-cysteine decreased from 84% to 20% (2,4 DNP) or 45% (probenecid) within one hour [19].

In ^{131}I-OIH, it decreased from 84% to 40% (2,4 DNP) or 65% probenecid. These results suggest that both ^{99m}Tc-cysteine and ^{131}I-OIH were eliminated via the renal tubular excretory pathway. Apparently 2,4 DNP influences more prominently the excretion of ^{99m}Tc-cysteine and ^{131}I-OIH than probenecid [19]. These findings imply that the same transport mechanism is utilized for the active secretion of these agents, thereby corresponding to the renal tubular transport enzymes. In overall, these findings suggest that ^{99m}Tc-cysteine can be used to assess renal function in conditions with no impairment of renal function [19].

^{99m}Tc-L, L-ethylenedicysteine (^{99m}Tc-L,L-EC) is a renal tubular tracer based on a bis-aminoethanethiol tetradentate ligand that has recently proven to be a valuable alternative for ^{99m}Tc-MAG_3. In comparison, studies have shown that the imaging properties of L, L –EC appear to be similar to those of MAG_3 [46]. In addition, the time to maximum activity for MAG_3, ^{99m}Tc-L,L-EC and OIH are similar although the time from peak to 50% of peak activity appears to be less for OIH than for the two ^{99m}Tc complexes [47].

With gamma camera studies, it has been shown that ^{99m}Tc-EC has comparable extraction, excretion and renogram patterns with ^{99m}Tc-MAG_3 and OIH. Studies also show that, the renal clearance of ^{99m}Tc-EC was 75% of OIH and it was higher than that of ^{99m}Tc-MAG_3. The higher renal clearance of ^{99m}Tc-EC with respect to ^{99m}Tc-MAG_3 can be attributed to the presence of

glomerular filtration of ^{99m}Tc-EC as a consequence of lower protein binding with higher free fraction and higher distribution volume.

^{99m}Tc-EC not only has the favourable physical characteristics of ^{99m}Tc labeling and simplicity of preparation, but also it seems to have strong potential in providing superior visual and quantitative evaluation of renal function [41]. ^{99m}Tc-EC shows low kidney retention and low liver uptake with rapid urinary excretion through primary route of active tubular secretion. It also provides high quality images [48].

2.4.6 ^{99m}Tc- ECMA

In an effort to develop an improved agent, a new ligand system, N, N' ethylene (cysteine)(mercaptoacetamide) (ECMA), was designed that the combined structural features of both MAG_3 and EC. Two isomers were prepared with D or L-cysteine and labeled with ^{99m}Tc. Biodistribution in rats showed that ^{99m}Tc-ECMA complexes are efficiently extracted by the kidneys (78-79% of the dose found in the kidneys and bladder 30 minutes post injection) with minimal hepatic uptake (5% for L-ECMA, 8% for D-ECMA). The renal clearance and extraction efficiency of ^{99m}Tc-L-ECMA was 93±11% and 102 ± 10% of OIH respectively. Plasma protein binding was 78±8%. The renal clearance and extraction efficiency of ^{99m}Tc-D-ECMA (65±10% and 89 ±10% of OIH respectively) were lower than those of ^{99m}Tc-L-ECMA, plasma protein binding was higher (96 ± 1%) [12].

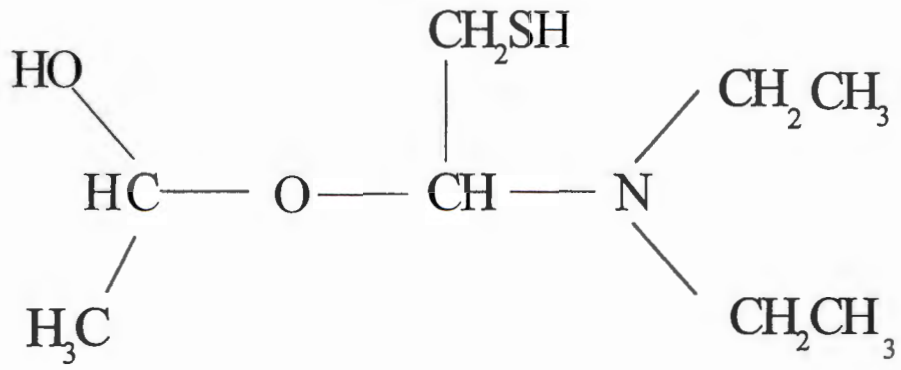

Figure 2.8: *Structure of ECMA*

2.4.7 ^{99m}Tc- HAG_3

Complexes of technetium with hydroxy compounds are much weaker than those with thiol-containing substances. For instance 2,3 dihydroxysuccinic acid (*fig 2.9)* is widely used as a weak chelating agent in exchange labeling reactions with ^{99m}Tc, whereas 2,3 dimercaptosuccinic acid (DMSA) forms stable complexes with ^{99m}Tc and has been used in nuclear medicine for years. Unlike a thiol, an alcohol does not suffer from stability problems in normal handling and storage conditions. Results obtained after using ^{99m}Tc-HAG_3 and ^{99m}Tc-MAG_3 were comparable. Liver uptake was lower for ^{99m}Tc-HAG_3 than for ^{99m}Tc-MAG_3. However, evaluation of ^{99m}Tc-HAG_3 in a human volunteer confirmed its favourable biological characteristics, namely a rapid and high uptake in the kidneys followed by a fast excretion into the urine, a high 1 hour plasma clearance and a low uptake in the intestines. Results also showed that the renogram of ^{99m}Tc-HAG_3 for the volunteer appeared slightly superior to that of ^{99m}Tc-MAG_3.

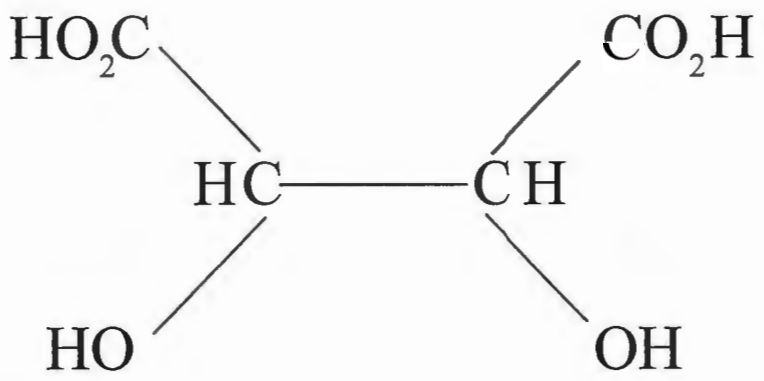

Figure 2.9: *Structure of HAG_3.*

Due to the lower protein binding to plasma proteins, a larger fraction of ^{99m}Tc-HAG_3 can be eliminated by glomerular filtration besides the active tubular extraction. For ^{99m}Tc-MAG_3, glomerular filtration is very limited due to its high (91%) binding to plasma proteins. The results indicate that the HAG_3 may be an easy-to-prepare substitute for ^{99m}Tc-MAG_3 with comparable renal excretion characteristics but lower hepatobiliary handling [9].

2.4.8 ^{99m}Tc- DACH

A new ^{99m}Tc-labeled renal tubular agent called 1,2 diaminocyclohexane (DACH) (*fig. 2.10*) has recently been introduced by Solaki et.al. This is a primary substituted ethylene diamine compound and forms a stable cationic complex with ^{99m}Tc. It is excreted via a cationic transport mechanism, like cyclosporine-a (CsA). Animal and human studies have shown promising results with ^{99m}Tc-DACH for renal imaging. Moreover, the clearance of this agent remained unaffected by pretreatment with the anionic tubular blocker, probenecid, but was significantly retarded by treatment with the cationic blocker, thiamine, confirming that this agent is secreted from tubules by a cationic transport mechanism. As a result, it is hypothesized that this agent could be helpful in the measurement of renal function in patients treated with cationic tubular secreted drugs such as CsA. Studies also revealed that ^{99m}Tc-DACH, a cation with the structure trans $[O_2\ (DACH)_2\ ^{99m}Tc]^+$, has recently been described as a potential alternative radiopharmaceutical to negatively charged tubular agents for renal studies.

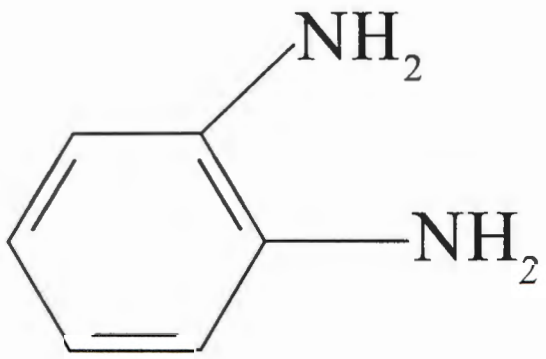

Figure 2.10: *Structure of DACH.*

It was also observed that ^{99m}Tc-DACH gives typical three-phase renograms and high quality images with rapid appearance of the kidneys and low background activity, in concordance with earlier reports. The slight liver uptake seen in the images does not jeopardise reliable calculation of right kidney function [49].

2.4.9 Orthoiodohippurate (OIH)

Radioiodinated orthoiodohippurate (OIH) is considered the principal agent for functional renal studies. Due to its extraction efficiency, it is useful in evaluating patients with impaired renal tubular function. The major disadvantage of OIH labeled with ^{131}I is the high radiation absorbed dose, especially in patients with urinary obstruction and poor scintigraphic image quality because of the high energy of the gamma rays (364 kev). ^{123}I-OIH has better physical characteristics, but the logistical problems and cost of this short lived, cyclotron-produced radionuclide are the major reasons for its limited use in routine clinical practice [50].

2.5 Complexes of ^{99m}Tc, with mercapto acids

A sulfhydryl group is far more nucleophilic than an aliphatic hydroxyl group and therefore the metal-sulfur bond is much stronger than the metal-oxygen bond. Complexes of ^{99m}Tc with mercapto carboxylic acids are relatively stable and more difficult to dissociate than the hydroxy carboxylic acid complexes.

The mechanism of renal accumulation of thiolate-containing tracer agents is not clearly understood. Their affinity for proteins is evident, as shown by their high protein binding in plasma from 82-97%, but knowledge about their exact renal pathway is lacking.

^{99m}Tc-DMSA is currently a routine first choice radiopharmaceutical for quantitative or visual determination of differential renal function. The mean renal uptake of ^{99m}Tc-DMSA at 3hr p.i in normal humans is about 50% of the administered dose, while 10% to 20% is excreted in urine during the first 2 hours after injection. The disadvantage of using ^{99m}Tc-DMSA is that imaging can start only 3-6 hours after administration.

^{99m}Tc-DMSA localizes specifically in the proximal convoluted tubule, where it binds mostly to soluble cytoplasmic proteins and mitochondria, and to a lesser extent to both microsomes and nuclei.

Labelling of DMSA with ^{99m}Tc at pH8 yields a high molecular size polynuclear Tc (V)-DMSA complex that is supposed to contain a $[TcO_4]^{3-}$ core. Its biological characteristics are distinct from those of the renal scanning agent ^{99m}Tc(III)-DMSA, as shown by the negligible renal retention. On the other hand, it exhibits selective tumor-seeking properties and clinical screening has demonstrated its usefulness in the detection and imaging of medullary thyroid carcinoma, head and neck tumors, in particular squamous carcinoma and rhabdomyosarcoma. Convenient methods for the preparation of this interesting ^{99m}Tc-labelled tumor agent have been reported [17].

MAG_3 (Mercaptoacetyltriglycine) has been regarded as one of the best kidney imaging agents. When combined with ^{99m}Tc, it offers high quality renal images and is widely accepted as an excellent renal radiopharmaceutical. The clearance of ^{99m}Tc-MAG_3 is approximately proportional to effective renal plasma flow measured with ^{131}I-orthoiodohippurate and can be used as an index of renal function. Camera-based methods have been described to evaluate ^{99m}Tc-MAG_3 clearance without blood sampling. Although less precise than techniques that require blood sampling, camera-based methods are convenient for both patients and Nuclear Medicine practitioners, and are suitable for routine clinical use [51]

2.6 Proposed Renal Radiopharmaceuticals

2.6.1 ^{99m}Tc-Biguanide Ligands As Potential Kidney Imaging Agents

Biguanide (*fig. 2.11*) may be considered as derived from the substitution of both the oxygen atoms of biuret by imino =NH groups. Biguanide and its derivatives contain nitrogen donor atoms. Its derivatives are well known for their hypoglycaemic and antimalarial activity. The precursors $[TcOCl_4]^-$ and $[ReOCl_3(XPh_3)_2]$, (where X=P=As) react rapidly under mild conditions with HL_{-n} (n=1-3, HL_{-1}= 1.1 dimethylbiguanide, HL_2= 1-phenethylbiguanide, HL_3= 1-phenyl-biguanide) forming stable, tricationic, violet, disubstituted complexes $[MO(HL_{1-3})_2]^{3+}$ (M=Tc, Re).

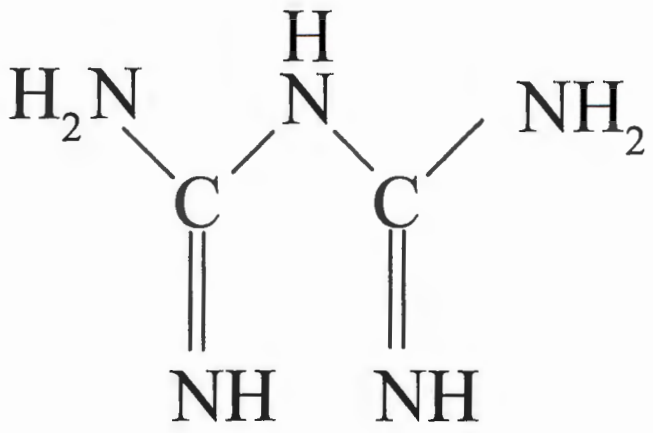

Figure 2.11: *Biguanide.*

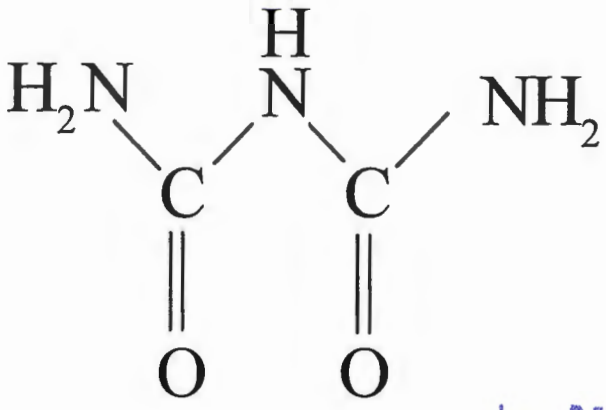

Figure 2.12: *Biuret.*

In the presence of a base, deprotonation of ligands occurs and the corresponding orange-yellow, monocationic complexes $[MO(L_n)_2]^+$ are formed. These are also obtained if a base is added to a solution of the violet compound. The pink nitridotechnetium precursor $[TcNCl_2(PPh_3)_2]$ in presence of NEt_3 reacts with HL_{1-3} ligands to form yellow, cationic, disubstituted complexes $[TcN(HL)_2]^{2+}$. Similarly, to oxo-compounds at strongly basic pH values deprotonation of ligands takes place and neutral complexes $[TcN(L_{1-3})_2]$ are isolated. Reactions with ITB give similar deprotonated complexes but do not require the presence of a base [3].

Biuret (*fig. 2.12*) and biguanide are considered to be strong σ and π donating ligands, which form stable complexes with transition metal ions in high or usual oxidation states utilising the availability of vacant d-orbitals of the metal, which may overlap, with the filled π orbitals of the ligand. They form highly coloured complexes with bivalent metal ions such as copper, nickel and cobalt [8].

Biodistribution studies results in mice show that the ^{99m}Tc-big complex has a ratio of %ID kidneys/liver, which is higher than other oxo-complexes. This fact is in accord with the increased lipophilicity in the sequence ^{99m}Tc-Big, ^{99m}Tc-Me_2Big, ^{99m}Tc-PhBig and ^{99m}Tc-PhetBig for which increased values of liver uptake are observed.

Table 2.1: *Biodistribution of ^{99m}TcOBig, ^{99m}TcOMe_2Big, ^{99m}TcOPhBig, ^{99m}TcOPhetBig in mice, %ID/organ ± SD [3].*

	Tc-Big		**Tc-Me_2Big**		**Tc-PhBig**		**Tc-PhetBig**	
ORGAN	*2min*	*30min*	*2min*	*30min*	*2min*	*30min*	*2min*	*30min*
Blood	17.2	6.2	2.8	1.3	2.0	1.2	2.6	1.3
Liver	8.7	5.2	18.7	12.3	49.5	24.8	57.1	28.5
Intestine	4.8	9.2	17.7	27.0	9.4	40.7	10.2	45.4
Lung	2.1	0.7	1.5	0.7	1.2	0.5	2.1	1.4
Kidneys	19.2	12.7	27.2	10.6	21.5	18.3	17.2	14.2
Stomach	0.9	0.6	1.3	1.2	0.5	0.7	1.3	1.2
Brain	0.2	0.1	0.2	0.2	0.0	0.0	0.0	0.0
Heart	0.7	0.2	0.6	0.5	0.3	0.2	0.3	0.1

For a comparison, qualitative gamma camera studies of ^{99m}Tc-Big and ^{99m}Tc-DMSA were performed in rabbits [3]. The ^{99m}Tc-Big complex is cleared faster than ^{99m}Tc-DMSA and for the same acquisition times images favour the ^{99m}Tc-Big. This complex reaches a peak at *ca.*6 min.p.i and the biological profiles revealed that good imaging could be obtained between 30-60 min p.i. [3].

In Table 2.1, the biodistribution of different biguanides is shown. In this work, a derivative of biguanide ITB, incorporating the "thio" (sulfur) group will be investigated as a potential kidney-imaging agent.

2.7 ^{99m}Tc-ITB (2-imino-4-thiobiuret) as a Potential Kidney Imaging Agent

Thiourea, the thiocarbonyl analogue of urea and a constituent of ITB, is one of the simplest organic molecules containing a thioamide group. Its structure and properties have been studied extensively by various experimental and theoretical techniques.

Extensive work has been done on the protonation of thiourea in aqueous solutions. It has been known since the middle of the 19th century that thiourea forms 1:1 compounds with strong acids such as HCl and H_2SO_4.

Two possible structures for monoprotonated thiourea can be found. They are the sulfonium form (*fig. 2.13*) and the ammonium form (*fig. 2.14*). On theoretical grounds the sulfonium structure should be preferred because of its resonance stabilization. However, on the basis of the infrared spectra of thiouronium salts in the solid state, Spinner had suggested N – protonation of thiourea [52]. On the other hand, ^{1}H NMR of the salts in solution indicated protonation of the sulfur atom. In subsequent UV and IR studies of thiouronium salts, the vibrational frequencies were assigned in favour of the sulfonium structure.

Conductivity studies of thiourea in $ClSO_3H$ were also interpreted in terms of monoprotonation on the sulfur atom. Semi-empirical SCF calculations have been used to demonstrate that the S-protonation is energetically favoured over the N-protonation.

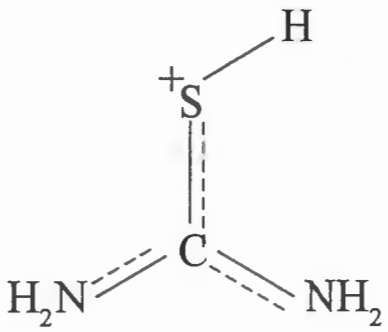

Figure 2.13: *Sulfonium-form structure of thiourea.*

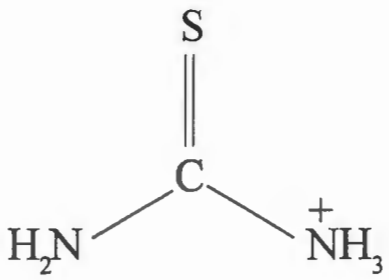

Figure 2.14: *Ammonium form structure of thiourea.*

Recently, Murgich *et.al* used ^{14}N nuclear quadropole resonance (NQR) spectroscopy to support S-protonation of thiourea in solution [52]. Although in the solid state the thiouronium monocation exists in the S-protonated form, as shown by X-ray diffraction data, the behaviour of thiourea in strong acids has not been clearly established. Birchall and Gillespie [52] studied the proton NMR spectra of thiourea in water, CF_3COOH, H_2SO_4 and FSO_3H. In water and CF_3COOH solution at 25°C, only one line due to the NH_2 group was observed. In more acidic solvents H_2SO_4 and FSO_3H, a new resonance appeared at about δ ^1H 5.0 which was attributed to the $C=SH^+$ group and the NH_2 group signal disappeared.

The observations were attributed to diprotonation with the first proton being attached to sulfur and exchanging only very slowly with the solvent and the

second proton being attached to nitrogen and exchanging rather rapidly with the solvent [52].

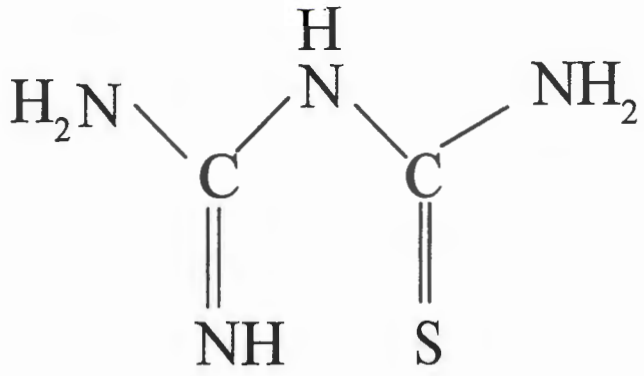

Figure 2.15: *The structure of 2-imino-4-thiobiouret (ITB)*

2.7.1 The Chemistry of 2 -imino-4-thiobiouret (ITB)

The results of pre-clinical trials [8,9] with biguanide ligands are encouraging. In this study, ITB, a ligand similar to biguanide is studied.

ITB was first prepared by Rathke [53], who obtained it by heating thiourea with thiophosgene at a temperature of 110-110°C or with phosphorus pentachloride at 100°C. However, Bamberger in 1883 obtained better results by digesting dicyandiamide or guanylurea salts with hydrogen sulfide water at 60-70°C, for several days. A further modification of the method consists in heating dicyandiamide or a substituted dicyandiamide in methanol solution of hydrogen sulfide at a temperature of 78-80°C.

Guanylurea is readily transformed into its sulfur analogue, 2-imino-4-thiobiuret, by heating any of its salts with hydrogen sulfide water.

$$H_2NC\ (=NH)\ NHCONH2 + H_2S \rightarrow H_2NC\ (=NH)NHCSNH_2 + H_2O$$

The reaction may be regarded as a case of sulfhydrolysis of guanylurea. The reverse change, the hydrolysis of 2-imino-4-thiobiuret to guanylurea, is also implied.

Metal complexes of 2-imino-4-thiobiuret (ITB) differ in certain cases from those of guanylurea, in their colour, composition and other properties. This is due to the metal sulphur bonds in the molecules of metal complexes of 2-imino-4-thiobiuret. It is believed that this ligand can react in either of its tautomeric forms (A or B) to give rise to inner metallic complexes of different structures, depending upon the nature of the metal [53].

However, 2-imino-4-thiobiuret closely resembles guanylurea, though it is a much weaker base than the latter. Its hydrochloride, $C_2H_6SN_4 \bullet HCl$, readily hydrolyzes in aqueous solution, giving an acid reaction [53].

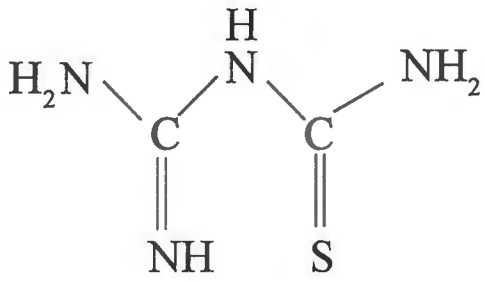

A

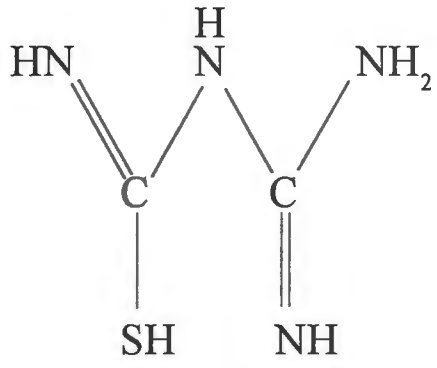

B

Precursors such as $[TcOCl_4]^-$ and $[ReOCl_3(XPh_3)_2]$ react under mild conditions with 1,1dimethylbiguanide(1) (*fig.2.16),* 1-phenethylbiguanide(2), 1-phenylbiguanide(3). Stable complexes were formed such as $[MO(HL1\text{-}3)_2]^{3+}$ (M=Tc,Re). With ITB the unexpected $[ReO(HL4)_2]^{3+}$, where HL4 = 2-imino-4-

thiobiuret is formed. The spontaneous deprotonation of HL4 gives the corresponding monocationic complex $[TcO(L4)_2]$ Cl [3].

With each type of ligand, the colour of the metal complex varies with the nature of the metal ion and its valency, as well as with the number of the ligand molecules in the complex. The colour is slightly modified by substitution in the ligand molecule. In colour, the metal complexes of guanylurea resemble more or less closely the corresponding complexes of biguanide. The metal complexes of 2-imino-4-thiobiuret, on the other hand, show somewhat darker colours. The metal complexes of biguanide are comparatively more stable than those of the guanylureas.

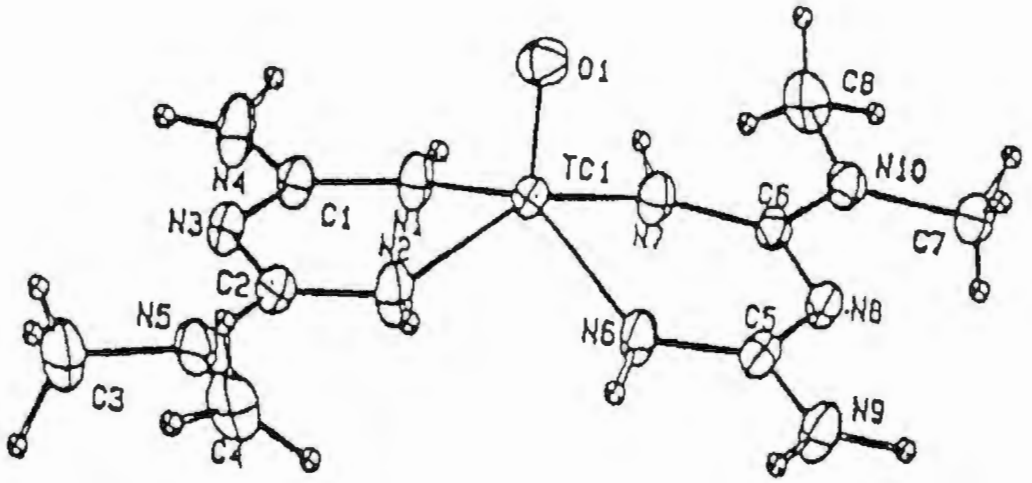

Figure 2.16: *Crystallographic structure of Tc-Biguanide complex.*

The molecules of biguanide, guanylurea and 2-imino-4-thiobiuret all possess active functional groups, which readily lend themselves to the formation of metal complexes in a suitably activated state of the molecule, most favorable for the purpose. The metal complexes of these ligands are usually cationic in nature, and the anhydrobases form hydroxides and salts. In most cases, the solubility of the complexes of the biguanide series is comparatively less than that of the corresponding complexes of the guanylurea series. All known

metal complexes of 2-imino-4-thiobiuret, on the other hand are practically insoluble [53].

The Cu(II) complex of ITB is brown, while that of the Ni(II) is orange, resembling the complexes of Ni(II) guanylurea and Ni(II) biguanide. The brown colour is due to copper-sulphur bond, which accounts for the rapid decomposition of the complex into copper sulfide on warming with dilute acid or alkali solution. Furthermore, while the copper complex contains only one molecule of 2-imino-4-thiobiuret per copper atom, the nickel atom combines as usual with two molecules of the ligand.

Nickel (II), bis (ITB), $[Ni\ (C_2H_5SN_4)_2]\bullet\ 5H_2O$ separates as an insoluble orange precipitate when a solution of nickel (II) sulfate is added to one of 2-imino-4-thiobiuret, which has been rendered strongly alkaline with sodium hydroxide. The substance is magnetic like all orange-yellow nickel (II) complexes and has therefore a square planar configuration with dsp^2 hybrid bonds. At 100°C, it loses water, forming an unhydrobase, and is readily decomposed by warm dilute acids through unaffected even by boiling alkalis [53].

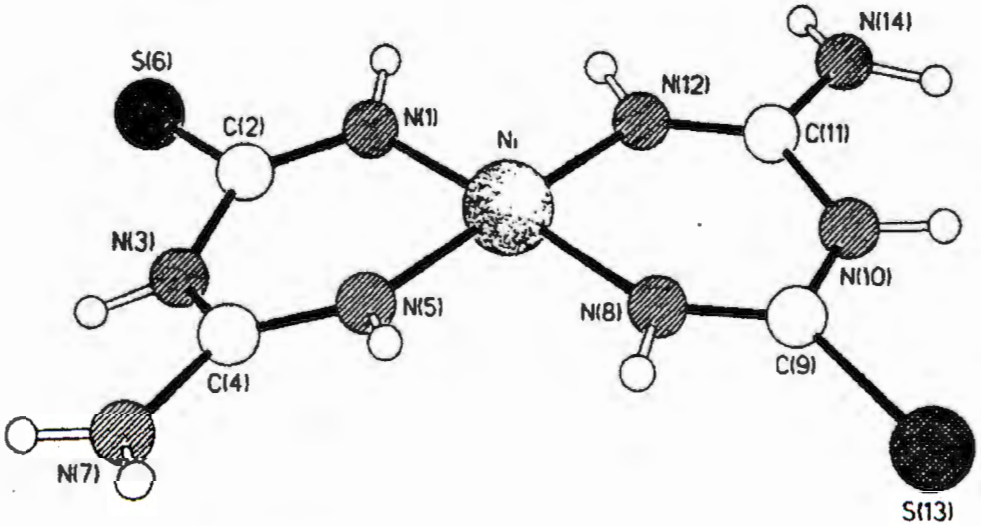

Figure 2.17: *Molecular structure of ITB-Ni(II).*

According to Ramon *et.al*, ITB can coordinate to metal centres using either 2 nitrogens (N,N) or one nitrogen and one sulfur (N,S). The molecular structure

in *fig. 2.17* reveals the coordination mode to be N, N'. This is in striking contrast to what is observed in the only other structurally characterized complex of this ligand with palladium, where N, S coordination occurs. This suggested that the non-coordinated sulfur atoms in *fig. 2.17* are available for coordination to additional metal centres [54].

CHAPTER 3 EXPERIMENTAL THEORY AND PROCEDURES

3.1. Experimental Procedure

All reagents used were of analytical grade. These were Merck 0.1 NaOH Titrisol, Riedel-de-Haen NaCl salt, Merck Potassium Hydrogen Phthalate, Merck HCl, Aldrich 2-Imino-4-thiobiuret, Analar sulphate salt of Copper and Merck chloride salts of Calcium, Magnesium, Nickel, Zinc.

EDTA titrations were performed on the Metrohm 702 SM Titrino using a Cu-selective electrode to determine metal concentration in 0.05 M metal solutions including Ca^{2+}, Mg^{2+}, Zn^{2+} and Ni^{2+}. The following solutions were prepared: 1.0 M EDTA, 0.01 M $CuSO_4$, pH 10 buffer solution. EDTA was standardized using primary standard Zn-solution. The standardized EDTA solution was then used to standardize 0.01 M $CuSO_4$.

The metal concentrations were determined by adding the following a beaker: 1.0ml metal solution, 5.0ml buffer solution of pH10, 1.0ml Cu-EDTA and filled to ± 70ml with demin water. The mixture was titrated with EDTA. This was repeated four (4) times for each different metal solution.

3.2. Potentiometry

The potentiometric method has since been used extensively in many branches of solution chemistry. It is an accurate and widely applicable technique for the study of solution equilibria. The potentials originate from two main types of phenomena: (1) oxidation-reduction equilibria and (2) the formation of ionic concentration gradients across membranes. If the reversible electron transfer reaction:

$$xX + yY + ... + ze - \Leftrightarrow pP + qQ + .. \qquad (4)$$

can occur, the potential acquired by an electrode in contact with equilibrium mixture of P, Q, X, Y, is given by the Nernst equation:

$$E = E_0 + \frac{RT}{zF} \ln \frac{[X]^x [Y]^y ..}{[P]^p [Q]^q ..} \qquad (5)$$

Where the standard electrode potential E_0 is the potential acquired when all species are at unit activity.

In general, the presence of any other oxidizing or reducing agent, which can react with species P, Q, X, or Y should be avoided. For instance sodium perchlorate is an unsuitable background salt for studies of cations that are strong reducing agents.

The electrodes usually employed to study ionic equilibria are reversible to metals ions, to protons, or to anions. The potential should reach that predicted by the Nernst equation within a reasonable time, particularly if the titration technique is used. The electrode should not be decomposed by the solution [55].

Potentiometry is a technique that is often used to calculate formation constants. It is considered by some to be necessary to evaluate calculated constants by a second technique to verify the results. In this study, the potentiometric data was analysed using the ESTA (Equilibrium Simulation by Titration Analysis) suite of computer programs written by May and Murray [56].

In an aqueous solution of definite pH containing the metal ion, M and a ligand L, the possibility of a large number of complexes coexisting in equilibrium exists. By utilising potentiometric methods, there is a possibility to determine which complexes are present as well as their formation (stability) constants [57].

There are a number of functions that may be defined in order to explain potentiometric data. The data obtained are usually in the form of titrant volume and potential pairs. The potential E is obtained from the Nernst equation where glass electrode is considered a probe for the free hydrogen ion concentration [58].

The Nernst equation is given as follows:

$$E = E_0 - H_{slope}.\ pH \qquad (6)$$

Where E_0 = the electrode constant

H_{slope} = the electrode response slope

pH = the negative logarithm of the free hydrogen ion concentration.

In a solution containing aquated metal ions M and ligands L, the following equations and equilibrium constants may describe the system at equilibrium:

$$M + L \rightleftharpoons ML \qquad K_1 = \frac{[ML]}{[M][L]} \qquad (7)$$

$$ML + L \rightleftharpoons ML_2 \qquad K_2 = \frac{[ML_2]}{[ML][L]} \qquad (8)$$

$$ML_2 + L \rightleftharpoons ML_3 \qquad K_3 = \frac{[ML_3]}{[ML_2][L]} \qquad (9)$$

$$ML_{N-1} + L \rightleftharpoons ML_N \qquad K_N = \frac{[ML_N]}{[ML_{N-1}][L]} \qquad (10)$$

$$M + L \rightleftharpoons ML \qquad \beta_1 = \frac{[ML]}{[M][L]} \qquad (11)$$

$$M + 2L \rightleftharpoons ML_2 \qquad \beta_2 = \frac{[ML_2]}{[M][L]^2} \qquad (12)$$

$$M + 3L \rightleftharpoons ML_3 \qquad \beta_3 = \frac{[ML_3]}{[M][L]^3} \qquad (13)$$

$$M + NL \rightleftharpoons ML_N \qquad \beta_N = \frac{[ML_N]}{[M][L]^N} \tag{14}$$

$$\beta_3 = \frac{[ML]}{[M][L]} \bullet \frac{[ML_2]}{[ML][L]} \bullet \frac{[ML_3]}{[ML_2][L]} \tag{15}$$

$$\beta_3 = K_1 \,.\, K_2 \,.\, K_3 \tag{16}$$

β_3 is the overall stability constant [4,59].

3.2.1 Experimental Procedure

Titrations were performed using a Metrohm Titroprocessor 670 with a Metrohm 665 Dosimat and a Metrohm combined glass electrode (Ag/AgCl reference). The electrode was calibrated regularly using strong acid – base titration data. Data were submitted to the program ESTA2A. The pK_w was held constant while E_0 and H_{slope} were refined. Very accurate values of E_0 were not essential as these values were refined by ESTA once a final model had been obtained [60].

The titration solutions were contained in a jacketed vessel through which water at 25.0 ± 0.1°C was circulated from a Grant W 14 thermostat bath [61]. The compositions of the titration solutions are listed in Table 3.1. These were performed beginning at low and ending at high pH by the addition of 0.050 M NaOH in 0.10 M NaCl. The NaOH solutions were made up so as to exclude the absorption of atmospheric carbon dioxide and standardised using potassium hydrogen phthalate.

Protonation constarts were calculated from data obtained from titrations of the ligand in the presence of various hydrochloric acid concentrations. Protonation constants were obtained for the ligand at different total ligand concentrations in the absence of metal ions. All titrations were performed under an inert atmosphere (by bubbling N_2 gas through the solution)[61] and

at a constant ionic strength of 0.15 mol dm^{-3} NaCl. In all cases, extreme care was taken to detect the onset of precipitation [62].

Table 3.1: *Composition of experimental solutions for potentiometric studies with ITB.*

Cation	Titration	0.05M ITB in 0.15M NaCl (ml)	0.05M HCl in 0.10M NaCl (ml)	0.15M NaCl (ml)	Metal ion Solution
H^+	1	5.00	10.00	35.00	
	2	10.00	10.00	30.00	
	3	15.00	10.00	25.00	
Ca^{2+}	1	5.00	10.00	34.00	1.00
	2	10.00	10.00	29.00	1.00
	3	15.00	10.00	24.00	1.00
	4	20.00	10.00	19.00	1.00
	5	25.00	10.00	14.00	1 .00
Mg^{2+}	1	5.00	10.00	34.00	1.00
	2	10.00	10.00	29.00	1.00
	3	15.00	10.00	24.00	1.00
	4	20.00	10.00	19.00	1.00
	5	25.00	10.00	14.00	1.00
Ni^{2+}	1	5.00	10.00	34.00	1.00
	2	10.00	10.00	29.00	1.00
	3	15.00	10.00	24.00	1.00
Zn^{2+}	1	15.00	10.00	24.00	1.00
	2	20.00	10.00	19.00	1.00
	3	25.00	10.00	14.00	1.00

Metal –ligand formation constants were calculated from titration data at three different metal– ligand ratios. Data were analysed by the ESTA library of programs. During the analysis the previously determined protonation constants were held constant. Hydrolysis constants and pK_w were taken from

the literature [63], and held constant during optimisation procedures (i.e ESTA2A).

Models were considered plausible if the Hamilton R – Factor and the standard deviations of log β values were low. Where more than one model was plausible, the model data were compared with experimental data using the deprotonation function, $\bar{Q}$ (the average number of protons released on complexation per metal ion), $\bar{Z}$ (the average number of ligands per metal ion), or the protonation function, $\bar{Z}_H$ (the average number of protons per ligand). The models giving rise to the best fit of the calculated to the experimental data were considered the most plausible [64].

3.2.2 Electrode Calibration

The relationship between E and -log $[H^+]$ should be linear. In practice, a sigmoidal curve is obtained. The "s" shape results from a number of contributing sources, at intermediate pH values (pH 3- pH 10.5) deviations occur due to low buffering capacity of the system. Non-linearity at extremes of pH is due to liquid junction effects (at low pH) and sodium-ion interference (high pH). (Rossoti, 1978). True linearity is only obtained in the pH regions 2 – 3 and 11 - 12. These calibration titrations were done weekly on each electrode by titrating hydrochloric acid with sodium hydroxide [65]. At pH less than 3 and greater than 11, the electrode is not stable. Data in these regions are usually ignored or given low weight.

The glass electrode functions as a result of ion exchange on the surface of a hydrated layer. The membrane of a glass electrode consists of chemically bonded Na_2O and SiO_2. In order for an electrode to operate, it must be soaked in water. During this process, the outer membrane becomes hydrated. The inner surface is already hydrated.

When the outer layer becomes hydrated, the sodium ions are exchanged for protons in the solution:

$$-SiO^- Na^+ + H^+ \rightleftharpoons -SiO^-H^+ + Na^+ \qquad (17)$$

When the electrode is dipped in an aqueous solution, a boundary potential is built up, which is determined by the activity of hydrogen ions in the external solution and the activity of hydrogen ions on the surface gel. One explanation of potential is that the ions will tend to move in the direction of lesser activity, much as at a liquid junction. The result is a microscopic layer of charge built up on the surface of the membrane, which represents a potential.

The pH region less than about 9 has a negligible error, but at pH values above this, the H^+ concentration is very small relative to that of other ions, and the electrode response to other ions such as Na^+, K^+, and so on becomes appreciable. In effect, the electrode appears to see more hydrogen ions than are present, and the pH reading is too low. In general, an electrode is preferred to work below pH 11 because it will provide faster response and greater stability due to its lower-resistance glass [66].

3.3 Computer Analysis of Titration Data

Equilibrium Simulation by Titration Analysis (ESTA) is a complex and sophisticated library of programs. It may be used to analyse potentiometric titration data and simulate equilibrium distribution of chemical species. Data were analysed on a computer using the ESTA suite of programs, which operate on titration data to yield overall formation constants defined by the following equation:

$$\beta_{pqr} = \frac{[M_p\ L_q\ H_r]}{[M]^p\,[L]^q[H]^r} \qquad (18)$$

The ESTA library of programs is used for simulating simple equilibrium distributions of chemical species and for the analysis of potentiometric titration data. The major objective is to provide a flexible tool for investigating phenomena associated with chemical interactions in solution and for their quantitative characterization. It is also used to analyse potentiometric titration

data and to manipulate titration data for a variety of other purposes. Accordingly, the best choice of objective function, the effects of various kinds of error and the most successful model selection strategy could be equivocally ascertained (because, when simulated data are used, the true result is known) [67].

3.3.1 ESTA 0: The preliminary Analysis Module

This module (ESTA0) permits various types of calculation, usually used in the preliminary analysis of titration data. Gran functions, pH, formation functions and deprotonation functions can be calculated from the observed data. The program only permits calculations for titrations in which there is a Hydrogen-ion sensing electrode. There is no limit to the number of points in a titration or to the number of titrations [60].

3.3.2 ESTA1: The simulation mode

The calculation done by this mode falls into two categories (i) species distribution calculations and (ii) potentiometric titration calculations. The latter include determination of emf values, formation constant – estimates, total analytical concentrations and initial burette concentrations. This program is commonly used to generate formation function value (task $\bar{Z}$), deprotonation function values (task $\bar{Q}$) and protonation values ($\bar{n}$). $\bar{Z}$ can be described as the number of ligands bound per metal ion at a certain pH value. $\bar{n}$ is the number of protons bound per ligand at a certain pH value in the absence of complexation. $\bar{Q}$ is the number of protons lost by the ligand per metal ion due to complexation taken at a certain pH value.

By using this program, graphs can be drawn of $\bar{Z}_H$ vs pH or, $\bar{Q}$ and $\bar{Z}$ vs pA observed and calculated functions can be compared and E_K^{obs}, E_K^{calc} evaluated respectively. If the calculated and observed curves match each other closely in the pH region of interest, the proposed model of formation constants can be accepted [56].

3.3.3 ESTA2: The optimisation module

ESTA2 involves two optimisation programs ESTA2A and ESTA2B which differ in the way data are weighted. They are used when it is desired to determine , for one or more parameters ,the "best" values , based on a least-square procedure applied to a whole system of titrations. In this way, it is possible for the following to be refined: formation constants, vessel and burette concentrations, electrode slope and initial vessel volume. It is also possible to group together, over any combinations of titrations, local parameters of the same type and with the same value so that they are refined together as a single parameter.

The objective function may be weighted or unweighted. The sum of squares of residuals may be minimized with respect to emf (OBJE) or total concentrations (OBJT) [60,67]. In this work, data were weighted.

Task OBJE permits the calculation of the weight, the objective function contribution based on emf's and the relative contributions of the most important errors to the weight at each titration point. The values calculated are those used by the optimizer for the specified formation constants, concentrations, electrode constants and associated errors.

Task OBJT is identical to OBJE in every way with two exceptions. These exceptions are :

(i) the objective function is based on the total electrode ion concentrations, and

(ii) Debye-Huckel, liquid junction and ion selectivity corrections are not allowed [60].

The approach is to model with ESTA2 the formation constants until the best values for the standard deviations and Hamilton factors are reached. The proposed model of formation constants is then tested by $\bar{Q}$ or $\bar{Z}$ comparison [56].

The final selection of the collection of species that best characterizes a particular metal-ligand-proton interaction is governed by a number of factors:

(i) The species chosen should be chemically feasible.

(ii) Optimisation of formation constants using OBJE allows selection upon the basis of statistical output, overall objective function and Hamilton R factor.

(iii) Optimised formation constants may be used to calculate theoretical $\bar{Z}$ and $\bar{Q}$ curves. Simulated curves are then compared to the original experimental curves, systems being selected upon the basis of goodness of theoretical to experimental fit [65].

3.3.4 The protonation formation function $\bar{Z}_H$

Let M_T, L_T and H_T represent the total concentrations and M, L and H represent the free concentrations of these 3 components. The formation function for protonated ligand, $\bar{Z}_H$ is defined as the average number of protons bound per ligand. In the absence of a metal, the equation is as follows:

$$\bar{Z}_H = [\text{bound H}]/L_T. \quad (19)$$

$$[\text{Bound H}] = H_T - H + [OH^-] \quad (20)$$

$$= H_T - H + k_w H^- \quad (21)$$

Where OH^- = hydroxide ion

K_w = dissociation constant of water

Therefore $\bar{Z}_H = (H_T - H - k_w H^-)/L_T$.

H_T and L_T are known from analytical determined concentration and k_w is a known constant. Glass electrode is used to measure H, and $\bar{Z}_H$ can be calculated at a number of pH (-log H) values. A protonation formation curve ($\bar{Z}_H$ versus pH) may be plotted [57,64].

3.3.5 The formation function, $\bar{Z}$

The formation function $\bar{Z}$ is defined as the average number of ligands bound per metal ion. This can be summarised by the following equation.

$$\bar{Z} = [\text{Ligand bound to } M_T]/M_T \quad (22)$$

$$\bar{Z} = (L_T - [\text{L not bound to M}])/M_T \quad (23)$$

$$= (L_T - [\text{bound H}]/\bar{Z}_H)\, M_T \quad (24)$$

$$= (L_T - \{H_T - H + k_w H^{-1}\}/\bar{Z})/M_T \quad (25)$$

The protonation formation constants for the ligand must be determined before $\bar{Z}$ can be calculated from the observed experimental points using the above equation (22).

$\bar{Z}$ is plotted against pA to get formation curves. Usually a number of titration's with different ligand to metal ratios are performed by starting at low and ending at high pH using strong base. Experimental formation curves are then obtained for all titration's. If the curves are superimposed, only mononuclear binary complexes are being formed. If the curves do not overlap, the protonated hydrolysis or polynuclear species are present [57].

Once modelling is completed, the calculated values are used to determine calculated values for H which can be substituted in equation (25). The resulting calculated formation curves are compared to experimental curves to test validity of the model [57].

3.3.6 The deprotonation function, $\bar{Q}$

The deprotonation function $\bar{Q}$, is defined as the average number of protons released per metal ion due to complexation. This can be represented by the following equation:

$$\bar{q} = \frac{(H^* - H_T)}{M_T} \tag{26}$$

Where H^* = The calculated total concentration of protons in the system at observed pH ignoring the presence of all metal complexes. The following mass balance equations need to be solved:

$$H^* = H - K_w.H^{-1} + \sum_{j=1}^{NJ} r[M_p L_q H_r] \tag{27}$$

Where p = 0 and NJ = number of complexes.

$$L_T = L + \sum_{j=1}^{NJ} q[M_p L_q H_r] \tag{28}$$

For binary systems a formation function $\bar{n}$, is defined for the ligand subsystems. This is equivalent to the average number of protons bound per ligand in the absence of the metal.

$$\bar{n} = \left(H^* - H + K_w H^{-1}\right) L_T^r \tag{29}$$

Thus an average proton stoichiometric coefficient, r may be calculated for any given M and L stoichiometry (p and q). The assumption is made here that the complex is predominant.

$$\bar{r} = q\bar{n} - \bar{Q}p \tag{30}$$

The deprotonation function may be calculated once a model has been established and the β values known. The validity of the model may be tested by comparing experimental and calculated deprotonation curves ($\bar{Q}$ vs pH) [57,64].

3.4 ECCLES *[Evaluate Constituent Concentration in Large Equilibrium System]*

ECCLES is a thermodynamic model of blood plasma, which is used to calculate the speciation of metal ions of interest in the presence of the ligand. Certain metal ions are considered essential to human life. These include metal ions such as calcium, magnesium, manganese, iron, cobalt, copper, nickel and zinc.

The metal ions that are present in blood plasma, may be classified into four distinct fractions:

(i) those that are incorporated rigidly into the metalloproteins and are non-exchangeable,

(ii) those that are relatively loosely bound by other types of protein and are in labile equilibrium with similar ions in solutions,

(iii) those that are complexed by the numerous low molecular weight ligands present including amino acid anions, carboxylates, carbonate, phosphate, salicylate and

(iv) the free (or aquated) metal ions [68].

Human blood plasma is known to contain about 20 amino acids, 12 essential metal ions, a number of other ligands, numerous low molecular weight [lmw] complexes as well as α/β macroglobulins such as albumin which complexes Zn very efficiently [56]. Sodium chloride is the chief contributor to the ionic strength of blood plasma (0.15 $mol.dm^{-3}$). The justification for using this substance is that, it acts as a supporting electrolyte in the formation-constant determination [68].

ECCLES calculates at pH 7.4, the competition of different ligands in blood plasma i.e. acids, amino acids for metal ions. It also determines whether the ligand will be able to mobilize the metal ions present in the blood plasma. The models indicate whether in blood plasma, a large proportion of metal ion of

interest would be complexed to the introduced ligand or pharmaceutical, thus making good organ uptake possible [69].

3.4.1 Program description

Most constants for complexation of metal ions with amino acid and low molecular weight complexes have been fed into the program by authors. Although these constants were obtained from the literature, some corrections for ionic strength were employed using Debye-Huckel and van Hoff-type extrapolations for temperature corrections.

In computation of the distribution of the metal ions other than Ca^{2+} among the low molecular weight complexes a range of plausible free concentrations for each, which bracketed an estimated average value, was taken. Since mixed –ligand (ternary) complex formation occurs widely in systems containing metal ions and two or more different ligands as many as possible ternary constants have been included in the program [56,68].

The procedure first calls in the program MIX to prepare input data for the program ECCLES. The user defines the system in terms of its components and their respective corrections and MIX generates the intermediate data file by performing three tasks. These tasks are:

(i) the selection of the applicable binary formation constants for the system in question,

(ii) calculating formation constants for all ternary complex species that may be assumed to exist according to the chosen binary formation constants, and

(iii) substitution, adjustment or extention of these constant estimates in respect of those for which experimental data has been collected.

The MIX program produces an output file that becomes the complete input for ECCLES. ECCLES is then run and it delivers the relative concentrations of all species in equilibrium [56].

May and Williams have defined plasma mobilising index (p.m.i) as the total concentration of l.m.m species of the metal after therapy / total concentration of l.m.m complexes before treatment. The equation is as follows:

$$\text{p.m.i} = \frac{\text{Total low molar mass metal ion concentration in presence of agent}}{\text{Total low molar mass concentration in normal plasma}}$$

The significance of p.m.i is that, it gives an indication as to which metal ions are mobilised by the added ligand [70].

3.4.2 Blood Plasma Modelling Experimental Procedure

All constants measured in this study were added to the ECCLES database. The ITB concentration used in modelling was 8.5×10^{-5} mol dm^{-3}. This value is representative of actual clinical amounts, and is similar to that previously employed during work using the ligands EDTMP, ADP and APDDMP [56]

For mobilisation studies, ECCLES was used to model ITB at different concentrations, starting from 8.5×10^{-10} mol.dm^{-3} to 8.5×10^{-2} mol.dm^{-3}. The program allowed the ligand concentration to be scanned in order to calculate the plasma mobilisation curves [63,69].

3.5 ITB labelling with ^{99m}Tc

The procedure was performed by Dr Werner Louw of the Radiochemistry Department of NECSA.

3.5.1 Experimental Procedure

All reagents were of analytically pure grade while purging with argon to deoxygenise all solutions used in preparing ^{99m}Tc-ITB. To 3mg ITB in an Ar-filled sealed vial, 0.5ml of water was added. After dissolution, 0.3ml 0.1 M NaOH was added followed by 0.2ml of $SnCl_2.2H_2O$ (1 mg /ml in 0.001N HCl)

solution. Immediately 0.5ml ^{99m}Tc-pertechnetate (freshly eluted from a ^{99}Mo/^{99m}Tc Peltek generator, NECSA, Pretoria, South Africa) was injected into the vial. The reaction mixture was incubated at room temperature for 15 minutes.

3.5.2 Radiochemical Control

The radiochemical purity of the ^{99m}Tc-ITB complex was assessed by ascending chromatography, using ITLC-SG (Gelman Sciences Inc., Ann Arbor, MI) strips developed with n-butanol saturated with 0.4 N HCl and Whatman No1 paper chromatography developed with acetone. After development, the strips were dried, cut into half and the origin and the front sections were counted.

CHAPTER 4 RESULTS AND DISCUSSION

4.1 Complexometric Titrations

The 0.01 M EDTA solution was standardised at 0.010683 M with Zn primary standard solution. The 0.01 M $CuSO_4$ solution was standardized at 0.010099M with the standardised EDTA solution.

The metal concentrations in the solutions prepared are reported in Table 4.1. Direct titrations were used for Ca^{2+}, Ni^{2+}, Zn^{2+}, Cu^{2+} and back titration for Mg^{2+}.

Table 4.1: *A summary of determined metal concentrations.*

Metal	***Concentrations determined***
Ni^{2+}	0.0517 ± 0.0004 M
Zn^{2+}	0.0483 ± 0.0004 M
Ca^{2+}	0.0476 ± 0.0006 M
Cu^{2+}	0.0485 ± 0.0005 M
Mg^{2+}	0.0495 ± 0.0004 M

4.2 Potentiometric Titrations

The results of modelling for ITB are found in Tables below. The low standard deviations of the β values and Hamilton R- Factors as well as the fact that calculated and experimental formation curves were all in good agreement, indicated that the chosen models were plausible.

4.2.1 Protonation of ITB

Table 4.2: *Protonation constant for ITB.*

Cation	*Equilibrium*	*Log K value*	*Hamilton R-factor*	*Hamilton R-limit*	*Data points*
H^+	$H + L \rightleftharpoons HL$	5.73 ± 0.01	0.0268	0.00108	600

All data were measured at 25.0 ± 0.1°C and I = 0.15 mol.dm^{-3} NaCl. In the above equilibrium, the charges on the ligand have been omitted for clarity (L = ITB, H = proton).

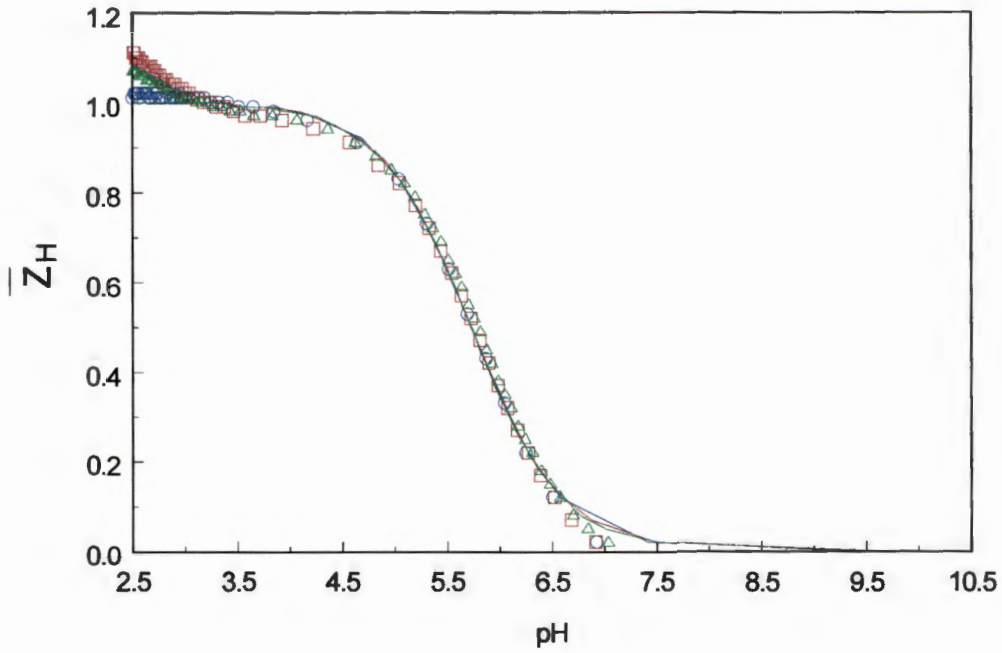

Figure 4.1: *The protonation formation curve for ITB.*

There is an infliction at $\bar{Z}_H$ =1 up to pH 5 (*fig. 4.1*). This indicates that one proton is bound to the ligand in this pH region and corresponds with HL found for the model. ITB has no dissociable protons and it can be assumed that protonation will occur at the sulphur atom.

Biguanide has almost the same structure as ITB, except that one imine group is replaced by sulphur. ITB has two tautomeric forms (see page 40, fig.A and fig.B) According to Hancock and Martell [71], the thiol group is weakly acidic (pK usually about 9 or 10), but binds to many metal ions with an enormous complexing strength. It is, like the neutral soft donors, particularly strongly bound by soft metal ions such as Ag(II) and Hg(II), and ligands such as DMSA, which has two thiol groups, are used in treatment of mercury poisoning.

Previous studies [72], have shown that 1,1dimethyl- biguanide had two pK_as, of about 3 and 11. In ITB, the "NH" in one amidine group is replaced by sulphur, a more acidic group. This lowers the second protonation formation constant to an undetectable value and the first constant to 5.73 as reported in the Table 4.2.

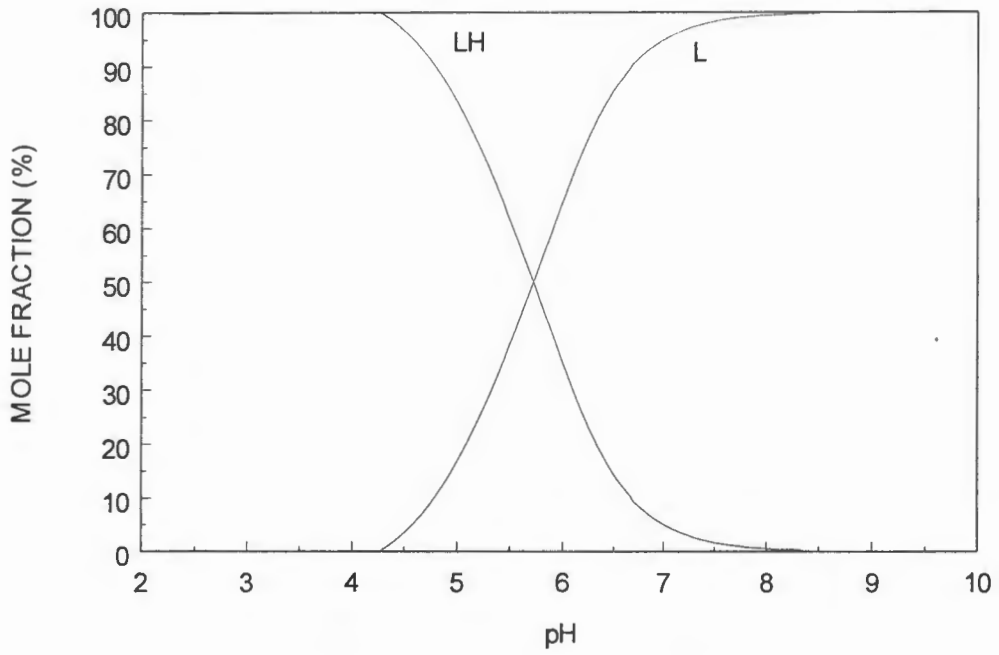

***Figure 4.2**: Species distribution curve for ITB at 25.0 ± 0.1°C in 0.15 mol dm^{-3} NaCl.*

The species distribution curves for ITB is shown in *fig.4.2*. The only protonated species present is HL, which dominates at lower pH values with mole fraction at 100%. From pH 5, the mole fraction of HL starts declining. On the other hand, the mole fraction of free ITB (L) increases as pH increases.

4.2.2 Complexation of Alkaline Earth Metals with ITB

Table 4.3: *Formation constants for Mg(II) and Ca(II) complexation by ITB.*

Cation	*Equilibrium*	*Log K or Log β*	*Hamilton R-factor*	*Hamilton R-limit*	*Data points*
Mg(II)	M+L⇌ ML ML+OH ⇌ MLH_{-1} M +L+OH ⇌ MLH_{-1}	2.36 ± 0.04 3.56 ± 0.05 5.92 ± 0.03	0.0281	0.00167	309
Ca(II)	M+L+OH ⇌ MLH_{-1}	5.43 ± 0.02	0.0231	0.00171	300

In these equilibria, the charges on the metal ions, the ligand and the complexes have been omitted for clarity (L = ITB, M = Mg^{2+}, Ca^{2+}, H = proton, OH = hydroxide).

According to the HSAB principle of Pearson [5], Ca(II) and Mg(II) are both hard acids. A hard acid is of a small size, with high positive charge density and usually does not contain unshared pairs of electrons in its valence shell. Therefore, Mg(II) is more acidic than Ca(II). This variation in acidity, depends on the difference in their atomic size, atomic radii and also the difference in their electronegativities.

Ca(II) has an ionic radius of 0.99Å while Mg(II) is 0.66Å. Based on their atomic size, Ca(II) is larger than Mg(II). According to the Irving – Williams series, there is increasing stability from Ba^{2+} to Mg^{2+} which is a measure of increasing acidity of the metal (largely due to decreasing size). This implies that metals with smaller atomic radii (and atomic number), tend to be more acidic than those with higher atomic radii and atomic number. Based on the above mentioned statement, Mg(II) is more acidic than Ca(II). This is reflected in the higher formation constant for Mg(II) over Ca(II) with ITB.

4.2.2.1 Magnesium (II) with ITB

For the MLH_{-1} species, inspection of the first hydrolysis constant for Mg(II) assists in ascertaining whether the proton is lost from coordinated water or the ligand, ITB. According to the literature [73], the first hydrolysis constant for Mg(II) is 2.58. If the proton were lost from a coordinated water molecule, we would not expect a value for the equilibrium constant to differ much from logK (MOH). In this case the proton is lost from the ligand, presumably from the thio-urea side of the molecule.

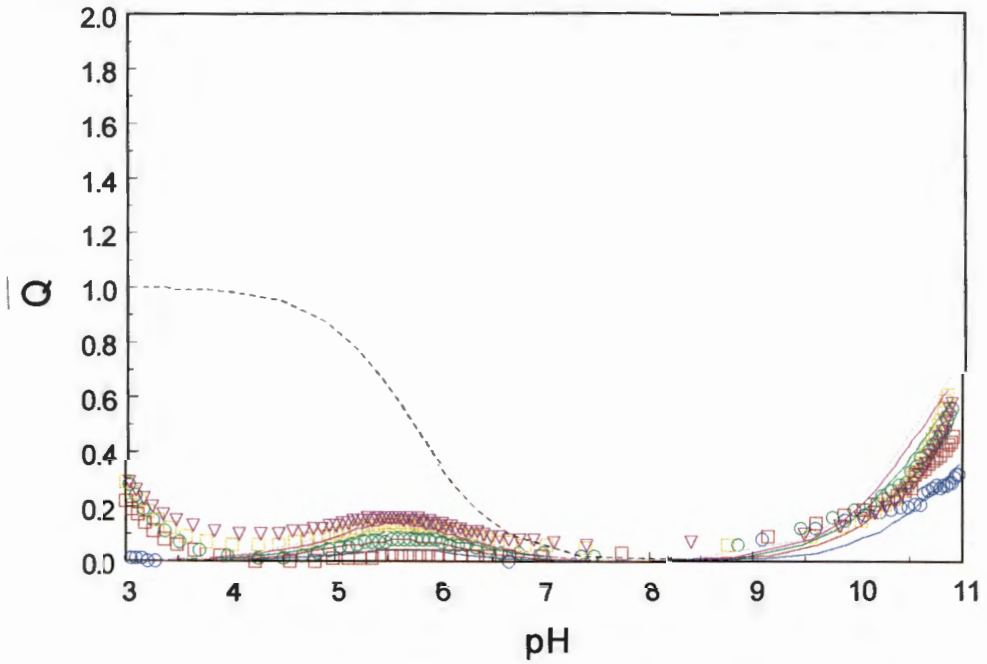

Figure 4.3: *Experimental (points) and calculated (lines) deprotonation curves for Mg(II) complexation by ITB.* $\bar{Q}$ *is the deprotonation function and the dashed line is* $\bar{n}$ *curve. The five separate titration M:L ratios are (o)1:1,(□) 1:2, (△)1:3, (◇)1:4 and (▽)1:5.*

The deprotonation curves *fig.4.3* show that the calculated and experimental $\bar{Q}$ curves follow each other satisfactorily. At high pH, $\bar{Q}$ rises above $\bar{n}$,

indicating that more protons are detected in the system than expected from the ligand. This is evidence of the ligand deprotonating as discussed above.

With reference to the $\bar{Z}$ curves (*fig.4.4*), there is some backfanning indicating the presence of an hydrolysis species [MLH_{-1} or ML(OH)] at low pA (negative logarithm of the free ligand concentration), indicating that more protons are lost on complexation than expected.

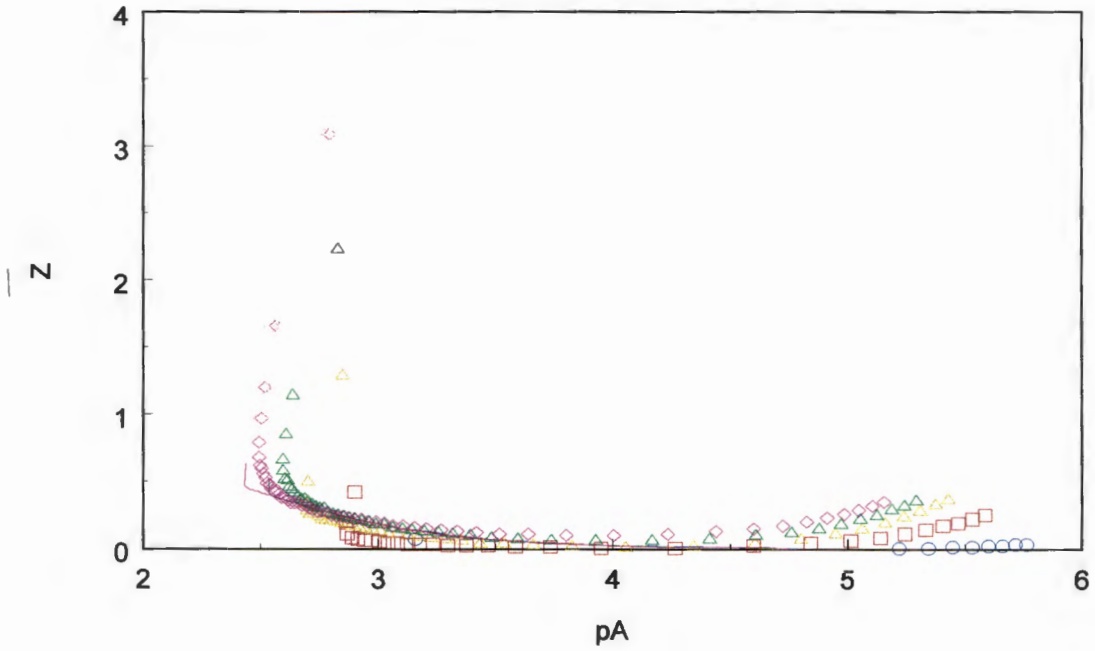

Figure 4.4: *The experimental and calculated formation curves for Mg(II) complexation by ITB. $\bar{Z}$ is the formation function and pA is the negative logarithm of the free ligand concentration. The five separate titration M:L ratios are (o)1:1,(□)1:2, (△)1:3, (◇)1:4 and (▽)1:5.*

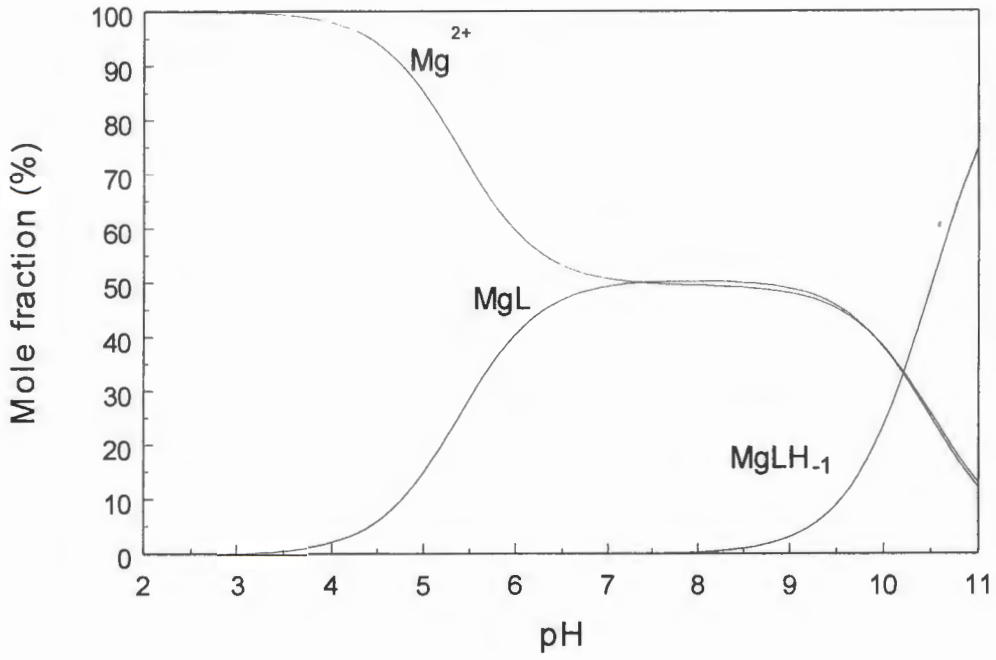

Figure 4.5: *Species distribution curves for complexation of Mg(II) by ITB at 25.0 ± 0.1°C in 0.15 mol dm^{-3} NaCl. The curves were generated from the M:L = 1:5 titration.*

The species distribution curves *fig 4.5* show that at low pH values, the mole fraction of Mg(II), was found to be at its maximum, *i.e.* 100%. However, it decreases gradually as the pH increases. The complex MgL, was present only at intermediate pH values. The second complex $MgLH_{-1}$, was also found at higher pH values and in large abundance (*i.e.* 75.0%) at pH 11. At pH 7.4, the Mg(II) and the complex $MgLH_{-1}$ were present at mole fraction of 50%.

4.2.2.2 Calcium (II) with ITB

In the case of Ca(II), the equilibrium was M + L + OH ⇌ MLH_{-1} and its logβ was found to be 5.43. The standard deviation obtained for the formation constant as well as the Hamilton R- factor are low and the calculated and experimental $\bar{Q}$ curves (*fig.4.6*) follow each other satisfactorily. This lends

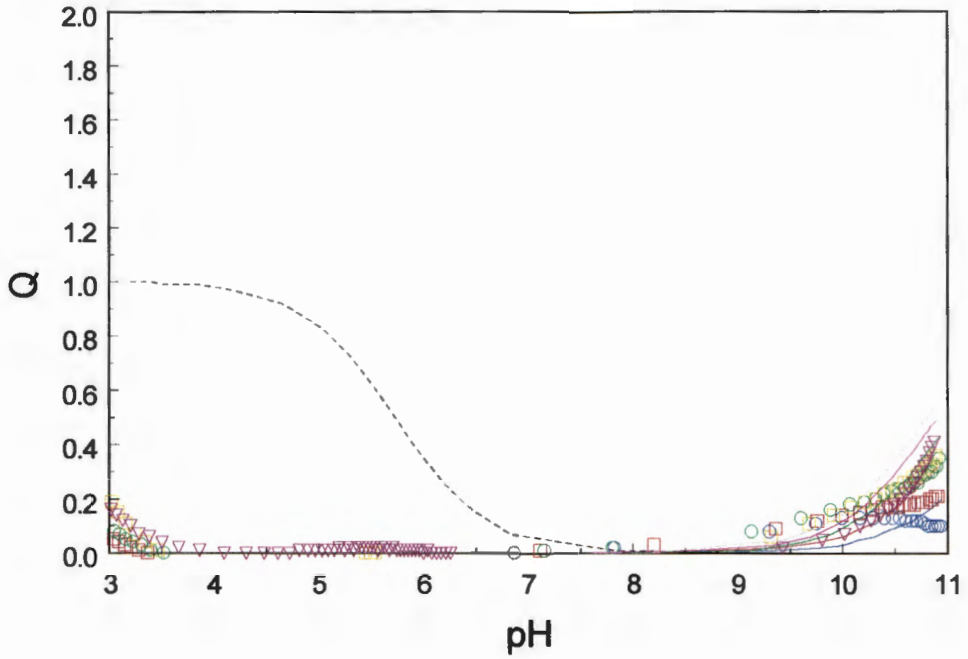

Figure 4.6: *Experimental (points) and calculated (lines) deprotonation curves for Ca(II) complexation by ITB.* $\bar{Q}$ *is the deprotonation function and the dashed line is* $\bar{n}$ *curve. The five separate titration M:L ratios are (o)1:1,(□) 1:2, (△)1:3, (◇)1:4 and (▽)1:5.*

confidence in the model obtained. At high pH, the $\bar{Q}$ rises above $\bar{n}$. When the $\bar{n}$ curve is below $\bar{Q}$, this is an indication that hydroxy species will be formed or the ligand loses more protons than expected [74]. This is verified by the presence of MLH_{-1} in the model. The $\bar{Q}$ curves also showed that below pH7, no complexation occurred. This implies that little Ca(II) is complexed at physiological pH by the ligand. This is an encouraging result as possible side effects due to mobilisation of Ca(II) will be minimised.

The $\bar{Z}$ curves showed that little or no complexation takes place as only few data points for $\bar{Z}$ rise above zero at high pH.

Modelling results, have shown both metal ions to have (11-1) models. The stability constants for the metal ions Ca(II) and Mg(II), were found to be 5.43 and 5.92 respectively, for this equilibrium. According to the Irving-Williams series, for a given ligand, the stability of complexes with dipositive metal ions follows the order: $Ba^{2+} < Sr^{2+} < Ca^{2+} < Mg^{2+} < Mn^{2+} < Fe^{2+} < Co^{2+} < Ni^{2+} < Cu^{2+} > Zn^{2+}$. This order arises in part from a decrease in size across the series and in part from the ligand field effects. The results obtained for both Ca (II) and Mg (II), thus follows the Irving Williams series, with Mg (II) stability being greater than Ca (II) stability [71].

For Ca(II), the ML species, as found for Mg(II), was absent. This is probably due to the very weak or non-existent complexation of Ca(II) at intermediate pH values by ITB.

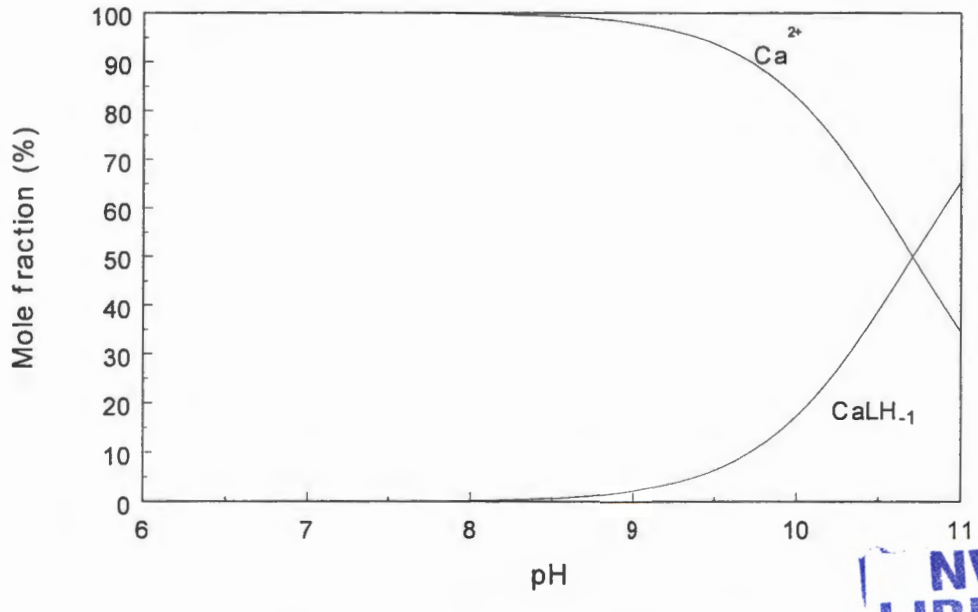

Figure 4.7: *Species distribution curves for the complexation of Ca(II) by ITB at 25°C and in 0.15 mol dm^{-3} NaCl. The curve was generated from the fifth titration (M:L = 1:5 ratio)*

The species distribution curves (*fig 4.7)* show that at low pH values, the mole fraction of Ca(II), is at its peak (100%), and as the pH increases, it decreases

to a lower value of 34.8% at pH 11. The only complex that is present is $CaLH_1$ with mole fraction of 65.2% at pH 11. As the ratio of metal to ligand increases, the abundance of the complex also tends to increase.

4.2.3 Complexation of Transitional Metals by ITB

Table 4.4: *Formation constant for Ni(II), Cu(II) and Zn(II) complexation by ITB.*

Cation	*Equilibrium*	*Log K*	*Hamilton R-factor*	*Hamilton R-limit*	*Data points*
Ni(II)	$M + 2L + 2OH \rightleftharpoons ML_2H_{-2}$	19.14 ± 0.01	0.0108	0.00157	190
Zn(II)	$M + 2L + 2OH \rightleftharpoons ML_2H_{-2}$	17.04 ± 0.02	0.0268	0.00139	337

4.2.3.1 Copper(II) with ITB

Formation constants of copper and ITB could not be determined potentiometrically due to immediate precipitate formation at low pH. The precipitate persisted over the whole pH range. ESTA is unable to interpretate data under these conditions. The precipitating complex is expected to be CuL_2H_{-2} as found for Zn(II) and Ni(II). This is a neutral species and therefore susceptible to precipitation.

4.2.3.2 Nickel (II) with ITB

Data points were deleted where precipitation occurred. The calculated and experimental deprotonation (*fig.4.8*) curves follow each other satisfactorily indicating the plausibility of the model. The $\bar{Q}$ curves obtained for nickel shows that $\bar{n}$ = 0 and $\bar{Q}$ = 2 at pH 8, thus two protons are lost by the ligand due to

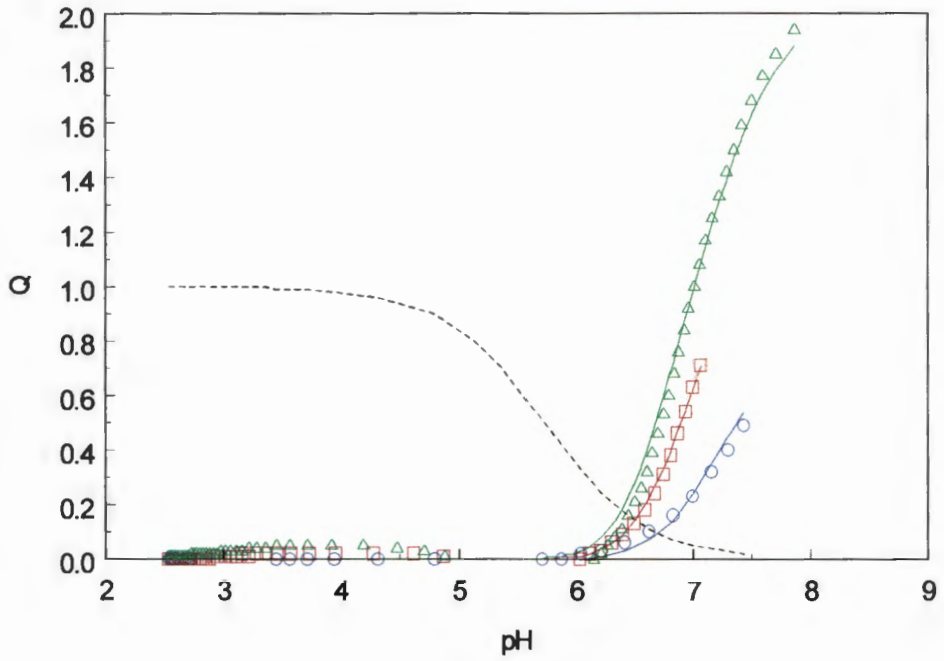

Figure 4.8: *Experimental (points) and calculated (lines) deprotonation curves for Ni(II) complexation by ITB.* $\bar{Q}$ *is the deprotonation function and the dashed line is* $\bar{n}$ *curve. The three separate titrations are represented by the symbols 1:1 (○), 1:2 (□) and1:3 (△) M:L ratios.*

complexation. From pH 6.5, the $\bar{n}$ curve is below the $\bar{Q}$ curves which is also an indication that more protons are detected in the system than expected from the ligand, thus, at pH 7 the modelled complex NiL_2H_{-2} predominates. The ML_2H_{-2} species in solution is expected to be similar to that in *fig.2.18*, found in the solid state. The colour of the precipitate generated at pH values higher than 8 was yellow-orange which corresponds to the colour reported for the compound in *fig.2.18*.

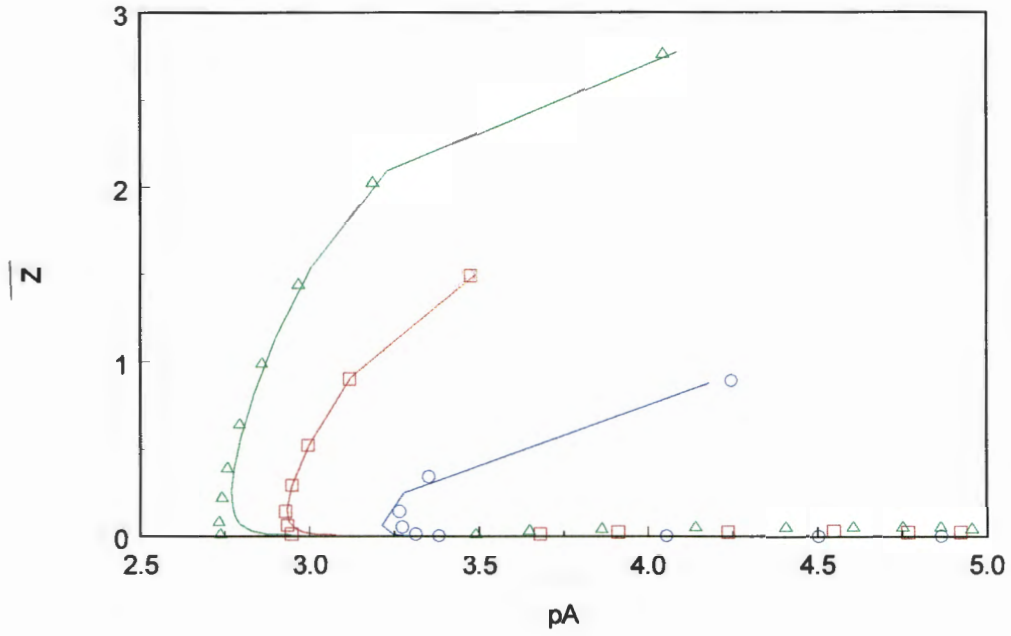

Figure 4.9: *Experimental points and calculated (lines) formation curves for Ni(II) complexation by ITB. $\overline{Z}$ is the formation function and the pA is the negative logarithm of the free ligand concentration. The three separate titration are represented by the symbols 1:1 (○), 1:2 (□) and1:3 (△) ratios.*

The calculated and experimental formation function curves $\overline{Z}$ are presented in *fig 4.9*. Backfanning observed at low pA indicates the loss of more protons due to complexation than expected.

The species distribution curves (*fig 4.10*) show that Ni(II) is complexed by ITB above pH6. It is fully complexed as NiL_2H_{-2} at pH 8.5 and precipitates. No other complexes were found since the data were deleted above pH 8. At physiological pH 7.4 ± 72% of the Ni(II) is complexed as NiL_2H_{-2}.

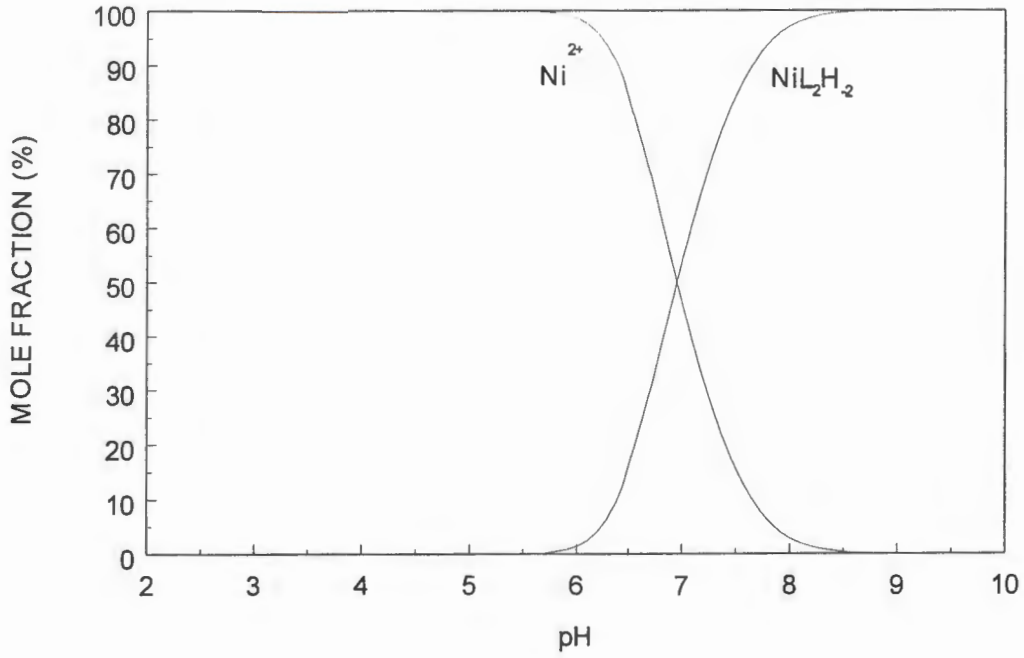

Figure 4.10: *Species distribution curves for the complexation of Ni(II) by ITB at 25.0 ± 0.1°C and 0.15 mol dm^{-3} NaCl. The curves were generated from the M:L=1:3 titration.*

4.2.3.3 Zinc(II) with ITB

Data points were deleted where precipitate occurred. The calculated and experimental deprotonation curves (*fig. 4.11*) follow each other satisfactorily indicating the plausibility of the model. At pH7, $\bar{n}$ is below $\bar{Q}$ curves which indicates that more protons are detected in the system than expected from the ligand. This can be represented by M + 2L - 2H ⇌ $M(LH_{-1})_2$ = ML_2H_{-2} which concludes that from pH7 the modelled complex ZnL_2H_{-2} predominates. The colour of precipitate obtained was white tiny particles which were at first difficult to notice. This probably is the reason why $\bar{Q}$ and $\bar{Z}$ fits are not as good as for Ni(II) and the standard deviation and the Hamilton R-factor if high

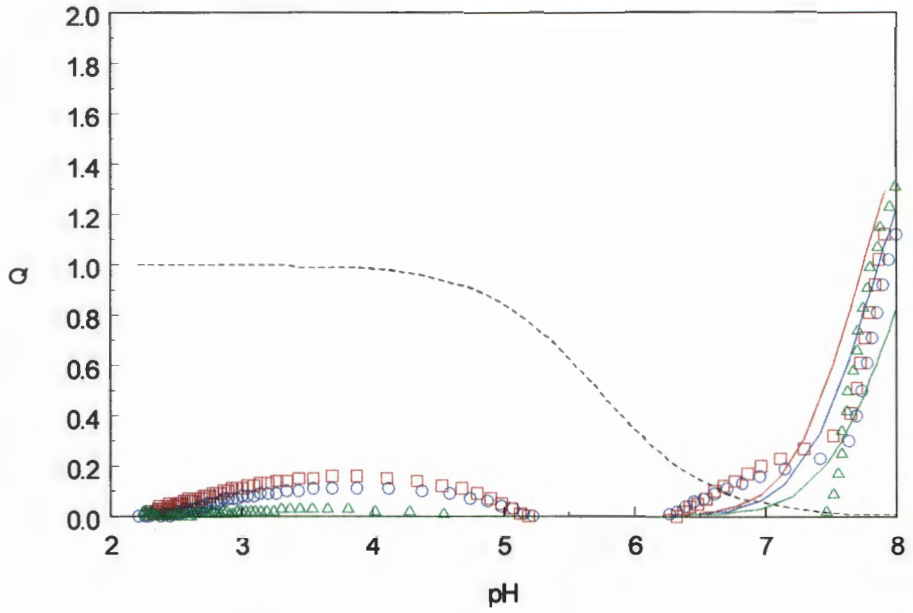

Figure 4.11: *Experimental (points) and calculated (lines) deprotonation curves for Zn(II) complexation by ITB.* $\bar{Q}$ *is the deprotonation function and the dashed line is* $\bar{n}$ *curve. The three separate titrations are represented by the symbols 1:1 (○), 1:2 (□) and1:3 (△) M:L ratios.*

The calculated and experimental formation function curves $\bar{Z}$ follow each other satisfactorily and are presented in *fig. 4.12.* Backfanning was observed at low pA values indicating the loss of more protons than expected as a result of complexation.

The species distribution curves (*fig.4.13)* show that Zn(II) is complexed by ITB above pH6. At pH 9, it is fully complexed as ZnL_2H_{-2} and hence it precipitates. Due to deletion of some data points at pH above 8, no other complexes could be found. At physiological pH 7.4, ± 30% of Zn(II) is complexed as ZnL_2H_{-2}.

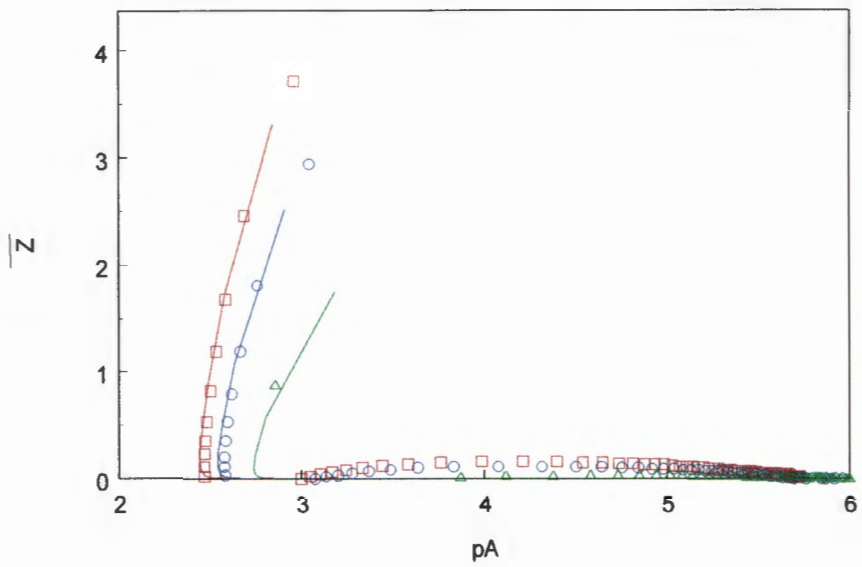

Figure 4.12: *Experimental points and calculated (lines) formation curves for Zn(II) complexation by ITB.* $\overline{Z}$ *is the formation function and the pA is the negative logarithm of the free ligand concentration. The three separate titration are represented by the symbols 1:1 (○), 1:2 (□) and1:3 (△) M:L ratios.*

Ni(II) and Zn(II) are both borderline acids. Ni(II) has an atomic radius of 0.69Å while Zn(II) has a radius of 0.74Å. Both these metal ions are transitional elements in the same period. Based on their atomic radii and atomic number, Ni(II) is more acidic than Zn(II).

Considering the metal ions with $3d^n$ configuration, the stability increases with the increase of atomic number. This is in accordance with the Irving-Williams's natural order of stability for complexes, which is Mn < Fe < Co < Ni < Cu > Zn [75].

Both metal ions have a (12-2) model. The stability constants for Ni(II) and Zn(II) were found to be 19.14 and 17.04 respectively. According to Irving Williams series, $Co^{2+} < Ni^{2+} < Cu^{2+} > Zn^{2+}$, Ni(II)'s stability is less than that of

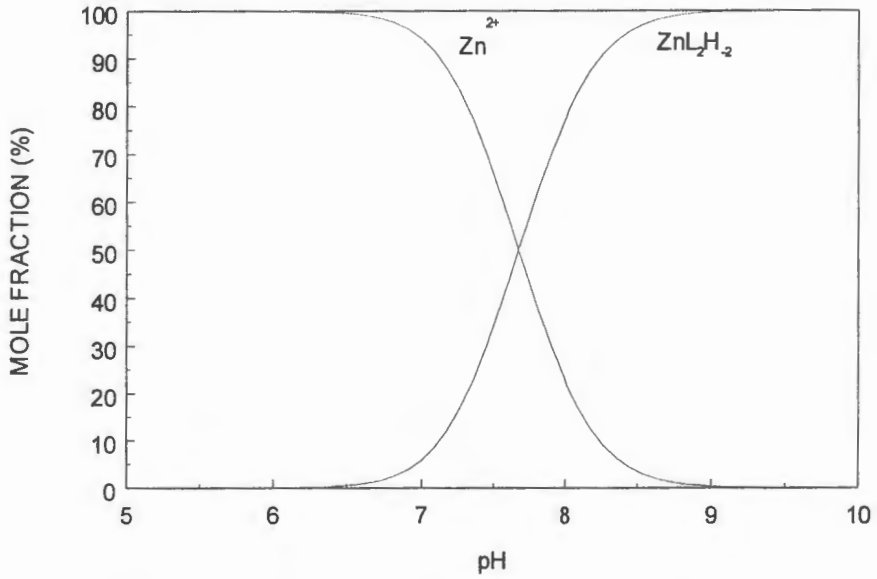

***Figure 4.13**: Species distribution curves for the complexation of Zn(II) by ITB at 25.0 ± 0.1°C and 0.15 mol dm^{-3} NaCl. The curves were generated from the M:L=1:3 titration*

Cu(II), which is greater than Zn(II). The results obtained are as follows: Ni(II) = 19.14 < Cu(II) = x > Zn(II) = 17.04. It is most unfortunate that Cu(II), could not be investigated, due to precipitate formation, with potentiometric methods. If Cu(II) should also follow the series, the following can be predicted: high formation constant and more stable than Ni(II) and Zn(II).

4.3 Results of ECCLES modelling with ITB

To determine the speciation of ITB in blood plasma under actual clinical conditions, a concentration of 8.5×10^{-5}M ITB was investigated. In experience with other radiopharmaceuticals, this represents a likely clinical concentration for the ligand.

The speciation results of ITB in blood plasma are given in Table 4.5 and *fig.4.14*. It can be seen that Mg(II) is the only metal ion complexed at

physiological pH and only to a very small extent. Therefore ITB will not mobilise Ca(II), Ni(II) and Zn(II) at physiological pH. This is a gratifying result as ITB will not be expected to produce side-effects due to metal-ion mobilisation.

Table 4.5: *Speciation of ITB in normal blood plasma as calculated by ECCLES. L=ITB*

Species	***Mol %***
L	87.7
$[MgL]^{2+}$	10.4
$[LH]^{+}$	1.9
$[MgLH_{-1}]^{+}$	0.0
$[CaLH_{-1}]^{+}$	0.0
ZnL_2H_{-2}	0.0
NiL_2H_{-2}	0.0

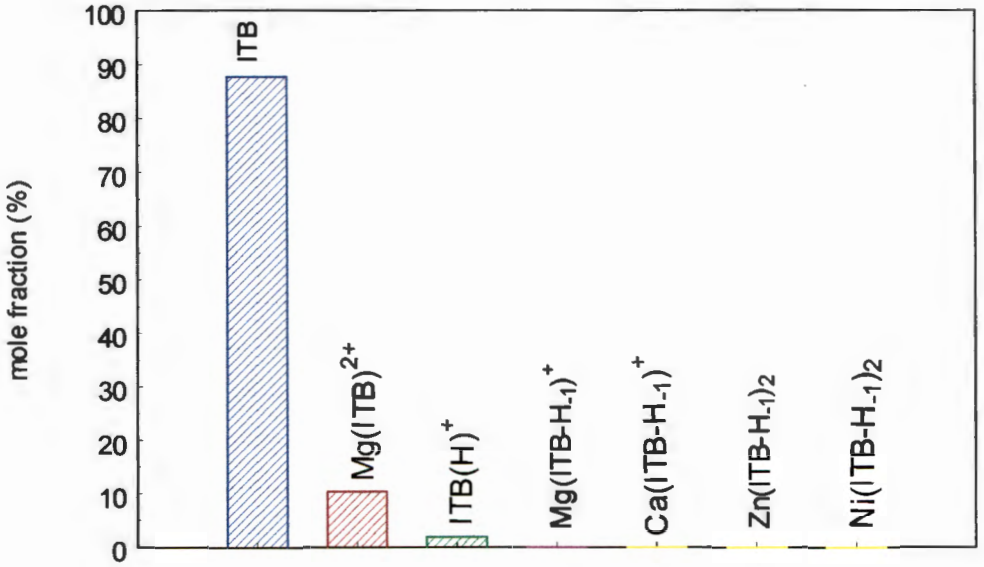

Figure 4.14*: Speciation of ITB in normal blood plasma.*

For comparison, the speciation of the blood plasma metal-ions were investigated in normal plasma and in the presence of ITB, (appendix D,E). The following results were observed: MgITB contributes 1.3% to the total Mg(II) speciation while CaITB, $Zn(ITB)_2H_{-2}$ and $Ni(ITB)_2H_{-2}$ do not contribute significantly to the total Ca(II), Zn(II) and Ni(II) speciation.

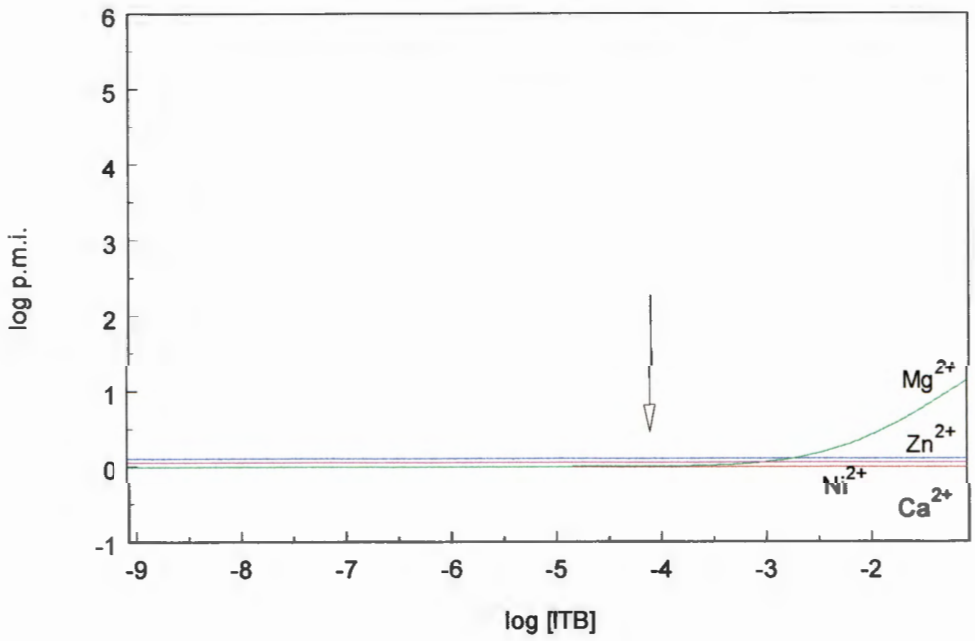

Figure 4.15: *p.m.i curve for ITB*

The graph in *fig. 4.15* shows the mobilisation of metal ions by ITB. The p.m.i curves show that the only significant mobilisation taking place is for Mg(II) at high ligand concentration, while Ca(II), Zn(II) and Ni(II) are not mobilised by ITB even at a concentration of 8.5×10^{-2}mol.dm^{-3}. The arrow indicates the likely clinical concentration of ITB. At this value, none of the metal ions are mobilised.

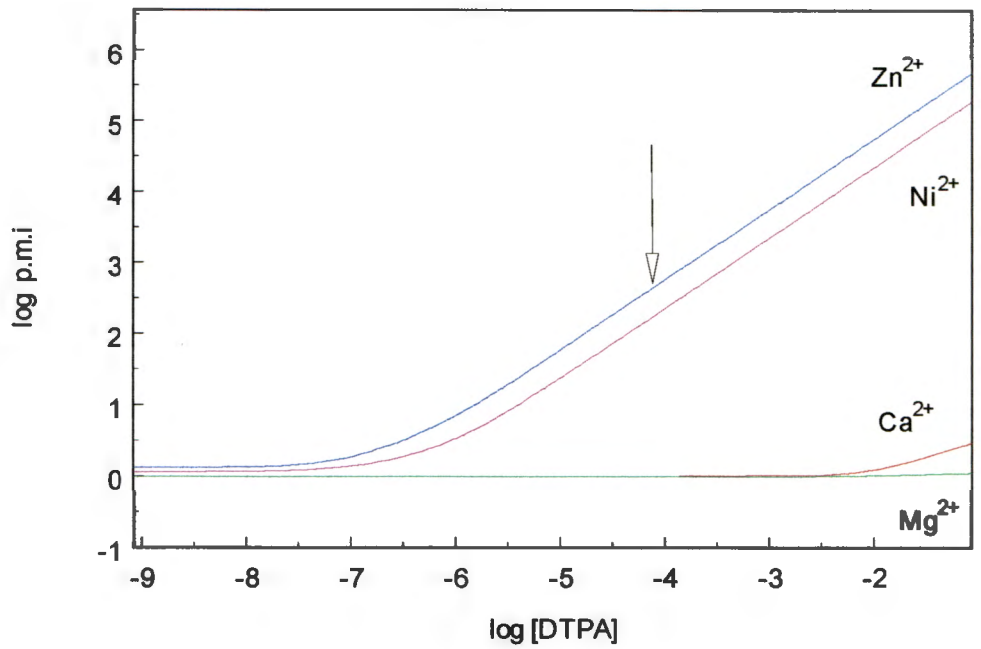

Figure 4.16: *p.m.i. curve for DTPA*

In contrast to this, DTPA, a ligand used in kidney imaging agents, significantly mobilises Zn(II) and Ni(II) as indicated in *fig. 4.16*. This illustrates the potential improvement of ITB over DTPA and other conventional ligands in minimising side-effects due to metal ion mobilisation.

4.4 Radiochemistry Results On ^{99m}Tc-ITB Labeling

Radioactive preparations with radiochemical purity of 92.26%, were identified. The ^{99m}Tc-ITB complex evaluated on Whatman no 1 paper remained at the origin, whereas on ITLC-SG it migrates with the solvent front as a single peak. In order to determine the amount of colloid formed, ITLC –t- butanol saturated with 0.4M HCl was used and the colloid formed was 2.38%.

CHAPTER 5 CONCLUSION AND FUTURE WORK

Labelling of ITB at pH7.4 with ^{99m}Tc, was more than 90%. Therefore at physiological pH, ITB strongly complexes ^{99m}Tc and not Ca(II), Mg(II), Zn(II) and Ni(II). This indicates the excellent selectivity offered by ITB for ^{99m}Tc over blood plasma metal-ions. This finding is sufficient to recommend that ^{99m}Tc-ITB be subjected to pre-clinical trials.

Future work will include the following:

(i) Investigational studies will be done on baboons. Furthermore, pre-clinical trials will carried out on animals and on terminal cancer patients. If positive results are obtained, Medicine Control Council approve the new radiopharmaceuticals i.e. (^{99m}Tc-ITB).

(ii) Polarography (instead of Potentiometry) should be used for metal ions that formed a precipitate with ITB, i.e. Cu(II), Ni(II) and Zn(II).

CHAPTER 6 REFERENCES

1. O Knoesen, Ferrocenyl Ligands in Complexes of Technetium and Rhenium, PhD Thesis, University of Pretoria, p 12-18, (2000).
2. D P. Swanson, H.M. Chilton, J H. Thrall, Pharmaceuticals in Imaging, p 280.
3. A. Marchi, M. Neves, I. Marvelli, M. Cattabriga, R. Rossi, V. Bertolasi, V. Ferretti, Technetium, Rhenium and other Metals in Chemistry and Nuclear Medicine, 5thedition, p 271-275, (1999).
4. Dr WKA Louw, NECSA, Radiochemistry Department, PO Box 582, Pretoria, South Africa.
5. D.M. Taylor and D.R. Williams, Trace Element Medicine and Chelation Therapy, p 33-35, (1995).
6. A Taylor,Jr, Radiology, vol. 136, p 449-453, (1980).
7. A.Piepsz, M Tondeur, J Kinthaert, H.R. Ham, European Journal of Nuclear Medicine, vol. 23 (2), p 195-198, (1996).
8. M. Neves, L. Gano, M. J Ribeiro, A. C. Santos, A. Marchi, C.S. Dimopolou and J.J. Pedroso de Lima, Nuclear Medicine and Biology, vol. 26, p 79 - 83, (1999).
9. A. Marchi, L. Marvelli, M. Cattabriga, R. Rossi, M. Neves, V. Bertolasi and V. Ferretti, Journal of Chemical Society, Dalton Trans, p 1937-1947, (1999).
10. H.P. Vanbilloen, N.A. Dezutter, B J. Cleynhens, A.M. Verbruggen, European Journal of Nuclear Medicine, vol. 24 (11), p 1374-1379, (1997).
11. M. Daly, W Jones, T Rudd and J Tremann, Journal of Nuclear Medicine, vol. 20, p 63-66, (1979).
12. L. Hansen, M. Lipowska, L.G. Marzilli and A. Taylor, Proceedings of the 43rd Annual meeting, vol. 37 (5), p 17N, (1996) supplement.
13. http://nm.mt.kmc.edu.tw/clinic/renal.html,p1.
14. L Kabasakal, European Journal of Nuclear Medicine, vol. 27 (3), p 351-357, (2000).
15. C.De Sadeleer, M Tondeur, K. Melis, M.B Van Espen and J Verelst, Journal of Nuclear Medicine, vol. 41 (1), p 23-26, (2000).

16. W.C. Eckelman, Journal of Nuclear Medicine Technology, vol. 20 (3), p 135-138, (2000).
17. A. Nunn, Radiopharmaceuticals Chemistry and Pharmacology, Drugs and the Pharmaceutical Sciences, 55, p366-369, (1993).
18. A R Fritzberg, Journal of Nuclear Medicine Technology, vol.12, p 178-181, (1984).
19. Ai-Yih-Wang, Journal of Radioanalytical and Nuclear Chemistry, vol. 230 (1-2), p 79-82, (1998).
20. http://urology channel.com/kidney cancer/index.shtml, p 1-16.
21. K. Zum. Winkel, H. Jost, F. Motzkus and G. Golde, IAEA, Dynamic studies with Radioisotopes in Medicine, p 229, (1971).
22. D. Blaufox, Journal of Nuclear Medicine, 32, p 1301-1309, (1991).
23. D. Jansen, The Principles of Physiology, 2nd edition, p 720.
24. N Oriuchi, T Inoue, I Hayashi, S Mizuiri, N Kosaka and J. Nishikawa, European Journal of Nuclear Medicine, vol. 23 (4), p 371-375, (1996).
25. A.Chachati, A. Meyers, J.P. Godon and P. Rigo, Journal of Nuclear Medicine, vol. 28, p 829-836, (1987).
26. R G Woolfson and G. H. Neild, European Journal of Nuclear Medicine, vol. 24 (5), p 557-570, (1997).
27. http://www.meb.unu-bonn.de/cancernet/101070.html, p 1-9.
28. http://www.uic.edu/com/uhrd/nucmed/introc.htm. p 1-3.
29. H.J. Glen, H.J. Glen, T.P. Haynie and T. Konikowiski, IAEA, Tumour Localization with Radioactive Agents, vol.II, p 82-89, (1976).
30. M L. Thakur, C.S. Marcus, S. Saeed, V. Palella, C. Minami, L. Diggles, H. Le Pham, R. Ahdoot and E.A. Kalinowski, Journal of Nuclear Medicine, vol. 41, p 107-110, (2000).
31. M. Neves and R. Fausto, Nuclear Medicine and Biology, vol. 26, p 85-89, (1999).
32. http://mfs.med.utokai.ac.jp/radiology/hypertension/tc99mdtpa.html.,
33. H.L. Atkins, J.F. Klopper, W.C. Eckelman, P. Richards, IAEA, p 251, (1972).

34. C. Constatinides, P. Kostamis, D. Binopoulos, A. Pachos and J. Constantes, IAEA; p 273, (1970).
35. A Taylor, D Eshima, A.R. Fritzberg, P.E. Christian and S. Kasina, Journal of Nuclear Medicine, vol. 27, p 795-803, (1986).
36. A. Nunn, Radiopharmaceuticals Chemistry and Pharmacology Drugs and the Pharmaceutical Sciences, 55, p 384-390, (1993).
37. S. Gacinovic, J. Buscombe, D. Costa, A.Hilson, J. Bomanji and P.J. Ell, Nuclear Medicine Communication, vol.17, p 596-602, (1996).
38. O. Knoesen, Ferrocenyl Ligands in Complexes of Technecium and Rhenium, PhD Thesis, University of Pretoria, p 23, (1999).
39. R. A. Kengen, Sytse Meijer, H. Beekhuis and D. Albertus Piers, Journal of Nuclear Medicine, vol. 32, p 1709-1712, (1991).
40. G.F. Fresco, F Digiorgio and G.L. Curti, Journal of Nuclear Medicine, vol. 36, p 1701-1706, (1995).
41. L. Kabasakal, H.T Turoglu, C. Onsel, K Ozker, I. Uslu, S. Atay, T. Cansiz, K. Sonmezoglü, E. Altiok, A.T. Isitman, T. Kapicioglü and I. Urgancioglü, Journal of Nuclear Medicine, vol. 36 (2), p 224-228, (1995).
42. A Taylor, P L. Corrigan, J Galt, E Garcia, R Folks, M Jones, A. Manatunga and D. Eshima, Journal of Nuclear Medicine, vol. 36, p 1689-1695, (1995).
43. V. Lee, J. Allard, J. Foster, K. Sheahan and P. Franklin, Journal of Nuclear Medicine, vol. 28, p 1911-1914, (1987).
44. R. Muller-Suur and H.U. Gutshe, Journal of Nuclear Medicine, vol. 36, p 1654-1658, (1995).
45. V. Nerom, G. Bosmans, A. Verbruggen, B. Cleynhens, D. Nosco and De Roo, European Journal of Nuclear Medicine, 37th Annual Meeting, p 806, (1999).
46. M. Stoffel, F. Jamar, C. Van Nerom, A. Verbruggen, T. Besse, J.P. Squifflet and C. Beckers, European Journal of Nuclear Medicine, vol. 23 (4), p 365-370, (1996).
47. A. Taylor, L. Hansen, D. Eshima, E. Malveaux, R. Folks, L. Shattuck, M. Lipowska and L. G. Martzilli, Journal of Nuclear Medicine, vol. 38, p 821-826, (1997).
48. L. Kabasakal, S. Atay, V.A. Vural, K. Ölzker, K. Sönmetzoglu, M. Demir, I. Uslu, A.T. Isitmam and C. Önsel , Journal of Nuclear Medicine, vol. 36 (8),

p 1398-1403, (1995).

49. K. Sonmezoglu, T. Yusuf, M. Demir, H. Soyman, L. Kabasakal, K.E. Britton, K. Solaki, M. Cem Mat and H. Özkara, European Journal of Nuclear Medicine, vol. 25 (12), p 1630-1636, (1998).
50. K. Otzker, L. Kabasakal, T.Cansiz, C. Önsel, H.B. Sayman, I. Uslu, S. Bozluolcay, T. Cni, T. Kapicioglu and I. Urganciglu, Journal of Nuclear Medicine, vol. 35 (5), p 840-845, (1994).
51. Y. Inoue, T. Ohtake, I. Yokoyama, K. Yoshikawa, S. Asai and K. Ohtomo, Journal of Nuclear Medicine, vol. 40 (5), p 793, (1999).
52. G. Olah, A. Burrichter, G. Rasul , K.O. Christe and G.K. Surya Prakash, Journal of American Society, vol. 119, p 4345-4352, (1997).
53. P. Ray, Chemical Review, vol. 61, p 316-327, (1961).
54. R. Vilar, D.M. Mingos, A.J.P. White and D. Williams, Chemical Communications, p 229-230, (1999).
55. . F.J.C. Rossotti and H. Rossotti, The Determination of Stability Constants, p127-128, (1961).
56. J.R. Zeevaart, Complexation of Trivalent Lanthanides by Three Diphosphonate ligands in Blood Plasma, p 18-37, (1997).
57. N.V. Jarvis, N,N–N',N'–Octaalkylimidodiphosphotetramide and Hydroxyalkylamine Ligands as Complexing Agents for f-Transition metals, p 90-94, (1991).
58. Application Bulletin Metrohm, No 101/2 e p 1-4.
59. A.F. Cotton and G. Wilkinson, Advanced Inorganic Chemistry, 4th ed, p 67-69, (1980).
60. K. Murray and P.M. May, ESTA notes
61. N. V.Jarvis and J. Wagener, Talanta, vol.41(5), p 747-754, (1994).
62. G. Berthon, B. Hacht, M.J Blais and P. May, Inorganica Chimica Acta 125, p 219-227, (1986).
63. J.R Zeevaart, N. Jarvis, W. Louw, G. Jackson, I. Cukrowski and C.J. Moutori, Journal of Inorganic Biochemistry, vol.73, p 265-272, (1999).
64. G. Jackson and M. Kelly, Journal of Chemical Society, p 2429, (1989).
65. J.A Findlow, J.R.Duffield and D.R Williams, Chemical Speciation and Bioavailability 2, p 3-32, (1990).
66. G. Christian, Analytical Chemistry, 5th ed, p 319-320.

67. P. May, K. Murray and D. Williams, Talanta, vol. 35 (11), p 825-830, (1988).
68. P. May and P. Linder, Journal of Chemical Society Daltons, p588-595, (1977).
69. J.R Zeevaart, N.V.Jarvis, I. Cukrowski and G.E.Jackson, South African Journal of Chemistry, vol. 50 (4) p 189-194, (1997).
70. D.M.Taylor and D.R. Williams, Trace Element Medicine and Chelation Therapy, p 39-41, (1995).
71. R D. Hancock and A.E. Martell, Chemical Review 89, p 1875-1914, (1989).
72. M. Edwin, Metal ion Speciation In Blood Plasma Incorporating Biguanide and Biuret As Potential Kidney Imaging Agents, MSc Thesis, University of The North West, (2000).
73. R.M Smith and A.E. Martell, Critical Stability Constants, vol.3, Plenum, New York, 2nd print, (1989).
74. G.E .Jackson, South African Chem, vol.35, p 89-92, (1982).
75. J E. Huheey, Inorganic Chemistry, Principles of Structures and Reactivity, 3rd edition, p 312-325, (1980).

CHAPTER 7 APPENDIXES

Appendix A: Potentiometic titration datasheet : initial and final values.

1. Protonation of ITB
2. Magnesium(II)-ITB
3. Calcium(II)-ITB
4. Nickel(II)-ITB
5. Zinc(II)-ITB

Appendix B: ESTA2A input data files of protonation titration and complexation titrations with ITB.

1. Protonation of ITB
2. Mg(II)-ITB
3. Ca(II)-ITB
4. Ni(II)-ITB
5. Zn(II)-ITB

Appendix C: ESTA2A output data files of protonation titration and complexation titrations with ITB.

1 Protonation of ITB
2. Mg(II)-ITB
3. Ca(II)-ITB
4. Ni(II)-ITB
5. Zn(II)-ITB

Appendix D: ECCLES input files.

Appendix E: ECCLES output files.

Appendix A

Potentiometric titration datasheet - Initial and final values

1 Protonation of ITB

	Titration 1	Titration 2	Titration 3
[ITB]	0.0009935	0.0019871	0.0029807
[Acid]			
initial	0.0098920	0.0095488	0.0095488
Final	0.0097760	0.0095399	0.0095542
[OH]	0.050812	0.050036	0.050036
E0			
Initial	406.126	405.663	405.952
Final	406.211	406.043	405.663
Gradient			
initial	58.764	58.711	58.711
Final	58.760	58.663	58.659

2 Magnesium(II) - ITB

	Titration 1	Titration 2	Titration 3	Titration 4	Titration 5
[ITB]	0.0009935	0.0019871	0.0029807	0.0040014	0.0050017
[Mg^{2+}]	0.0009904	0.0009904	0.0009904	0.0009904	0.0009904
[Acid]					
initial	0.0095429	0.0093807	0.0093807	0.0094647	0.0094647
Final	0.0096070	0.0095931	0.0095364	0.0097249	0.0097269
[OH]	0.050036	0.050036	0.050036	0.0504515	0.0504515
E0					
Initial	408.452	409.090	409.090	405.015	405.015
Final	407.874	401.962	398.411	394.415	395.226
Gradient					
Initial	58.730	58.780	58.780	59.057	59.057
Final	58.794	58.453	58.277	58.700	58.660

3 Calcium (II) - ITB

	Titration 1	Titration 2	Titration 3	Titration 4	Titration 5
[ITB]	0.0009935	0.0019871	0.0029807	0.0040014	0.0050017
$[Ca^{2+}]$	0.0009515	0.0009515	0.0009515	0.0009515	0.0009515
[Acid]					
initial	0.0096129	0.0096129	0.0097890	0.0098620	0.0098481
Final	0.0096954	0.0096774	0.0098101	0.0096945	0.0098172
[OH]	0.050036	0.050036	0.050036	0.0504515	0.0504515
E0					
Initial	403.628	403.628	401.654	398.920	403.541
Final	399.663	399.555	397.811	394.316	397.952
Gradient					
Initial	58.636	58.636	58.711	58.160	58.774
Final	58.555	58.628	58.734	58.267	58.892

4 Nickel(II) - ITB

	Titration 1	Titration 2	Titration 3
[ITB]	0.0009935	0.0019871	0.0029807
$[Ni^{2+}]$	0.0010341	0.0010341	0.0010341
[Acid]			
initial	0.0096889	0.0096730	0.0096889
Final	0.0096157	0.0095617	0.0096216
[OH]	0.050036	0.050036	0.050036
E0			
Initial	398.774	405.326	398.774
Final	398.964	401.064	398.547
Gradient			
Initial	58.203	58.557	58.203
Final	58.164	58.558	58.146

5 Zinc(II) - ITB

	Titration 1	Titration 2	Titration 3
[ITB]	0.0039709	0.0049636	0.0024818
$[Zn^{2+}]$	0.0009655	0.0009655	0.0009655
[Acid]			
initial	0.0101321	0.0101588	0.0081390
Final	0.0101009	0.0099075	0.0081429
[OH]	0.051214	0.051214	0.048200
E0			
Initial	405.395	403.748	407.971
Final	405.705	404.391	409.719
Gradient			
Initial	58.707	58.696	58.532
Final	58.623	58.415	58.869

Appendix B

Esta2a input datafiles of protonation titration and complexation titrations with ITB.

See disk 1

HITB1.DAT	original and final datafile
MGITBM.DAT	original datafile
MGITBM2.DAT	final datafile
CAITBJ.DAT	original datafile
CAITBJ2.DAT	final datafile
NIITB2.DAT	original datafile
NIITB6.DAT	final datafile
ZNITBE.DAT	original datafile
ZNITBE1.DAT	final datafile

Appendix C

Esta2a final output files of protonation titration and complexation titrations with ITB.

1 H-ITB model

```
PROGRAM ESTA2A          VERSION 3.0

  TASK OBJE  1       ITB0-ACID
  MODL     ITB0 H +1
  CPLX 0  1 -13.7900  ITB0( 0) H +1(-1)
  CPLX 1  1   5.7274  ITB0( 1) H +1( 1)
  CONC
  VESL IVOL    50.000  0 0
  VESL ITB0   .0009935  0 0
  VESL H +1   .0097760  0 0
  BUR1 H +1  -.0508120  0 0
  ELEC
  ZERO H +1    406.211    0
  GRAD H +1     58.760    0
  WGHT 1
  VESL ITB0   .0000019
  VESL H +1   .0000197
  BUR1 H +1  -.0001000
  ZERO H +1      .250
  GRAD H +1      .020
  TITR RNDE      .0010
  EOBS RNDE      .0800
  DATA

  CONC
  VESL IVOL    50.000  0 0
  VESL ITB0   .0019871  0 0
  VESL H +1   .0095399  0 0
  BUR1 H +1  -.0500360  0 0
  ELEC
  ZERO H +1    406.043    0
  GRAD H +1     58.663    0
  WGHT 1
  VESL ITB0   .0000039
  VESL H +1   .0000190
  BUR1 H +1  -.0001000
  ZERO H +1      .250
  GRAD H +1      .020
  TITR RNDE      .0010
  EOBS RNDE      .0800
  DATA

  CONC
  VESL IVOL    50.000  0 0
  VESL ITB0   .0029807  0 0
  VESL H +1   .0095542  0 0
  BUR1 H +1  -.0500360  0 0
  ELEC
  ZERO H +1    405.952    0
  GRAD H +1     58.659    0
  WGHT 1
  VESL ITB0   .0000059
  VESL H +1   .0000190
  BUR1 H +1  -.0001000
```

```
  TITR RNDE    .0010
  EOBS RNDE    .0800
  DATA


OPTIMIZATION CYCLE  0
**********
OVERALL OBJE OBJECTIVE FUNCTION:   6.2067E+02     (N-R ITERATIONS:  1093)
FORMATION CONSTANTS:
---------
COMPLEX NUMBER:      2
 LOG BETA:      5.7274

GAUSS-NEWTON:          INITIAL SLOPE =  -1.0602E-05

                SLOPE AT PREDICTED SOLUTION =  -4.6709E-08


OPTIMIZATION CYCLE  1
**********
OVERALL OBJE OBJECTIVE FUNCTION:   6.2067E+02     (N-R ITERATIONS:  2512)
FORMATION CONSTANTS:
---------
COMPLEX NUMBER:      2
 LOG BETA:           5.7274
 STD DEVN:           0.0113

GAUSS-NEWTON:          INITIAL SLOPE =  -2.0579E-10


OPTIMIZATION CYCLE  2   (CONVERGENCE)
**********
OVERALL OBJE OBJECTIVE FUNCTION:   6.2067E+02     (N-R ITERATIONS:  3931)
FORMATION CONSTANTS:
---------
COMPLEX NUMBER:      2
 LOG BETA:           5.7274
 STD DEVN:           0.0113
NO SIGNIFICANTLY CORRELATED PARAMETERS FOUND
HAMILTON R-FACTOR:  0.02682
HAMILTON  R-LIMIT:  0.00108
NO. OF TITRATIONS:   3       NO. OF POINTS:  600
Stop - Program terminated.
```

2 Mg(II)-ITB model

```
PROGRAM ESTA2A          VERSION 3.0

  TASK OBJE  1       ITB-MG+2
  MODL     MG+2 ITB0 H +1
  CPLX 0  1 -13.7900  MG+2( 0) ITB0( 0) H +1(-1)
  CPLX 0  1   5.7274  ITB0( 1) H +1( 1)
  CPLX 1  1   2.3558  MG+2( 1) ITB0( 1) H +1( 0)
  CPLX 1  1  -7.8525  MG+2( 1) ITB0( 1) H +1(-1)
  CONC
  VESL IVOL    50.000  0 0
  VESL ITB0   .0009935  0 0
  VESL MG+2   .0009904  0 0
  VESL H +1   .0096070  0 0
  BUR1 H +1  -.0500360  0 0
  ELEC
  ZERO H +1    407.874    0
  GRAD H +1     58.794    0
  WGHT 1
  VESL ITB0   .0000020
  VESL MG+2   .0000020
  VESL H +1   .0000190
  BUR1 H +1  -.0001000
  ZERO H +1       .250
  GRAD H +1       .020
  TITR RNDE      .0010
  EOBS RNDE      .0800
  DATA

  CONC
  VESL IVOL    50.000  0 0
  VESL ITB0   .0019871  0 0
  VESL MG+2   .0009904  0 0
  VESL H +1   .0095931  0 0
  BUR1 H +1  -.0500360  0 0
  ELEC
  ZERO H +1    401.962    0
  GRAD H +1     58.453    0
  WGHT 1
  VESL ITB0   .0000040
  VESL MG+2   .0000020
  VESL H +1   .0000190
  BUR1 H +1  -.0001000
  ZERO H +1       .250
  GRAD H +1       .020
  TITR RNDE      .0010
  EOBS RNDE      .0800
  DATA

  CONC
  VESL IVOL    50.000  0 0
  VESL ITB0   .0029807  0 0
  VESL MG+2   .0009904  0 0
  VESL H +1   .0095364  0 0
  BUR1 H +1  -.0500360  0 0
  ELEC
  ZERO H +1    398.411    0
  GRAD H +1     58.277    0
  WGHT 1
  VESL ITB0   .0000060
  VESL MG+2   .0000020
  VESL H +I   .0000190
  BUR1 H +1  .0001000
```

```
GRAD H +1      .020
TITR RNDE      .0010
EOBS RNDE      .0800
DATA

CONC
VESL IVOL     50.000  0 0
VESL ITB0   .0040014  0 0
VESL MG+2   .0009904  0 0
VESL H +1   .0097249  0 0
BUR1 H +1  -.0504515  0 0
ELEC
ZERO H +1    394.415    0
GRAD H +1     58.700    0
WGHT 1
VESL ITB0   .0000080
VESL MG+2   .0000020
VESL H +1   .0000190
BUR1 H +1  -.0001000
ZERO H +1      .250
GRAD H +1      .020
TITR RNDE      .0010
EOBS RNDE      .0800
DATA

CONC
VESL IVOL     50.000  0 0
VESL ITB0   .0050017  0 0
VESL MG+2   .0009904  0 0
VESL H +1   .0097269  0 0
BUR1 H +1  -.0504515  0 0
ELEC
ZERO H +1    395.226    0
GRAD H +1     58.660    0
WGHT 1
VESL ITB0   .0000080
VESL MG+2   .0000020
VESL H +1   .0000190
BUR1 H +1  -.0001000
ZERO H +1      .250
GRAD H +1      .020
TITR RNDE      .0010
EOBS RNDE      .0800
DATA


OPTIMIZATION CYCLE  0
*********************
OVERALL OBJE OBJECTIVE FUNCTION:    2.8417E+02      (N-R ITERATIONS:  654)
FORMATION CONSTANTS:
--------------------
COMPLEX NUMBER:       3         4
 LOG BETA:          2.3558    -7.8525

GAUSS-NEWTON:            INITIAL SLOPE =  -7.1948E-06

                  SLOPE AT PREDICTED SOLUTION  =  -3.3470E-07


OPTIMIZATION CYCLE  1
*********************
OVERALL OBJE OBJECTIVE FUNCTION:    2.8417E+02      (N-R ITERATIONS:  1498)
FORMATION CONSTANTS:
--------------------
```

LOG BETA: 2.3558 -7.8525
STD DEVN: 0.0420 0.0257

GAUSS-NEWTON: INITIAL SLOPE = -3.1022E-08

OPTIMIZATION CYCLE 2 (CONVERGENCE)
****
OVERALL OBJE OBJECTIVE FUNCTION: 2.8417E+02 (N-R ITERATIONS: 2343)
FORMATION CONSTANTS:

COMPLEX NUMBER: 3 4
LOG BETA: 2.3558 -7.8525
STD DEVN: 0.0420 0.0257
NO SIGNIFICANTLY CORRELATED PARAMETERS FOUND
HAMILTON R-FACTOR: 0.02808
HAMILTON R-LIMIT: 0.00167
NO. OF TITRATIONS: 5 NO. OF POINTS: 309
Stop - Program terminated.

3 Ca(II)-ITB model

```
PROGRAM ESTA2A        VERSION 3.0

 TASK OBJE 1       ITB-CA+2
 MODL     CA+2 ITB0 H +1
 CPLX 0  1 -13.7900  CA+2( 0) ITB0( 0) H +1(-1)
 CPLX 0  1  5.7274  ITB0( 1) H +1( 1)
 CPLX 1  1  -8.3600  CA+2( 1) ITB0( 1) H +1(-1)
 CONC
 VESL IVOL    50.000  0 0
 VESL ITB0   .0009935  0 0
 VESL CA+2   .0009515  0 0
 VESL H +1   .0096954  0 0
 BUR1 H +1  -.0500360  0 0
 ELEC
 ZERO H +1   399.663   0
 GRAD H +1    58.555   0
 WGHT 1
 VESL ITB0   .0000020
 VESL CA+2   .0000020
 VESL H +1   .0000240
 BUR1 H +1  -.0001000
 ZERO H +1      .250
 GRAD H +1      .020
 TITR RNDE      .0010
 EOBS RNDE      .0800
 DATA

 CONC
 VESL IVOL    50.000  0 0
 VESL ITB0   .0019871  0 0
 VESL CA+2   .0009515  0 0
 VESL H +1   .0096774  0 0
 BUR1 H +1  -.0500360  0 0
 ELEC
 ZERO H +1   399.555   0
 GRAD H +1    58.628   0
 WGHT 1
 VESL ITB0   .0000040
 VESL CA+2   .0000020
 VESL H +1   .0000200
 BUR1 H +1  -.0001000
 ZERO H +1      .250
 GRAD H +1      .020
 TITR RNDE      .0010
 EOBS RNDE      .0800
 DATA

 CONC
 VESL IVOL    50.000  0 0
 VESL ITB0   .0029807  0 0
 VESL CA+2   .0009515  0 0
 VESL H +1   .0098101  0 0
 BUR1 H +1  -.0500360  0 0
 ELEC
 ZERO H +1   397.811   0
 GRAD H +1    58.734   0
 WGHT 1
 VESL ITB0   .0000060
 VESL CA+2   .0000020
 VESL H +1   .0000200
 BUR1 H +1  -.0001000
 ZERO H +1      .250
```

```
TITR RNDE     .0010
EOBS RNDE     .0800
DATA

CONC
VESL IVOL    50.000  0 0
VESL ITB0   .0040014  0 0
VESL CA+2   .0009515  0 0
VESL H +1   .0096945  0 0
BUR1 H +1  -.0504515  0 0
ELEC
ZERO H +1    394.315    0
GRAD H +1     58.267    0
WGHT 1
VESL ITB0   .0000080
VESL CA+2   .0000020
VESL H +1   .0000200
BUR1 H +1  -.0001000
ZERO H +1      .250
GRAD H +1      .020
TITR RNDE     .0010
EOBS RNDE     .0800
DATA

CONC
VESL IVOL    50.000  0 0
VESL ITB0   .0050017  0 0
VESL CA+2   .0009515  0 0
VESL H +1   .0098172  0 0
BUR1 H +1  -.0504515  0 0
ELEC
ZERO H +1    397.952    0
GRAD H +1     58.892    0
WGHT 1
VESL ITB0   .0000080
VESL CA+2   .0000020
VESL H +1   .0000200
BUR1 H +1  -.0001000
ZERO H +1      .250
GRAD H +1      .020
TITR RNDE     .0010
EOBS RNDE     .0800
DATA


OPTIMIZATION CYCLE  0
*********************
OVERALL OBJE OBJECTIVE FUNCTION:    1.8339E+02      (N-R ITERATIONS:  627)
FORMATION CONSTANTS:
--------------------
COMPLEX NUMBER:      3
 LOG BETA:               -8.3600

GAUSS-NEWTON:           INITIAL SLOPE =  -2.6683 E-02

                SLOPE AT PREDICTED SOLUTION =  -2.3685E-03


OPTIMIZATION CYCLE  1
*********************
OVERALL OBJE OBJECTIVE FUNCTION:    1.8338E+02      (N-R ITERATIONS: 1427)
FORMATION CONSTANTS:
--------------------
COMPLEX NUMBER:      3
```

STD DEVN: 0.0223

GAUSS-NEWTON: INITIAL SLOPE = -2.1228E-04

OPTIMIZATION CYCLE 2 (CONVERGENCE)
****
OVERALL OBJE OBJECTIVE FUNCTION: 1.8338E+02 (N-R ITERATIONS: 2227)
FORMATION CONSTANTS:

COMPLEX NUMBER: 3
LOG BETA: -8.3651
STD DEVN: 0.0224
NO SIGNIFICANTLY CORRELATED PARAMETERS FOUND
HAMILTON R-FACTOR: 0.02311
HAMILTON R-LIMIT: 0.00171
NO. OF TITRATIONS: 5 NO. OF POINTS: 300
Stop - Program terminated.

4 Ni(II)-ITB model

```
PROGRAM ESTA2A          VERSION 3.0

  TASK OBJE  1      ITB-NI+2
  MODL     NI+2 ITB0 H +1
  CPLX 0  1 -13.7900  NI+2( 0) ITB0( 0) H +1(-1)
  CPLX 0  1   5.7274  ITB0( 1) H +1( 1)
  CPLX 0  1  -9.7900  NI+2( 1) ITB0( 0) H +1(-1)
  CPLX 0  1 -19.5800  NI+2( 1) ITB0( 0) H +1(-2)
  CPLX 0  1 -30.3700  NI+2( 1) ITB0( 0) H +1(-3)
  CPLX 0  1 -26.8600  NI+2( 4) ITB0( 0) H +1(-4)
  CPLX 1  1  -8.4400  NI+2( 1) ITB0( 2) H +1(-2)
  CONC
  VESL IVOL    50.000  0 0
  VESL ITB0   .0009935  0 0
  VESL NI+2   .0010341  0 0
  VESL H +1   .0096157  0 0
  BUR1 H +1  -.0500360  0 0
  ELEC
  ZERO H +1    398.964    0
  GRAD H +1     58.164    0
  WGHT 1
  VESL ITB0   .0000020
  VESL NI+2   .0000020
  VESL H +1   .0000190
  BUR1 H +1  -.0001000
  ZERO H +1      .250
  GRAD H +1      .020
  TITR RNDE      .0010
  EOBS RNDE      .0800
  DATA

  CONC
  VESL IVOL    50.000  0 0
  VESL ITB0   .0019871  0 0
  VESL NI+2   .0010341  0 0
  VESL H +1   .0095617  0 0
  BUR1 H +1  -.0500360  0 0
  ELEC
  ZERO H +1    401.064    0
  GRAD H +1     58.558    0
  WGHT 1
  VESL ITB0   .0000040
  VESL NI+2   .0000020
  VESL H +1   .0000190
  BUR1 H +1  -.0001000
  ZERO H +1      .250
  GRAD H +1      .020
  TITR RNDE      .0010
  EOBS RNDE      .0800
  DATA

  CONC
  VESL IVOL    50.000  0 0
  VESL ITB0   .0029807  0 0
  VESL NI+2   .0010341  0 0
  VESL H +1   .0096215  0 0
  BUR1 H +1  -.0500360  0 0
  ELEC
  ZERO H +1    398.547    0
  GRAD H +1     58.146    0
  WGHT 1
  VESL ITB0   .0000060
```

```
VESL H +1   .0000190
BUR1 H +1  -.0001000
ZERO H +1      .250
GRAD H +1      .020
TITR RNDE      .0010
EOBS RNDE      .0800
DATA


OPTIMIZATION CYCLE  0
**********
OVERALL OBJE OBJECTIVE FUNCTION:    4.8045E+01      (N-R ITERATIONS:  360)
FORMATION CONSTANTS:
---------
COMPLEX NUMBER:      7
 LOG BETA:      -8.4400

GAUSS-NEWTON:           INITIAL SLOPE =  -1.4204E-02

                SLOPE AT PREDICTED SOLUTION  =   4.9088E-05


OPTIMIZATION CYCLE  1
**********
OVERALL OBJE OBJECTIVE FUNCTION:    4.8037E+01      (N-R ITERATIONS:  846)
FORMATION CONSTANTS:
---------
COMPLEX NUMBER:      7
 LOG BETA:           -8.4421
 STD DEVN:           0.0090

GAUSS-NEWTON:           INITIAL SLOPE =  -1.6960E-07


OPTIMIZATION CYCLE  2   (CONVERGENCE)
**********
OVERALL OBJE OBJECTIVE FUNCTION:    4.8037E+01      (N-R ITERATIONS: 1332)
FORMATION CONSTANTS:
---------
COMPLEX NUMBER:      7
 LOG BETA:           -8.4421
 STD DEVN:           0.0090
NO SIGNIFICANTLY CORRELATED PARAMETERS FOUND
HAMILTON R-FACTOR:  0.01082
HAMILTON  R-LIMIT:  0.00157
NO. OF TITRATIONS:   3       NO. OF POINTS:  190
Stop - Program terminated.
```

5 Zn(II)-ITB MODEL

```
PROGRAM ESTA2A          VERSION 3.0


TASK OBJE 1       ITB-ZN+2
MODL     ZN+2 ITB0 H +1
CPLX 0  1 -13.7900  ZN+2( 0) ITB0( 0) H +1(-1)
CPLX 0  1  -8.7900  ZN+2( 1) ITB0( 0) H +1(-1)
CPLX 0  1 -17.5800  ZN+2( 1) ITB0( 0) H +1(-2)
CPLX 0  1 -27.7700  ZN+2( 1) ITB0( 0) H +1(-3)
CPLX 0  1 -39.1600  ZN+2( 1) ITB0( 0) H +1(-4)
CPLX 0  1  -8.5900  ZN+2( 2) ITB0( 0) H +1(-1)
CPLX 0  1   5.7274  ITB0( 1) H +1( 1)
CPLX 1  1 -10.5600  ZN+2( 1) ITB0( 2) H +1(-2)
CONC
VESL IVOL    50.000  0 0
VESL ITB0   .0039709  0 0
VESL ZN+2   .0009655  0 0
VESL H +1   .0101009  0 0
BUR1 H +1  -.0512140  0 0
ELEC
ZERO H +1    405.705    0
GRAD H +1     58.623    0
WGHT 1
VESL ITB0   .0000080
VESL ZN+2   .0000020
VESL H +1   .0000200
BUR1 H +1  -.0001020
ZERO H +1       .250
GRAD H +1       .020
TITR RNDE       .0010
EOBS RNDE       .0800
DATA

CONC
VESL IVOL    50.000  0 0
VESL ITB0   .0049636  0 0
VESL ZN+2   .0009655  0 0
VESL H +1   .0099075  0 0
BUR1 H +1  -.0512140  0 0
ELEC
ZERO H +1    404.391    0
GRAD H +1     58.415    0
WGHT 1
VESL ITB0   .0000090
VESL ZN+2   .0000020
VESL H +1   .0000200
BUR1 H +1  -.0001020
ZERO H +1       .250
GRAD H +1       .020
TITR RNDE       .0010
EOBS RNDE       .0800
DATA

CONC
VESL IVOL    60.000  0 0
VESL ITB0   .0024818  0 0
VESL ZN+2   .0009655  0 0
VESL H +1   .0081429  0 0
BUR1 H +1  -.0482000  0 0
ELEC
ZERO H +1    409.719    0
GRAD H +1     58.869    0
```

```
  VESL ITB0  .0000050
  VESL ZN+2  .0000016
  VESL H +1  .0000160
  BUR1 H +1 -.0000964
  ZERO H +1     .250
  GRAD H +1     .020
  TITR RNDE     .0010
  EOBS RNDE     .0800
  DATA


OPTIMIZATION CYCLE  0
*********************
OVERALL OBJE OBJECTIVE FUNCTION:   3.7507E+02      (N-R ITERATIONS:  610)
FORMATION CONSTANTS:
--------------------
COMPLEX NUMBER:      8
 LOG BETA:          -10.5600

GAUSS-NEWTON:           INITIAL SLOPE =      -7.4412E-01

                SLOPE AT PREDICTED SOLUTION =    -2.1666E-02


OPTIMIZATION CYCLE  1
*********************
OVERALL OBJE OBJECTIVE FUNCTION:   3.7481E+02      (N-R ITERATIONS: 1419)
FORMATION CONSTANTS:
--------------------
COMPLEX NUMBER:      8
 LOG BETA:          -10.5410
 STD DEVN:           0.0233

GAUSS-NEWTON:           INITIAL SLOPE =      -6.2874E-04


OPTIMIZATION CYCLE  2   (CONVERGENCE)
*********************
OVERALL OBJE OBJECTIVE FUNCTION:   3.7481E+02      (N-R ITERATIONS: 2228)
FORMATION CONSTANTS:
--------------------
COMPLEX NUMBER:      8
 LOG BETA:          -10.5404
 STD DEVN:           0.0233
NO SIGNIFICANTLY CORRELATED PARAMETERS FOUND
HAMILTON R-FACTOR:  0.02679
HAMILTON  R-LIMIT:  0.00139
NO. OF TITRATIONS:  3       NO. OF POINTS:  337
Stop - Program terminated.
```

Appendix D

ECCLES modelling input files

See Disk 1

The ECCLES input files containing the concentrations and complexation constants used.

NorITB.MOD (ITB scan from 8.5×10^{-10} to 8.5×10^{-2})

NorITB1.MOD (ITB)

Appendix E

ECCLES modelling output files

The ECCLES output, with respect to monitored components

```
****      ****      ****      *         *****     *****
         *         *          *         *         *
***      *         *          *         ****      *****
         *         *          *         *             *
****      ****      ****      *****     *****     *****
-----------------------------------------------------------------------------




><><><><><><><><><><><><><><><><><><><><><><><><><><><><><><><><><><><><><><><>
>
>                        NORMAL PLASMA WITH ALL THE METALS
>
>
>  EXCLUDING ITB                                                         100392
>
><><><><><><><><><><><><><><><><><><><><><><><><><><><><><><><><><><><><><><><>



UTPUT SUPRESSED.
ONITORED COMPONENTS:  CA+2 MG+2 ZN+2 NI+2
O SCAN REQUIRED.
CCLES DATA CHECKING PROCEDURES EMPLOYED.
HERE ARE 18 SPECIES WITH DEFINED CONCENTRATIONS.

ATA INPUT SUCCESSFULLY COMPLETED.
OTAL NUMBER OF COMPONENTS =  52  (LIMIT = 115 )
UMBER OF COMPONENTS WITH FIXED FREE CONCENTRATIONS = 12  (LIMIT = 15 )
OTAL NUMBER OF SPECIES =  4987  (LIMIT =  5000 )
OTAL NUMBER OF COMPONENTS ENTERED IN KEY ARRAY = 17407  (LIMIT = 18000 )

XPERIMENTAL PH =       7.398                CALCULATED LOG KW =    -13.3116
```

ONCENTRATIONS OF THE FREE COMPONENTS.

COMP. NO.	FREE CONC.	REAL TOTAL	CALC. TOTAL	COMP. NAME
1	3.597142E-06	3.700000E-04	3.700000E-04	ALA1
2	3.375804E-07	2.400000E-05	2.400000E-05	ABA1
3	3.665891E-06	9.500000E-05	9.499999E-05	ARG0
4	4.275294E-06	5.500000E-05	5.500000E-05	ASN1
5	6.518598E-08	5.000000E-06	5.000000E-06	ASP2
6	9.272521E-09	2.300000E-05	2.300000E-05	CYS2
7	6.180418E-07	4.000000E-05	4.000000E-05	CIS2
8	1.264413E-06	2.700000E-05	2.700000E-05	CIT1
9	7.676385E-07	4.800000E-05	4.800000E-05	GLU2
10	2.436659E-05	5.210000E-04	5.210000E-04	GLN1
11	3.371017E-06	2.430000E-04	2.430000E-04	GLY1
12	3.226903E-06	8.500000E-05	8.500001E-05	HIS1
13	9.007221E-11	1.000000E-08	1.000000E-08	HSN0
14	8.577172E-08	7.000000E-06	7.000001E-06	HYP1
15	6.940376E-07	6.500000E-05	6.500000E-05	ILE1
16	1.618587E-06	1.240000E-04	1.240000E-04	LEU1
17	6.500972E-09	1.780000E-04	1.780000E-04	LYS1
18	1.135893E-06	2.900000E-05	2.900000E-05	MET1
19	5.684671E-09	5.800000E-05	5.800000E-05	ORN1
20	2.515039E-06	6.400000E-05	6.399999E-05	PHE1
21	2.861981E-07	2.110000E-04	2.110000E-04	PRO1
22	5.569534E-06	1.220000E-04	1.220000E-04	SER1
23	9.243447E-06	1.500000E-04	1.500000E-04	THR1
24	2.297071E-07	1.000000E-05	1.000000E-05	TRP1
25	3.496343E-09	5.800000E-05	5.800001E-05	TYR2
26	3.043186E-06	2.270000E-04	2.270000E-04	VAL1
27	3.234148E-05	2.450000E-02	2.450000E-02	CO32
28	3.306920E-08	3.810000E-04	3.810000E-04	PO43
29	1.399999E-05	1.400000E-05	1.400000E-05	SCN1
30	2.672677E-10	1.380000E-04	1.380000E-04	SIL2
31	2.039919E-04	2.110000E-04	2.110000E-04	SO42
32	6.548429E-07	2.400000E-05	2.400000E-05	NH30
33	2.645373E-05	1.130000E-04	1.130000E-04	CTA3
34	1.748671E-03	1.818000E-03	1.818000E-03	LTA1
35	3.188940E-05	3.500000E-05	3.500000E-05	MLA2
36	9.792929E-06	1.200000E-05	1.200000E-05	OXA2
37	9.412581E-05	9.500000E-05	9.500000E-05	PVA1
38	1.217195E-11	5.000000E-06	5.000000E-06	SLA2
39	4.018534E-05	4.200000E-05	4.200000E-05	SCA2
40	4.784818E-08	4.300000E-05	4.300000E-05	ACA2
41	4.000000E-08	FIXED FREE CONC.	3.005372E-02	H +1
42	1.220000E-06	FIXED FREE CONC.	1.322464E-06	OH-1
43	1.130000E-03	FIXED FREE CONC.	1.460676E-03	CA+2
44	5.200000E-04	FIXED FREE CONC.	6.717570E-04	MG+2
45	1.000000E-20	FIXED FREE CONC.	2.453152E-13	CU+2
46	1.000000E-17	FIXED FREE CONC.	5.603324E-10	CU+1
47	1.000000E-11	FIXED FREE CONC.	4.997208E-11	FE+2
48	1.000000E-23	FIXED FREE CONC.	1.185664E-11	FE+3
49	1.000000E-12	FIXED FREE CONC.	1.796520E-12	MN+2
50	1.000000E-09	FIXED FREE CONC.	2.215783E-07	ZN+2
51	1.000000E-14	FIXED FREE CONC.	5.936220E-11	PB+2
52	1.000000E-18	FIXED FREE CONC.	1.757598E-14	NI+2

ONITOR COMPONENT CA+2 — FREE CONC. = 1.1300E-03 77.

SPECIES NO.	SPECIES CONC.		LOG STAB. CONST.	COMPOSITION.
850	1.1612E-04	7.9%	10.90	CO32(1) CA+2(1) H +1(1)
1001	5.4396E-05	3.7%	3.26	CTA3(1) CA+2(1)
898	4.1928E-05	2.9%	6.05	PO43(1) CA+2(1)
1061	3.9426E-05	2.7%	1.30	LTA1(1) CA+2(1)
849	2.9029E-05	2.0%	2.90	CO32(1) CA+2(1)
899	7.4914E-06	.5%	12.70	PO43(1) CA+2(1) H +1(1)
516	6.6096E-06	.5%	20.75	LYS1(1) CA+2(1) H +1(2)
649	4.0908E-06	.3%	11.50	PRO1(1) CA+2(1) H +1(1)
938	3.6534E-06	.3%	1.20	SO42(1) CA+2(1)
292	2.7665E-06	.2%	9.40	GLN1(1) CA+2(1) H +1(1)
1082	2.2737E-06	.2%	1.80	MLA2(1) CA+2(1)
5	2.0469E-06	.1%	10.10	ALA1(1) CA+2(1) H +1(1)
324	1.9182E-06	.1%	10.10	GLY1(1) CA+2(1) H +1(1)
714	1.3212E-06	.1%	9.50	THR1(1) CA+2(1) H +1(1)
4926	1.1675E-06	.1%	14.65	LTA1(1) PO43(1) CA+2(1) H +1(1
1188	9.0604E-07	.1%	1.30	SCA2(1) CA+2(1)
260	8.7155E-07	.1%	10.40	GLU2(1) CA+2(1) H +1(1)
817	8.6789E-07	.1%	9.80	VAL1(1) CA+2(1) H +1(1)
68	8.3046E-07	.1%	9.70	ARG0(1) CA+2(1) H +1(1)
682	7.9608E-07	.1%	9.50	SER1(1) CA+2(1) H +1(1)
363	7.3101E-07	.1%	9.70	HIS1(1) CA+2(1) H +1(1)
1113	6.9822E-07	.0%	1.80	OXA2(1) CA+2(1)
1147	5.9812E-07	.0%	.75	PVA1(1) CA+2(1)
482	5.8113E-07	.0%	9.90	LEU1(1) CA+2(1) H +1(1)
4549	5.2273E-07	.0%	4.00	CTA3(1) LTA1(1) CA+2(1)
96	4.8540E-07	.0%	9.40	ASN1(1) CA+2(1) H +1(1)
1062	3.4554E-07	.0%	2.00	LTA1(2) CA+2(1)
4662	3.0524E-07	.0%	11.20	LTA1(1) GLN1(1) CA+2(1) H +1(1
623	2.8555E-07	.0%	9.40	PHE1(1) CA+2(1) H +1(1)
232	2.8068E-07	.0%	17.40	CIS2(1) CA+2(1) H +1(2)
231	2.7935E-07	.0%	10.00	CIS2(1) CA+2(1) H +1(1)
291	2.7534E-07	.0%	1.00	GLN1(1) CA+2(1)
585	2.5817E-07	.0%	19.40	ORN1(1) CA+2(1) H +1(2)
4577	2.5340E-07	.0%	11.95	LTA1(1) ALA1(1) CA+2(1) H +1(1
452	2.4918E-07	.0%	9.90	ILE1(1) CA+2(1) H +1(1)
900	2.3802E-07	.0%	18.60	PO43(1) CA+2(1) H +1(2)
4676	2.1164E-07	.0%	11.90	LTA1(1) GLY1(1) CA+2(1) H +1(1
778	1.9990E-07	.0%	19.50	TYR2(1) CA+2(1) H +1(2)
4792	1.7969E-07	.0%	12.90	LTA1(1) PRO1(1) CA+2(1) H +1(1
4925	1.7662E-07	.0%	15.65	CTA3(1) PO43(1) CA+2(1) H +1(1
67	1.6491E-07	.0%	1.60	ARG0(1) CA+2(1)
557	1.6236E-07	.0%	9.50	MET1(1) CA+2(1) H +1(1)
713	1.3150E-07	.0%	1.10	THR1(1) CA+2(1)
4836	1.2992E-07	.0%	11.25	LTA1(1) THR1(1) CA+2(1) H +1(1
681	1.2557E-07	.0%	1.30	SER1(1) CA+2(1)
95	1.2135E-07	.0%	1.40	ASN1(1) CA+2(1)
4880	1.2055E-07	.0%	11.70	LTA1(1) VAL1(1) CA+2(1) H +1(1
515	1.1698E-07	.0%	11.60	LYS1(1) CA+2(1) H +1(1)
161	1.1403E-07	.0%	9.30	CIT1(1) CA+2(1) H +1(1)
4571	1.1216E-07	.0%	3.15	LTA1(1) SCA2(1) CA+2(1)
1166	1.0977E-07	.0%	14.30	SLA2(1) CA+2(1) H +1(1)
4939	1.0314E-07	.0%	22.85	GLN1(1) PO43(1) CA+2(1) H +1(2
4556	9.9870E-08	.0%	3.20	LTA1(1) MLA2(1) CA+2(1)

ONITOR COMPONENT MG+2 FREE CONC. = 5.2000E-04 77.

SPECIES NO.	SPECIES CONC.		LOG STAB. CONST.	COMPOSITION.
869	3.3715E-05	5.0%	10.70	CO32(1) MG+2(1) H +1(1)
1042	3.0095E-05	4.5%	3.34	CTA3(1) MG+2(1)
1071	2.2841E-05	3.4%	1.40	LTA1(1) MG+2(1)
868	1.3359E-05	2.0%	2.90	CO32(1) MG+2(1)
917	1.0902E-05	1.6%	13.20	PO43(1) MG+2(1) H +1(1)
538	8.5724E-06	1.3%	21.20	LYS1(1) MG+2(1) H +1(2)
945	3.3544E-06	.5%	1.50	SO42(1) MG+2(1)
308	3.1979E-06	.5%	9.80	GLN1(1) MG+2(1) H +1(1)
342	2.7914E-06	.4%	10.60	GLY1(1) MG+2(1) H +1(1)
663	2.3699E-06	.4%	11.60	PRO1(1) MG+2(1) H +1(1)
24	1.8794E-06	.3%	10.40	ALA1(1) MG+2(1) H +1(1)
83	1.5214E-06	.2%	10.30	ARG0(1) MG+2(1) H +1(1)
1131	1.2791E-06	.2%	2.40	OXA2(1) MG+2(1)
730	1.2131E-06	.2%	9.80	THR1(1) MG+2(1) H +1(1)
832	1.0032E-06	.1%	10.20	VAL1(1) MG+2(1) H +1(1)
497	8.4567E-07	.1%	10.40	LEU1(1) MG+2(1) H +1(1)
383	8.4499E-07	.1%	10.10	HIS1(1) MG+2(1) H +1(1)
699	7.3094E-07	.1%	9.80	SER1(1) MG+2(1) H +1(1)
243	6.4429E-07	.1%	10.70	CIS2(1) MG+2(1) H +1(1)
277	6.3565E-07	.1%	10.60	GLU2(1) MG+2(1) H +1(1)
307	6.3504E-07	.1%	1.70	GLN1(1) MG+2(1)
1098	5.2438E-07	.1%	1.50	MLA2(1) MG+2(1)
115	4.4569E-07	.1%	9.70	ASN1(1) MG+2(1) H +1(1)
4462	4.2677E-07	.1%	14.55	LTA1(1) PO43(1) MG+2(1) H +1(1
1200	3.3119E-07	.0%	1.20	SCA2(1) MG+2(1)
637	3.3007E-07	.0%	9.80	PHE1(1) MG+2(1) H +1(1)
466	2.8804E-07	.0%	10.30	ILE1(1) MG+2(1) H +1(1)
1156	2.7524E-07	.0%	.75	PVA1(1) MG+2(1)
382	2.6594E-07	.0%	2.20	HIS1(1) MG+2(1)
244	2.5772E-07	.0%	17.70	CIS2(1) MG+2(1) H +1(2)
729	2.4090E-07	.0%	1.70	THR1(1) MG+2(1)
606	2.3704E-07	.0%	19.70	ORN1(1) MG+2(1) H +1(2)
341	2.2068E-07	.0%	2.10	GLY1(1) MG+2(1)
4086	2.1439E-07	.0%	3.95	CTA3(1) LTA1(1) MG+2(1)
4201	1.9841E-07	.0%	11.35	LTA1(1) GLN1(1) MG+2(1) H +1(1
82	1.9063E-07	.0%	2.00	ARG0(1) MG+2(1)
570	1.8767E-07	.0%	9.90	MET1(1) MG+2(1) H +1(1)
801	1.8354E-07	.0%	19.80	TYR2(1) MG+2(1) H +1(2)
698	1.8274E-07	.0%	1.80	SER1(1) MG+2(1)
537	1.7023E-07	.0%	12.10	LYS1(1) MG+2(1) H +1(1)
174	1.6594E-07	.0%	9.80	CIT1(1) MG+2(1) H +1(1)
114	1.4027E-07	.0%	1.80	ASN1(1) MG+2(1)
918	1.3789E-07	.0%	18.70	PO43(1) MG+2(1) H +1(2)
4216	1.3757E-07	.0%	12.05	LTA1(1) GLY1(1) MG+2(1) H +1(1
4116	1.3084E-07	.0%	12.00	LTA1(1) ALA1(1) MG+2(1) H +1(1
4334	1.0410E-07	.0%	13.00	LTA1(1) PRO1(1) MG+2(1) H +1(1
1072	1.0033E-07	.0%	1.80	LTA1(2) MG+2(1)
605	9.3922E-08	.0%	11.90	ORN1(1) MG+2(1) H +1(1)
23	9.3748E-08	.0%	1.70	ALA1(1) MG+2(1)
4461	9.1196E-08	.0%	15.70	CTA3(1) PO43(1) MG+2(1) H +1(1
4475	8.4400E-08	.0%	23.10	GLN1(1) PO43(1) MG+2(1) H +1(2
831	7.9311E-08	.0%	1.70	VAL1(1) MG+2(1)
55	7.0217E-08	.0%	10.00	ABA1(1) MG+2(1) H +1(1)

ONITOR COMPONENT ZN+2 FREE CONC. = 1.0000E-09

SPECIES NO.	SPECIES CONC.		LOG STAB. CONST.	COMPOSITION.
213	5.0629E-08	22.8%	17.77	CYS2(2) ZN+2(1)
2222	2.5555E-08	11.5%	14.93	CYS2(1) HIS1(1) ZN+2(1)
2503	1.7590E-08	7.9%	22.89	CYS2(1) CIS2(1) ZN+2(1) H +1(1
2207	1.3931E-08	6.3%	13.79	CYS2(1) GLN1(1) ZN+2(1)
2315	9.0789E-09	4.1%	14.02	CYS2(1) THR1(1) ZN+2(1)
392	6.2920E-09	2.8%	6.29	HIS1(1) ZN+2(1)
2214	5.5906E-09	2.5%	14.25	CYS2(1) GLY1(1) ZN+2(1)
2191	4.8770E-09	2.2%	14.16	ALA1(1) CYS2(1) ZN+2(1)
2298	4.8197E-09	2.2%	13.97	CYS2(1) SER1(1) ZN+2(1)
219	4.4305E-09	2.0%	24.11	CYS2(2) ZN+2(1) H +1(1)
218	3.6915E-09	1.7%	8.60	CYS2(1) ZN+2(1)
2224	3.2778E-09	1.5%	10.62	GLN1(1) HIS1(1) ZN+2(1)
2389	2.9506E-09	1.3%	11.26	CYS2(1) LTA1(1) ZN+2(1)
2194	2.8719E-09	1.3%	13.86	ASN1(1) CYS2(1) ZN+2(1)
2345	2.8545E-09	1.3%	14.01	CYS2(1) VAL1(1) ZN+2(1)
2507	2.8305E-09	1.3%	19.55	HIS1(1) CIS2(1) ZN+2(1) H +1(1
393	2.8027E-09	1.3%	11.43	HIS1(2) ZN+2(1)
253	2.7607E-09	1.2%	6.65	CIS2(1) ZN+2(1)
2548	2.7054E-09	1.2%	24.05	CYS2(1) LYS1(1) ZN+2(1) H +1(1
1145	2.4482E-09	1.1%	11.31	OXA2(1) ZN+2(1) OH-1(1)
2249	2.1945E-09	1.0%	14.16	CYS2(1) LEU1(1) ZN+2(1)
2371	2.1197E-09	1.0%	10.40	HIS1(1) CTA3(1) ZN+2(1)
1057	2.0914E-09	.9%	10.81	CTA3(1) ZN+2(1) OH-1(1)
2479	2.0326E-09	.9%	21.23	HIS1(1) CYS2(1) ZN+2(1) H +1(1
2283	1.8150E-09	.8%	14.84	CYS2(1) PRO1(1) ZN+2(1)
2426	1.3903E-09	.6%	13.19	CYS2(1) OXA2(1) ZN+2(1)
1054	1.3724E-09	.6%	4.72	CTA3(1) ZN+2(1)
2625	1.3295E-09	.6%	23.03	CYS2(1) PO43(1) ZN+2(1) H +1(1
2193	1.2802E-09	.6%	13.58	ARG0(1) CYS2(1) ZN+2(1)
2216	1.1475E-09	.5%	10.99	ALA1(1) HIS1(1) ZN+2(1)
2302	1.1340E-09	.5%	10.80	HIS1(1) SER1(1) ZN+2(1)
2573	1.0446E-09	.5%	23.69	CYS2(1) ORN1(1) ZN+2(1) H +1(1
2453	1.0029E-09	.5%	12.43	CYS2(1) SCA2(1) ZN+2(1)
2200	9.3833E-10	.4%	14.12	CYS2(1) GLU2(1) ZN+2(1)
2597	8.8689E-10	.4%	23.83	CYS2(1) TYR2(1) ZN+2(1) H +1(1
2168	8.3139E-10	.4%	11.62	CIS2(1) HIS1(1) ZN+2(1)
873	8.1624E-10	.4%	11.80	CO32(1) ZN+2(1) H +1(1)
2541	7.1437E-10	.3%	26.35	CIS2(1) HIS1(1) ZN+2(1) H +1(2
2393	6.9422E-10	.3%	8.09	HIS1(1) LTA1(1) ZN+2(1)
2219	6.7570E-10	.3%	10.69	ASN1(1) HIS1(1) ZN+2(1)
2349	6.7161E-10	.3%	10.84	HIS1(1) VAL1(1) ZN+2(1)
2525	6.6426E-10	.3%	28.86	CYS2(1) CIS2(1) ZN+2(1) H +1(2
738	6.2493E-10	.3%	4.83	THR1(1) ZN+2(1)
2367	5.4662E-10	.2%	12.35	CYS2(1) CTA3(1) ZN+2(1)
2238	5.4148E-10	.2%	13.93	CYS2(1) ILE1(1) ZN+2(1)
2253	5.1632E-10	.2%	10.99	HIS1(1) LEU1(1) ZN+2(1)
2505	4.8403E-10	.2%	17.91	GLN1(1) CIS2(1) ZN+2(1) H +1(1
2287	4.2702E-10	.2%	11.66	HIS1(1) PRO1(1) ZN+2(1)
2477	4.1310E-10	.2%	19.66	GLN1(1) CYS2(1) ZN+2(1) H +1(1
2408	4.0350E-10	.2%	12.14	CYS2(1) MLA2(1) ZN+2(1)
317	3.9518E-10	.2%	4.21	GLN1(1) ZN+2(1)
2330	3.9208E-10	.2%	14.27	CYS2(1) TRP1(1) ZN+2(1)
2488	3.4284E-10	.2%	20.00	THR1(1) CYS2(1) ZN+2(1) H +1(1

NITOR COMPONENT NI+2 FREE CONC. = 1.0000E-18 .

PECIES NO.	SPECIES CONC.		LOG STAB. CONST.	COMPOSITION.
389	7.5435E-15	42.9%	14.86	HIS1(2) NI+2(1)
1744	3.2808E-15	18.7%	17.04	CYS2(1) HIS1(1) NI+2(1)
211	1.4269E-15	8.1%	19.22	CYS2(2) NI+2(1)
1747	6.8483E-16	3.9%	12.94	GLN1(1) HIS1(1) NI+2(1)
388	6.7420E-16	3.8%	8.32	HIS1(1) NI+2(1)
1890	4.0236E-16	2.3%	13.13	HIS1(1) THR1(1) NI+2(1)
1745	3.9337E-16	2.2%	14.30	CIS2(1) HIS1(1) NI+2(1)
1748	3.8155E-16	2.2%	13.55	GLY1(1) HIS1(1) NI+2(1)
1725	2.9785E-16	1.7%	15.12	CYS2(1) GLN1(1) NI+2(1)
1741	1.8610E-16	1.1%	13.13	ASN1(1) HIS1(1) NI+2(1)
1885	1.7500E-16	1.0%	15.31	CYS2(1) THR1(1) NI+2(1)
1710	1.7109E-16	1.0%	16.48	CYS2(1) CIS2(1) NI+2(1)
1870	1.6967E-16	1.0%	12.98	HIS1(1) SER1(1) NI+2(1)
1734	1.6594E-16	.9%	15.73	CYS2(1) GLY1(1) NI+2(1)
1931	1.4032E-16	.8%	13.15	HIS1(1) VAL1(1) NI+2(1)
2083	1.2411E-16	.7%	23.17	HIS1(1) LYS1(1) NI+2(1) H +1(1
1740	1.0069E-16	.6%	12.93	ARG0(1) HIS1(1) NI+2(1)
1701	8.0940E-17	.5%	15.31	ASN1(1) CYS2(1) NI+2(1)
1865	7.3793E-17	.4%	15.15	CYS2(1) SER1(1) NI+2(1)
1794	7.0457E-17	.4%	13.13	HIS1(1) LEU1(1) NI+2(1)
1834	6.9077E-17	.4%	12.93	HIS1(1) PHE1(1) NI+2(1)
1053	6.6134E-17	.4%	12.31	CTA3(1) NI+2(1) OH-1(1)
1926	6.1028E-17	.3%	15.34	CYS2(1) VAL1(1) NI+2(1)
2078	5.3980E-17	.3%	25.35	CYS2(1) LYS1(1) NI+2(1) H +1(1
1746	4.7747E-17	.3%	13.28	GLU2(1) HIS1(1) NI+2(1)
1852	4.4203E-17	.3%	13.68	HIS1(1) PRO1(1) NI+2(1)
1700	4.3790E-17	.2%	15.11	ARG0(1) CYS2(1) NI+2(1)
2007	4.2628E-17	.2%	12.13	HIS1(1) OXA2(1) NI+2(1)
2139	3.8411E-17	.2%	22.93	HIS1(1) TYR2(1) NI+2(1) H +1(1
210	3.6915E-17	.2%	9.60	CYS2(1) NI+2(1)
1742	3.5722E-17	.2%	14.23	ASP2(1) HIS1(1) NI+2(1)
2112	3.5120E-17	.2%	22.68	HIS1(1) ORN1(1) NI+2(1) H +1(1
1819	3.5004E-17	.2%	12.98	HIS1(1) MET1(1) NI+2(1)
1789	3.0643E-17	.2%	15.31	CYS2(1) LEU1(1) NI+2(1)
1781	3.0211E-17	.2%	13.13	HIS1(1) ILE1(1) NI+2(1)
1829	3.0043E-17	.2%	15.11	CYS2(1) PHE1(1) NI+2(1)
1962	2.4071E-17	.1%	9.63	HIS1(1) LTA1(1) NI+2(1)
1717	2.0766E-17	.1%	15.47	CYS2(1) GLU2(1) NI+2(1)
1847	1.9225E-17	.1%	15.86	CYS2(1) PRO1(1) NI+2(1)
2002	1.8540E-17	.1%	14.31	CYS2(1) OXA2(1) NI+2(1)
2134	1.6706E-17	.1%	25.11	CYS2(1) TYR2(1) NI+2(1) H +1(1
1702	1.5536E-17	.1%	16.41	ASP2(1) CYS2(1) NI+2(1)
1743	1.5512E-17	.1%	12.58	CIT1(1) HIS1(1) NI+2(1)
2107	1.5274E-17	.1%	24.86	CYS2(1) ORN1(1) NI+2(1) H +1(1
1814	1.5224E-17	.1%	15.16	CYS2(1) MET1(1) NI+2(1)
1739	1.4695E-17	.1%	13.13	ABA1(1) HIS1(1) NI+2(1)
1776	1.3140E-17	.1%	15.31	CYS2(1) ILE1(1) NI+2(1)
1911	1.1219E-17	.1%	13.18	HIS1(1) TRP1(1) NI+2(1)
1957	1.0469E-17	.1%	11.81	CYS2(1) LTA1(1) NI+2(1)
1769	7.4496E-18	.0%	13.43	HIS1(1) HYP1(1) NI+2(1)
1984	6.9572E-18	.0%	10.83	HIS1(1) MLA2(1) NI+2(1)
1703	6.7466E-18	.0%	14.76	CIT1(1) CYS2(1) NI+2(1)
1699	6.3911E-18	.0%	15.31	ABA1(1) CYS2(1) NI+2(1)

LL DONE ECCLES', SAID MORIARTY.

```
***      ****      ****      *        *****      *****
        *         *          *        *          *
**      *         *          *        ****       *****
        *         *          *        *              *
***      ****      ****      *****    *****      *****
------------------------------------------------------
```

```
<><><><><><><><><><><><><><><><><><><><><><><><><><><><><><><><><><><><><><><><>

                     NORMAL PLASMA WITH ALL THE METALS

 INCLUDING ITB                                                        100392

<><><><><><><><><><><><><><><><><><><><><><><><><><><><><><><><><><><><><><><><>
```

```
TPUT SUPRESSED.
NITORED COMPONENTS:  ITB0 CA+2 MG+2 ZN+2 NI+2
 SCAN REQUIRED.
CLES DATA CHECKING PROCEDURES EMPLOYED.
ERE ARE 18 SPECIES WITH DEFINED CONCENTRATIONS.

TA INPUT SUCCESSFULLY COMPLETED.
TAL NUMBER OF COMPONENTS =  53  (LIMIT = 115 )
MBER OF COMPONENTS WITH FIXED FREE CONCENTRATIONS = 12  (LIMIT = 15 )
TAL NUMBER OF SPECIES =  4988  (LIMIT =  5000 )
TAL NUMBER OF COMPONENTS ENTERED IN KEY ARRAY = 17410  (LIMIT = 18000 )

PERIMENTAL PH =       7.398               CALCULATED LOG KW =    -13.3116
```

NCENTRATIONS OF THE FREE COMPONENTS.

COMP. NO.	FREE CONC.	REAL TOTAL	CALC. TOTAL	COMP. NAME
1	7.450190E-05	8.500000E-05	8.500000E-05	ITB0
2	3.597142E-06	3.700000E-04	3.700000E-04	ALA1
3	3.375804E-07	2.400000E-05	2.400000E-05	ABA1
4	3.665891E-06	9.500000E-05	9.499999E-05	ARG0
5	4.275294E-06	5.500000E-05	5.500000E-05	ASN1
6	6.518598E-08	5.000000E-06	5.000000E-06	ASP2
7	9.272521E-09	2.300000E-05	2.300000E-05	CYS2
8	6.180418E-07	4.000000E-05	4.000000E-05	CIS2
9	1.264413E-06	2.700000E-05	2.700000E-05	CIT1
10	7.676385E-07	4.800000E-05	4.800000E-05	GLU2
11	2.436659E-05	5.210000E-04	5.210000E-04	GLN1
12	3.371017E-06	2.430000E-04	2.430000E-04	GLY1
13	3.226903E-06	8.500000E-05	8.500001E-05	HIS1
14	9.007221E-11	1.000000E-08	1.000000E-08	HSN0
15	8.577172E-08	7.000000E-06	7.000001E-06	HYP1
16	6.940376E-07	6.500000E-05	6.500000E-05	ILE1
17	1.618587E-06	1.240000E-04	1.240000E-04	LEU1
18	6.500972E-09	1.780000E-04	1.780000E-04	LYS1
19	1.135900E-06	2.900000E-05	2.900000E-05	MET1
20	5.684671E-09	5.800000E-05	5.800000E-05	ORN1
21	2.515039E-06	6.400000E-05	6.399999E-05	PHE1
22	2.861981E-07	2.110000E-04	2.110000E-04	PRO1
23	5.569534E-06	1.220000E-04	1.220000E-04	SER1
24	9.243447E-06	1.500000E-04	1.500000E-04	THR1
25	2.297071E-07	1.000000E-05	1.000000E-05	TRP1
26	3.496343E-09	5.800000E-05	5.800001E-05	TYR2
27	3.043186E-06	2.270000E-04	2.270000E-04	VAL1
28	3.234148E-05	2.450000E-02	2.450000E-02	CO32
29	3.306920E-08	3.810000E-04	3.810000E-04	PO43
30	1.399999E-05	1.400000E-05	1.400000E-05	SCN1
31	2.672681E-10	1.380000E-04	1.380000E-04	SIL2
32	2.039919E-04	2.110000E-04	2.110000E-04	SO42
33	6.548429E-07	2.400000E-05	2.400000E-05	NH30
34	2.645373E-05	1.130000E-04	1.130000E-04	CTA3
35	1.748671E-03	1.818000E-03	1.818000E-03	LTA1
36	3.188940E-05	3.500000E-05	3.500000E-05	MLA2
37	9.792929E-06	1.200000E-05	1.200000E-05	OXA2
38	9.412581E-05	9.500000E-05	9.500000E-05	PVA1
39	1.217195E-11	5.000000E-06	5.000000E-06	SLA2
40	4.018534E-05	4.200000E-05	4.200000E-05	SCA2
41	4.784818E-08	4.300000E-05	4.300000E-05	ACA2
42	4.000000E-08	FIXED FREE CONC.	3.005532E-02	H +1
43	1.220000E-06	FIXED FREE CONC.	1.345123E-06	OH-1
44	1.130000E-03	FIXED FREE CONC.	1.460685E-03	CA+2
45	5.200000E-04	FIXED FREE CONC.	6.806456E-04	MG+2
46	1.000000E-20	FIXED FREE CONC.	2.453152E-13	CU+2
47	1.000000E-17	FIXED FREE CONC.	5.603324E-10	CU+1
48	1.000000E-11	FIXED FREE CONC.	4.997207E-11	FE+2
49	1.000000E-23	FIXED FREE CONC.	1.185664E-11	FE+3
50	1.000000E-12	FIXED FREE CONC.	1.796520E-12	MN+2
51	1.000000E-09	FIXED FREE CONC.	2.215777E-07	ZN+2
52	1.000000E-14	FIXED FREE CONC.	5.936220E-11	PB+2
53	1.000000E-18	FIXED FREE CONC.	1.757598E-14	NI+2

NITOR COMPONENT CA+2 FREE CONC. = 1.1300E-03 77.

PECIES NO.	SPECIES CONC.		LOG STAB. CONST.	COMPOSITION.
850	1.1612E-04	7.9%	10.90	CO32(1) CA+2(1) H +1(1)
1001	5.4396E-05	3.7%	3.26	CTA3(1) CA+2(1)
898	4.1928E-05	2.9%	6.05	PO43(1) CA+2(1)
1061	3.9426E-05	2.7%	1.30	LTA1(1) CA+2(1)
849	2.9029E-05	2.0%	2.90	CO32(1) CA+2(1)
899	7.4914E-06	.5%	12.70	PO43(1) CA+2(1) H +1(1)
516	6.6096E-06	.5%	20.75	LYS1(1) CA+2(1) H +1(2)
649	4.0908E-06	.3%	11.50	PRO1(1) CA+2(1) H +1(1)
938	3.6534E-06	.3%	1.20	SO42(1) CA+2(1)
292	2.7665E-06	.2%	9.40	GLN1(1) CA+2(1) H +1(1)
1082	2.2737E-06	.2%	1.80	MLA2(1) CA+2(1)
5	2.0469E-06	.1%	10.10	ALA1(1) CA+2(1) H +1(1)
324	1.9182E-06	.1%	10.10	GLY1(1) CA+2(1) H +1(1)
714	1.3212E-06	.1%	9.50	THR1(1) CA+2(1) H +1(1)
4927	1.1675E-06	.1%	14.65	LTA1(1) PO43(1) CA+2(1) H +1(1
1188	9.0604E-07	.1%	1.30	SCA2(1) CA+2(1)
260	8.7155E-07	.1%	10.40	GLU2(1) CA+2(1) H +1(1)
817	8.6789E-07	.1%	9.80	VAL1(1) CA+2(1) H +1(1)
68	8.3046E-07	.1%	9.70	ARG0(1) CA+2(1) H +1(1)
682	7.9608E-07	.1%	9.50	SER1(1) CA+2(1) H +1(1)
363	7.3101E-07	.1%	9.70	HIS1(1) CA+2(1) H +1(1)
1113	6.9822E-07	.0%	1.80	OXA2(1) CA+2(1)
1147	5.9812E-07	.0%	.75	PVA1(1) CA+2(1)
482	5.8113E-07	.0%	9.90	LEU1(1) CA+2(1) H +1(1)
4550	5.2273E-07	.0%	4.00	CTA3(1) LTA1(1) CA+2(1)
96	4.8540E-07	.0%	9.40	ASN1(1) CA+2(1) H +1(1)
1062	3.4554E-07	.0%	2.00	LTA1(2) CA+2(1)
4663	3.0524E-07	.0%	11.20	LTA1(1) GLN1(1) CA+2(1) H +1(1
623	2.8555E-07	.0%	9.40	PHE1(1) CA+2(1) H +1(1)
232	2.8068E-07	.0%	17.40	CIS2(1) CA+2(1) H +1(2)
231	2.7935E-07	.0%	10.00	CIS2(1) CA+2(1) H +1(1)
291	2.7534E-07	.0%	1.00	GLN1(1) CA+2(1)
585	2.5817E-07	.0%	19.40	ORN1(1) CA+2(1) H +1(2)
4578	2.5340E-07	.0%	11.95	LTA1(1) ALA1(1) CA+2(1) H +1(1
452	2.4918E-07	.0%	9.90	ILE1(1) CA+2(1) H +1(1)
900	2.3802E-07	.0%	18.60	PO43(1) CA+2(1) H +1(2)
4677	2.1164E-07	.0%	11.90	LTA1(1) GLY1(1) CA+2(1) H +1(1
778	1.9990E-07	.0%	19.50	TYR2(1) CA+2(1) H +1(2)
4793	1.7969E-07	.0%	12.90	LTA1(1) PRO1(1) CA+2(1) H +1(1
4926	1.7662E-07	.0%	15.65	CTA3(1) PO43(1) CA+2(1) H +1(1
67	1.6491E-07	.0%	1.60	ARG0(1) CA+2(1)
557	1.6236E-07	.0%	9.50	MET1(1) CA+2(1) H +1(1)
713	1.3150E-07	.0%	1.10	THR1(1) CA+2(1)
4837	1.2992E-07	.0%	11.25	LTA1(1) THR1(1) CA+2(1) H +1(1
681	1.2557E-07	.0%	1.30	SER1(1) CA+2(1)
95	1.2135E-07	.0%	1.40	ASN1(1) CA+2(1)
4881	1.2055E-07	.0%	11.70	LTA1(1) VAL1(1) CA+2(1) H +1(1
515	1.1698E-07	.0%	11.60	LYS1(1) CA+2(1) H +1(1)
161	1.1403E-07	.0%	9.30	CIT1(1) CA+2(1) H +1(1)
4572	1.1216E-07	.0%	3.15	LTA1(1) SCA2(1) CA+2(1)
1166	1.0977E-07	.0%	14.30	SLA2(1) CA+2(1) H +1(1)
4940	1.0314E-07	.0%	22.85	GLN1(1) PO43(1) CA+2(1) H +1(2
4557	9.9870E-08	.0%	3.20	LTA1(1) MLA2(1) CA+2(1)

NITOR COMPONENT MG+2 FREE CONC. = 5.2000E-04 76.

PECIES NO.	SPECIES CONC.		LOG STAB. CONST.	COMPOSITION.
869	3.3715E-05	5.0%	10.70	CO32(1) MG+2(1) H +1(1)
1042	3.0095E-05	4.4%	3.34	CTA3(1) MG+2(1)
1071	2.2841E-05	3.4%	1.40	LTA1(1) MG+2(1)
868	1.3359E-05	2.0%	2.90	CO32(1) MG+2(1)
917	1.0902E-05	1.6%	13.20	PO43(1) MG+2(1) H +1(1)
1213	8.8750E-06	1.3%	2.36	ITB0(1) MG+2(1)
538	8.5724E-06	1.3%	21.20	LYS1(1) MG+2(1) H +1(2)
945	3.3544E-06	.5%	1.50	SO42(1) MG+2(1)
308	3.1979E-06	.5%	9.80	GLN1(1) MG+2(1) H +1(1)
342	2.7914E-06	.4%	10.60	GLY1(1) MG+2(1) H +1(1)
663	2.3699E-06	.3%	11.60	PRO1(1) MG+2(1) H +1(1)
24	1.8794E-06	.3%	10.40	ALA1(1) MG+2(1) H +1(1)
83	1.5214E-06	.2%	10.30	ARG0(1) MG+2(1) H +1(1)
1131	1.2791E-06	.2%	2.40	OXA2(1) MG+2(1)
730	1.2131E-06	.2%	9.80	THR1(1) MG+2(1) H +1(1)
832	1.0032E-06	.1%	10.20	VAL1(1) MG+2(1) H +1(1)
497	8.4567E-07	.1%	10.40	LEU1(1) MG+2(1) H +1(1)
383	8.4499E-07	.1%	10.10	HIS1(1) MG+2(1) H +1(1)
699	7.3094E-07	.1%	9.80	SER1(1) MG+2(1) H +1(1)
243	6.4429E-07	.1%	10.70	CIS2(1) MG+2(1) H +1(1)
277	6.3565E-07	.1%	10.60	GLU2(1) MG+2(1) H +1(1)
307	6.3504E-07	.1%	1.70	GLN1(1) MG+2(1)
1098	5.2438E-07	.1%	1.50	MLA2(1) MG+2(1)
115	4.4569E-07	.1%	9.70	ASN1(1) MG+2(1) H +1(1)
4464	4.2677E-07	.1%	14.55	LTA1(1) PO43(1) MG+2(1) H +1(1
1200	3.3119E-07	.0%	1.20	SCA2(1) MG+2(1)
637	3.3007E-07	.0%	9.80	PHE1(1) MG+2(1) H +1(1)
466	2.8804E-07	.0%	10.30	ILE1(1) MG+2(1) H +1(1)
1156	2.7524E-07	.0%	.75	PVA1(1) MG+2(1)
382	2.6594E-07	.0%	2.20	HIS1(1) MG+2(1)
244	2.5772E-07	.0%	17.70	CIS2(1) MG+2(1) H +1(2)
729	2.4090E-07	.0%	1.70	THR1(1) MG+2(1)
606	2.3704E-07	.0%	19.70	ORN1(1) MG+2(1) H +1(2)
341	2.2068E-07	.0%	2.10	GLY1(1) MG+2(1)
4088	2.1439E-07	.0%	3.95	CTA3(1) LTA1(1) MG+2(1)
4203	1.9841E-07	.0%	11.35	LTA1(1) GLN1(1) MG+2(1) H +1(1
82	1.9063E-07	.0%	2.00	ARG0(1) MG+2(1)
570	1.8767E-07	.0%	9.90	MET1(1) MG+2(1) H +1(1)
801	1.8354E-07	.0%	19.80	TYR2(1) MG+2(1) H +1(2)
698	1.8274E-07	.0%	1.80	SER1(1) MG+2(1)
537	1.7023E-07	.0%	12.10	LYS1(1) MG+2(1) H +1(1)
174	1.6594E-07	.0%	9.80	CIT1(1) MG+2(1) H +1(1)
114	1.4027E-07	.0%	1.80	ASN1(1) MG+2(1)
918	1.3789E-07	.0%	18.70	PO43(1) MG+2(1) H +1(2)
4218	1.3757E-07	.0%	12.05	LTA1(1) GLY1(1) MG+2(1) H +1(1
4118	1.3084E-07	.0%	12.00	LTA1(1) ALA1(1) MG+2(1) H +1(1
4336	1.0410E-07	.0%	13.00	LTA1(1) PRO1(1) MG+2(1) H +1(1
1072	1.0033E-07	.0%	1.80	LTA1(2) MG+2(1)
605	9.3922E-08	.0%	11.90	ORN1(1) MG+2(1) H +1(1)
23	9.3748E-08	.0%	1.70	ALA1(1) MG+2(1)
4463	9.1196E-08	.0%	15.70	CTA3(1) PO43(1) MG+2(1) H +1(1
4477	8.4400E-08	.0%	23.10	GLN1(1) PO43(1) MG+2(1) H +1(2
831	7.9311E-08	.0%	1.70	VAL1(1) MG+2(1)

NITOR COMPONENT ZN+2 FREE CONC. = 1.0000E-09 .

SPECIES NO.	SPECIES CONC.		LOG STAB. CONST.	COMPOSITION.
213	5.0629E-08	22.8%	17.77	CYS2(2) ZN+2(1)
2227	2.5555E-08	11.5%	14.93	CYS2(1) HIS1(1) ZN+2(1)
2507	1.7590E-08	7.9%	22.89	CYS2(1) CIS2(1) ZN+2(1) H +1(1
2212	1.3931E-08	6.3%	13.79	CYS2(1) GLN1(1) ZN+2(1)
2320	9.0789E-09	4.1%	14.02	CYS2(1) THR1(1) ZN+2(1)
392	6.2920E-09	2.8%	6.29	HIS1(1) ZN+2(1)
2219	5.5906E-09	2.5%	14.25	CYS2(1) GLY1(1) ZN+2(1)
2196	4.8770E-09	2.2%	14.16	ALA1(1) CYS2(1) ZN+2(1)
2303	4.8197E-09	2.2%	13.97	CYS2(1) SER1(1) ZN+2(1)
219	4.4305E-09	2.0%	24.11	CYS2(2) ZN+2(1) H +1(1)
218	3.6915E-09	1.7%	8.60	CYS2(1) ZN+2(1)
2229	3.2778E-09	1.5%	10.62	GLN1(1) HIS1(1) ZN+2(1)
2394	2.9506E-09	1.3%	11.26	CYS2(1) LTA1(1) ZN+2(1)
2199	2.8719E-09	1.3%	13.86	ASN1(1) CYS2(1) ZN+2(1)
2350	2.8545E-09	1.3%	14.01	CYS2(1) VAL1(1) ZN+2(1)
2511	2.8305E-09	1.3%	19.55	HIS1(1) CIS2(1) ZN+2(1) H +1(1
393	2.8027E-09	1.3%	11.43	HIS1(2) ZN+2(1)
253	2.7607E-09	1.2%	6.65	CIS2(1) ZN+2(1)
2552	2.7054E-09	1.2%	24.05	CYS2(1) LYS1(1) ZN+2(1) H +1(1
1145	2.4482E-09	1.1%	11.31	OXA2(1) ZN+2(1) OH-1(1)
2254	2.1945E-09	1.0%	14.16	CYS2(1) LEU1(1) ZN+2(1)
2376	2.1197E-09	1.0%	10.40	HIS1(1) CTA3(1) ZN+2(1)
1057	2.0914E-09	.9%	10.81	CTA3(1) ZN+2(1) OH-1(1)
2483	2.0326E-09	.9%	21.23	HIS1(1) CYS2(1) ZN+2(1) H +1(1
2288	1.8150E-09	.8%	14.84	CYS2(1) PRO1(1) ZN+2(1)
2431	1.3903E-09	.6%	13.19	CYS2(1) OXA2(1) ZN+2(1)
1054	1.3724E-09	.6%	4.72	CTA3(1) ZN+2(1)
2629	1.3295E-09	.6%	23.03	CYS2(1) PO43(1) ZN+2(1) H +1(1
2198	1.2802E-09	.6%	13.58	ARG0(1) CYS2(1) ZN+2(1)
2221	1.1475E-09	.5%	10.99	ALA1(1) HIS1(1) ZN+2(1)
2307	1.1340E-09	.5%	10.80	HIS1(1) SER1(1) ZN+2(1)
2577	1.0446E-09	.5%	23.69	CYS2(1) ORN1(1) ZN+2(1) H +1(1
2457	1.0029E-09	.5%	12.43	CYS2(1) SCA2(1) ZN+2(1)
2205	9.3833E-10	.4%	14.12	CYS2(1) GLU2(1) ZN+2(1)
2601	8.8689E-10	.4%	23.83	CYS2(1) TYR2(1) ZN+2(1) H +1(1
2173	8.3139E-10	.4%	11.62	CIS2(1) HIS1(1) ZN+2(1)
873	8.1624E-10	.4%	11.80	CO32(1) ZN+2(1) H +1(1)
2545	7.1437E-10	.3%	26.35	CIS2(1) HIS1(1) ZN+2(1) H +1(2
2398	6.9422E-10	.3%	8.09	HIS1(1) LTA1(1) ZN+2(1)
2224	6.7570E-10	.3%	10.69	ASN1(1) HIS1(1) ZN+2(1)
2354	6.7161E-10	.3%	10.84	HIS1(1) VAL1(1) ZN+2(1)
2529	6.6426E-10	.3%	28.86	CYS2(1) CIS2(1) ZN+2(1) H +1(2
738	6.2493E-10	.3%	4.83	THR1(1) ZN+2(1)
2372	5.4662E-10	.2%	12.35	CYS2(1) CTA3(1) ZN+2(1)
2243	5.4148E-10	.2%	13.93	CYS2(1) ILE1(1) ZN+2(1)
2258	5.1632E-10	.2%	10.99	HIS1(1) LEU1(1) ZN+2(1)
2509	4.8403E-10	.2%	17.91	GLN1(1) CIS2(1) ZN+2(1) H +1(1
2292	4.2702E-10	.2%	11.66	HIS1(1) PRO1(1) ZN+2(1)
2481	4.1310E-10	.2%	19.66	GLN1(1) CYS2(1) ZN+2(1) H +1(1
2413	4.0350E-10	.2%	12.14	CYS2(1) MLA2(1) ZN+2(1)
317	3.9518E-10	.2%	4.21	GLN1(1) ZN+2(1)
2335	3.9208E-10	.2%	14.27	CYS2(1) TRP1(1) ZN+2(1)
2492	3.4284E-10	.2%	20.00	THR1(1) CYS2(1) ZN+2(1) H +1(1

NITOR COMPONENT NI+2 FREE CONC. = 1.0000E-18 .

SPECIES NO.	SPECIES CONC.		LOG STAB. CONST.	COMPOSITION.
389	7.5435E-15	42.9%	14.86	HIS1(2) NI+2(1)
1749	3.2808E-15	18.7%	17.04	CYS2(1) HIS1(1) NI+2(1)
211	1.4269E-15	8.1%	19.22	CYS2(2) NI+2(1)
1752	6.8483E-16	3.9%	12.94	GLN1(1) HIS1(1) NI+2(1)
388	6.7420E-16	3.8%	8.32	HIS1(1) NI+2(1)
1895	4.0236E-16	2.3%	13.13	HIS1(1) THR1(1) NI+2(1)
1750	3.9337E-16	2.2%	14.30	CIS2(1) HIS1(1) NI+2(1)
1753	3.8155E-16	2.2%	13.55	GLY1(1) HIS1(1) NI+2(1)
1730	2.9785E-16	1.7%	15.12	CYS2(1) GLN1(1) NI+2(1)
1746	1.8610E-16	1.1%	13.13	ASN1(1) HIS1(1) NI+2(1)
1890	1.7500E-16	1.0%	15.31	CYS2(1) THR1(1) NI+2(1)
1715	1.7109E-16	1.0%	16.48	CYS2(1) CIS2(1) NI+2(1)
1875	1.6967E-16	1.0%	12.98	HIS1(1) SER1(1) NI+2(1)
1739	1.6594E-16	.9%	15.73	CYS2(1) GLY1(1) NI+2(1)
1936	1.4032E-16	.8%	13.15	HIS1(1) VAL1(1) NI+2(1)
2088	1.2411E-16	.7%	23.17	HIS1(1) LYS1(1) NI+2(1) H +1(1
1745	1.0069E-16	.6%	12.93	ARG0(1) HIS1(1) NI+2(1)
1706	8.0940E-17	.5%	15.31	ASN1(1) CYS2(1) NI+2(1)
1870	7.3793E-17	.4%	15.15	CYS2(1) SER1(1) NI+2(1)
1799	7.0457E-17	.4%	13.13	HIS1(1) LEU1(1) NI+2(1)
1839	6.9077E-17	.4%	12.93	HIS1(1) PHE1(1) NI+2(1)
1053	6.6134E-17	.4%	12.31	CTA3(1) NI+2(1) OH-1(1)
1931	6.1028E-17	.3%	15.34	CYS2(1) VAL1(1) NI+2(1)
2083	5.3980E-17	.3%	25.35	CYS2(1) LYS1(1) NI+2(1) H +1(1
1751	4.7747E-17	.3%	13.28	GLU2(1) HIS1(1) NI+2(1)
1857	4.4203E-17	.3%	13.68	HIS1(1) PRO1(1) NI+2(1)
1705	4.3790E-17	.2%	15.11	ARG0(1) CYS2(1) NI+2(1)
2012	4.2628E-17	.2%	12.13	HIS1(1) OXA2(1) NI+2(1)
2144	3.8411E-17	.2%	22.93	HIS1(1) TYR2(1) NI+2(1) H +1(1
210	3.6915E-17	.2%	9.60	CYS2(1) NI+2(1)
1747	3.5722E-17	.2%	14.23	ASP2(1) HIS1(1) NI+2(1)
2117	3.5120E-17	.2%	22.68	HIS1(1) ORN1(1) NI+2(1) H +1(1
1824	3.5005E-17	.2%	12.98	HIS1(1) MET1(1) NI+2(1)
1794	3.0643E-17	.2%	15.31	CYS2(1) LEU1(1) NI+2(1)
1786	3.0211E-17	.2%	13.13	HIS1(1) ILE1(1) NI+2(1)
1834	3.0043E-17	.2%	15.11	CYS2(1) PHE1(1) NI+2(1)
1967	2.4071E-17	.1%	9.63	HIS1(1) LTA1(1) NI+2(1)
1722	2.0766E-17	.1%	15.47	CYS2(1) GLU2(1) NI+2(1)
1852	1.9225E-17	.1%	15.86	CYS2(1) PRO1(1) NI+2(1)
2007	1.8540E-17	.1%	14.31	CYS2(1) OXA2(1) NI+2(1)
2139	1.6706E-17	.1%	25.11	CYS2(1) TYR2(1) NI+2(1) H +1(1
1707	1.5536E-17	.1%	16.41	ASP2(1) CYS2(1) NI+2(1)
1748	1.5512E-17	.1%	12.58	CIT1(1) HIS1(1) NI+2(1)
2112	1.5274E-17	.1%	24.86	CYS2(1) ORN1(1) NI+2(1) H +1(1
1819	1.5224E-17	.1%	15.16	CYS2(1) MET1(1) NI+2(1)
1744	1.4695E-17	.1%	13.13	ABA1(1) HIS1(1) NI+2(1)
1781	1.3140E-17	.1%	15.31	CYS2(1) ILE1(1) NI+2(1)
1916	1.1219E-17	.1%	13.18	HIS1(1) TRP1(1) NI+2(1)
1962	1.0469E-17	.1%	11.81	CYS2(1) LTA1(1) NI+2(1)
1774	7.4496E-18	.0%	13.43	HIS1(1) HYP1(1) NI+2(1)
1989	6.9572E-18	.0%	10.83	HIS1(1) MLA2(1) NI+2(1)
1708	6.7466E-18	.0%	14.76	CIT1(1) CYS2(1) NI+2(1)
1704	6.3911E-18	.0%	15.31	ABA1(1) CYS2(1) NI+2(1)

WELL DONE ECCLES', SAID MORIARTY.